

Genetically Programmed Protein-based Hydrogels with Tunable Mechanical Properties

Inaugural dissertation

to obtain the academic degree

Doctor rerum naturalium (Dr. rer. nat.)

submitted to the Department of Biology, Chemistry, Pharmacy

of

Freie Universität Berlin

from

Jun Zhu

from Guangdong, China

Berlin, 2023

This work was performed between November 2017 and July 2022 under the supervision of Univ.-Prof. Dr. Kerstin G. Blank in the Mechano(bio)chemistry research group at the Max Planck Institute of Colloids and Interfaces and Prof. Dr. Petra Knaus at the Institute of Chemistry and Biochemistry at Freie Universität Berlin.

I hereby declare that I have prepared and written my dissertation “*Genetically Programmed Protein-based Hydrogels with Tunable Mechanical Properties*” independently. Furthermore, no sources and aids other than those indicated have been used. Intellectual property of other authors has been marked accordingly. I also declare that I have not submitted the dissertation in this or any other form to any other institution.

1st Reviewer: Prof. Dr. Petra Knaus

2nd Reviewer: Univ.-Prof. Dr. Kerstin G. Blank

Date of oral defense: 2024. 12th. Feb

Acknowledgements

First and foremost, I want to express my sincere gratitude to my supervisor, Univ.-Prof. Dr. Kerstin G. Blank, for her scientific and non-scientific guidance and support throughout the past years. As my expertise primarily lies in gene editing and protein expression, I had very little knowledge about material and polymer science when starting the project. Her patience and cross-disciplinary understanding opened my eyes to the fascinating realm of biological materials science. For me, the most essential thing I have learnt is to think critically. I also want to express my gratitude to Prof. Dr. Petra Knaus for accepting me as an external PhD student in her group. I acknowledge the “*Guangzhou Elite Scholarship Project*” for funding support.

I am deeply appreciative of all my colleagues from the Mechano(bio)chemistry research group for providing such a warm, welcoming, and international working atmosphere. Thank you all for your warm company, encouragement and patience. We had countless scientific discussions, interesting talks, and so many kinds of delicious cakes and desserts in the coffee corner. We also had a great time in many restaurants, international dinner evenings, and an amazing trip to Canada. I will always remember the times when we were together, no matter where I will go in the future. Thank you, Reinhild, Ayesha and Dr. Melis, you were always there when I was depressed. Thank you, Zeynep, for the help and suggestions with this thesis. Thank you, Geonho, for all the support with rheology. Thank you, Isabell, for your warm patience that always encouraged me to ask all my “stupid” questions. Your positive attitude impressed and refreshed me when I failed in experiments. Thank you, Russell and Eesha, for a lot of suggestions on the thesis so that I can be here.

I would also like to thank the technicians of the group, Reinhild Dünnebacke and Margit Rößner. Without your continuous efforts to organize everything effectively to keep the lab running smoothly, my daily research life would not have been so pleasant.

It was a struggle and tough for me during COVID times. With a lot of experimental work to complete, most of which was time-consuming, I was extremely anxious when I was stuck in Wuhan for four months. I had to go through quarantine and work from home in Germany. I am proud of myself for my unwavering dedication to my work, and I am grateful to all my Chinese friends in Golm for their support during those challenging times.

Lastly, I want to express my heartfelt gratitude to my parents and sister for their endless encouragement and love.

List of Publications

Jun Zhu, Geonho Song, Isabell Tunn, Ayesha Talib, Kerstin G. Blank;
Engineering protein-based star-polymers for hydrogel synthesis, *in preparation*

Table of Contents

Acknowledgements	V
List of Publications.....	VII
Table of Contents.....	IX
List of Abbreviations and Acronyms.....	XIII
List of Figures	XV
List of Tables.....	XVII
Summary	XIX
Zusammenfassung	XXIII
1. Introduction	1
1.1 Classification of hydrogels based on their source	1
1.1.1 Natural hydrogels	1
1.1.2 Synthetic hydrogels.....	2
1.1.3 Genetically engineered protein-based hydrogels.....	3
1.2 Rationally designed protein-based hydrogels	4
1.2.1 Random coil polypeptides	5
1.2.2 Chemical and physical cross-links	8
1.2.3 Network topology	12
1.3 Bottom-up control of hydrogel properties	15
1.4 Aims of this thesis	19
2. Materials and Methods	22
2.1 Gene design and cloning	22
2.1.1 DsRed variants.....	22
2.1.2 DsRed-ELP _n -SpyCatcher-His and DsRed-ELP _n -SpyTag-His.....	22
2.1.3 DsRed-X-A4 and DsRed-X-B4.....	23
2.2 Protein expression	24
2.2.1 DsRed variants.....	24

2.2.2	Expression of DsRed star proteins.....	25
2.2.3	Purification of ELP-containing fusion proteins.....	25
2.3.	Protein characterization	27
2.3.1	SDS-PAGE.....	27
2.3.2	MALDI-TOF.....	27
2.3.3	Dynamic light scattering.....	27
2.4	Hydrogel synthesis	28
2.4.1	DsRed-sPEG hybrid hydrogel.....	28
2.4.2	Hydrogels based on DsRed-ELP star proteins.....	29
2.5	Rheology	29
2.5.1	Time sweeps to measure hydrogel gelation time.....	30
2.5.2	Strain amplitude sweeps to determine the linear viscoelastic range..	31
2.5.3.	Rotational stress-strain experiment.....	31
2.5.4	Frequency sweep to determine the relaxation time.....	31
2.5.5	Step-strain experiment to probe self-healing.....	31
2.5.6	Rheo-optical measurements.....	32
2.6	Determination of SpyCatcher/SpyTag coupling efficiency	32
3.	Results	34
3.1	Suitability of DsRed as a tetrameric core for protein-based star-polymers	34
3.1.1	Experimental setup and design.....	34
3.1.2	Protein design, expression and purification.....	36
3.1.3	Protein characterization by SDS-PAGE and MALDI-TOF.....	38
3.1.4	Fluorescence spectroscopy.....	39
3.1.5	Hydrogel characterization.....	40
3.2	Chemically cross-linked DsRed-ELP star polymers	45
3.2.1	Experimental setup and design.....	45

3.2.2 Protein expression, purification and characterization.....	47
3.2.3 Synthesis and characterization of hydrogels.....	51
3.2.4 Influence of protein concentration and RCPP length on hydrogel properties.....	53
3.2.5 Determination of the fraction of SpyCatcher/SpyTag cross-links	58
3.3 Physically cross-linked DsRed-ELP_n star polymers (initial design)	60
3.3.1 Experimental setup and design.....	60
3.3.2 Protein expression, purification and characterization.....	61
3.4 Physically cross-linked DsRed-ELP₃ and DsRed-PAS₈ star polymers	65
3.4.1 Experimental setup and design.....	65
3.4.2 Expression and characterization of the redesigned CC fusion proteins	67
3.4.3 Self-healing test of a CC-cross-linked hydrogel	72
4. Discussion	74
4.1 Suitability of DsRed as a tetrameric core for protein-based hydrogels	74
4.2 Chemically crosslinked recombinant protein-based hydrogels	76
4.3 Physically crosslinked recombinant protein-based hydrogels	78
5. Conclusions and Future Perspectives	81
6. References	83
7. Appendix	98
S1. Amino acid sequences	98
S1.1 Sequences of the DsRed variants used in Chapter 3.1	98
S1.2 Sequences of the DsRed-ELP star proteins used in chapter 3.2	100

S1.3 Sequences of the DsRed-ELP star proteins used in chapter 3.3	103
S1.4 Sequences of the DsRed-ELP and DsRed-PAS star proteins used in chapter 3.4	105
S2. List of primers	108
S3. MALDI-TOF of the proteins used.....	109
S3.1 MALDI-TOF of the DsRed variants used in chapter 3.1	109
S3.2 MALDI-TOF of the DsRed-ELP star proteins used in chapter 3.2	111

List of abbreviations and acronyms

AFM	atomic force microscope
Abs	Absorbance
°C	degrees Celsius
CC	coiled coil
CD	circular dichroism
Cys	Cysteine
Da	Dalton
DLS	dynamic light scattering
DNA	deoxyribonucleic acid
DsRed	red fluorescent protein from <i>Discosoma</i> sp.
E	Young's modulus
ECM	extracellular matrix
<i>E. coli</i>	<i>Escherichia coli</i>
ELP	elastin-like polypeptide
FRET	fluorescence resonance energy transfer
G'	storage modulus
G''	loss modulus
His	Histidine
histag	sequence of 6 consecutive His residues for IMAC purification
IMAC	immobilized metal ion affinity chromatography
IPTG	isopropylthio- β -galactoside
LB	Luria-Bertani medium
LCST	lower critical solution temperature
LVE	linear viscoelastic (region)
M	mol L ⁻¹
Mal	Maleimide
MALDI-TOF	matrix-assisted laser desorption/ionization time-of flight
MW	molecular weight
OD ₆₀₀	optical density at a wavelength of 600 nm
Pa	Pascal
PAS	polypeptide consisting of proline, serine and alanine

PDB	protein data bank
PDB ID	protein data bank identification code
PEG	polyethylene glycol
PHA	Polyhydroxyalkanoate
PBS	phosphate-buffered saline
RCP	random coil polypeptide
SDS	sodium dodecyl sulfate
SDS-PAGE	sodium dodecyl sulfate polyacrylamide gel electrophoresis
sPEG	4-arm star-PEG
TB	terrific broth
TCEP	tris(2-carboxyethyl)phosphine
UV/VIS	ultraviolet-visible spectroscopy
WT	Wildtype

List of Figures

Figure 1. Classification of hydrogels based on different properties.

Figure 2. Structure of elastin-like polypeptides (ELPs).

Figure 3. Coiled coil structure.

Figure 4. Structure of the fluorescent protein DsRed.

Figure 5. Network structure with defects.

Figure 6. Bottom-up strategy for the design of hydrogels with controlled properties.

Figure 7. Schematic diagram illustrating the inverse transition cycle (ITC) method used for the purification of ELP-fusion proteins.

Figure 8. Preparation of DsRed-PEG hydrogels based on the thiol-maleimide reaction.

Figure 9. DsRed variants used in this project.

Figure 10. Experimental setup intended to probe a possible color change when DsRed tetramers dissociate as a result of the applied shear force.

Figure 11. Protein expression cassettes for the DsRed variants 3CY, 2CH, 2TH, 2THG.

Figure 12. SDS-PAGE analysis of the expressed and purified DsRed mutants.

Figure 13. Fluorescence excitation spectrum of the DsRed mutants, recorded at an emission wavelength of 620 nm.

Figure 14. Time sweep performed to monitor gelation after mixing DsRed 3CY and sPEG-Mal.

Figure 15. Amplitude sweeps of the DsRed(3CY)-Cys/sPEG-Mal hydrogel.

Figure 16. Rotational stress-strain experiment of the DsRed(3CY)-Cys/sPEG-Mal hydrogel.

Figure 17. Rheo-fluorescence setup.

Figure 18. Components of the SpyCatcher-SpyTag crosslinked hydrogel.

Figure 19. SDS-PAGE of all DsRed-ELP_n-SpyCatcher-His and DsRed-ELP_n-SpyTag-His proteins.

Figure 20. Dynamic light scattering of the DsRed-ELP₃ star proteins.

Figure 21. Spectroscopic characterization of the different DsRed-ELP star proteins.

Figure 22. Synthesis and properties of the DsRed-ELP₅-SpyCatcher-His/DsRed-ELP₅-SpyTag-His hydrogel.

Figure 23. Amplitude sweeps of SpyCatcher/SpyTag crosslinked hydrogels, highlighting the effect of different protein concentrations.

Figure 24. Amplitude sweeps of SpyCatcher/SpyTag crosslinked hydrogels, highlighting the effect of different RCPP lengths.

Figure 25. Frequency sweeps of DsRed-ELP₅-SpyCatcher-His/DsRed-ELP₅-SpyTag-His hydrogels, containing different protein concentrations.

Figure 26. SDS-PAGE to determine the coupling efficiency of SpyCatcher and SpyTag in the hydrogel.

Figure 27. Physically cross-linked hydrogel based on DsRed-ELP star proteins containing two different CC-forming peptides.

Figure 28. Expression cassettes for the star proteins His-DsRed(3CY)-linker-A4 and B4-linker-DsRed(3CY)-His.

Figure 29. Expression test of His-DsRed(3CY)-ELP_n-A4 and B4-ELP_n-DsRed(3CY)-His.

Figure 30. SDS-PAGE of the proteins His-DsRed(3CY)-ELP_n-A4 and B4-ELP_n-DsRed(3CY)-His.

Figure 31. Sequences of the CC-forming peptides.

Figure 32. Expression cassette with the general layout of the DsRed_C117T-ELP_n/PAS_n-CC-His proteins.

Figure 33. Visualization of protein expression for the DsRed_C117T-ELP_n/PAS_n-CC-His constructs.

Figure 34. SDS-PAGE of the DsRed_C117T-ELP₃-CC-His proteins.

Figure 35. Increase of DsRed fluorescence in BLR(DE3) expression cultures.

Figure 36. Comparison of the expression of DsRed_C117T-ELP₃-A4-His in BL21(DE3) and BLR(DE3).

Figure 37. Step strain experiment of the CC cross-linked hydrogel.

List of Tables

Table 1. Preparation of SpyCatcher-SpyTag cross-linked hydrogels.

Table 2. Overview of DsRed mutants.

Table 3. Yield and measured molecular weight (MW_{meas}) of the purified DsRed derivatives.

Table 4. Overview of DsRed-ELP star proteins with a SpyCatcher or SpyTag.

Table 5. Molecular weight of DsRed-ELP star proteins with a SpyCatcher or SpyTag.

Table 6. Total mass fraction of protein in the different SpyCatcher/SpyTag cross-linked hydrogels.

Table 7. Molecular weight and yield of the DsRed-ELP star proteins fused to the CC-forming peptides A4 and B4.

Table 8. Properties of the different DsRed(3CY)-ELP_n/PAS_n-CC-His fusion proteins.

Table 9. Comparison of the RCPP proteins ELP and PAS to PEG.

Summary

Hydrogels are widely used as biomaterials for cell culture and tissue engineering. They consist of natural biopolymers (e.g., collagen, elastin, hyaluronic acid) or synthetic polymers (e.g., polyethylene glycol, polylactic acid, polyacrylamide). The mechanical properties of hydrogels, such as stiffness, toughness and stress relaxation, depend primarily on the molecular building blocks and the spatial organization of polymeric network chains and cross-links (network topology). Star-shaped, 4-arm polyethylene glycol (sPEG) is a widely used hydrogel building block. sPEG displays a very low polydispersity and carries exactly one terminal cross-linking site per arm. As a result, almost ideal covalently cross-linked networks have been synthesized from sPEG building blocks. In this thesis, my goal was to replace sPEG with a purely protein-based, 4-arm polymer building block, based on the tetrameric fluorescent protein DsRed and random coil polypeptides (RCPP). This strategy allowed for the recombinant production of fusion proteins consisting of DsRed, RCPP and a covalent or dynamic cross-linking unit thus providing purely protein-based hydrogels. More importantly, it gives access to sequence-controlled RCPPs with an exactly determined number of monomer units per chain (i.e., monodispersity). Employing a modular gene design, the length of the RCPPs can be easily varied and also polymer lengths beyond commercially available sPEGs can easily be obtained.

In a first series of experiments, three different variants of DsRed were tested for their suitability to serve as the tetrameric core of the fusion proteins. Key criteria were their expression level in an *E. coli* expression system as well as their stability in a hydrogel network. The different variants were engineered so that they carry exactly one Cys residue per monomeric unit. The Cys residues were used to cross-link the DsRed proteins with maleimide-terminated sPEG to obtain a hydrogel network. After cross-linking, DsRed becomes the mechanically weakest link in the network and is expected to show force-induced dissociation when the hydrogel experiences strain. To probe possible pulling geometry effects,

Cys was introduced either at the C-terminus or at an internal, surface-exposed position. Hydrogels were formed for all tested DsRed variants whereas no cross-linking took place for a Cys-free mutant. A simple stress-strain experiment was performed where the fluorescence signal of DsRed was monitored in parallel. It has been proposed that a shift from red to green fluorescence may occur upon tetramer dissociation; however, no such change was observed over a large range of applied strains. These experiments suggest that DsRed possesses a high stability and is well suited as a tetrameric core.

Continuing with one DsRed variant, I genetically fused elastin-like polypeptides (ELPs) of controlled length to the C-terminus of the fluorescent protein. The fusion protein was further extended with either SpyCatcher or SpyTag to test the possibility of using this protein ligation system as a permanent covalent cross-link. I systematically varied the length of the ELP chain and tested the influence of this parameter on the resulting hydrogel properties, in combination with the total protein concentration. Rheology experiments show purely elastic behavior with a stiffness of around 10,000 Pa for the best hydrogel obtained (ELP length of 132 nm and protein concentration of 2 mM). This is a clear improvement over other protein-based hydrogels, which often show a stiffness less than 1000 Pa. The linear viscoelastic region scaled with ELP length, which is a clear indication that the hydrogels are indeed cross-linked via the terminal SpyCatcher/SpyTag fusion partners. Overall, these results show that purely protein-based hydrogels can be synthesized with a high level of molecular control, similar to what has already been obtained with sPEGs in other experiments.

For most cell culture applications, dynamically cross-linked hydrogels are of advantage. It has been shown that cells respond to the viscoelastic properties of the hydrogel and the presence of dynamic bonds further allows cell migration and proliferation. In the next step, I thus replaced the SpyCatcher/SpyTag system with reversible coiled coil (CC) cross-links. To prevent hydrogel formation during recombinant protein expression, a heterodimeric CC (AB) was used. In contrast

to the SpyCatcher/SpyTag system, expression and purification of these fusion proteins was more challenging. The DsRed-ELP-A fusion protein showed a low expression yield. DsRed-ELP-B had a strong tendency to aggregate, which most likely originated from the tendency of the B sequence to form homodimers. Preliminary experiments, where the B peptide was modified to reduce homodimer stability, did not show a significant improvement. Further optimization of the sequences is thus necessary before a sufficient amount of protein can be obtained for hydrogel synthesis.

The above results have shown that ELPs are excellent RCPPs for hydrogel synthesis; however, ELPs also undergo a phase transition in response to salt concentration and temperature. As a possible replacement for ELPs, I tested another protein-based repeat sequence, consisting of serine, alanine and proline. Even though this PAS sequence has already been used as a replacement for PEG in protein therapeutics, its application as a hydrogel building block is novel. Initial expression and purification tests with the fusion proteins DsRed-PAS-A and DsRed-PAS-B also show a low yield, even lower than for the corresponding ELP fusion proteins.

Overall, in this thesis I have tested several protein-based modules that can be used as tetrameric cores, random coil polymers and cross-linking modules for the synthesis of protein-based hydrogels. The results obtained from the above work show the potential of protein-based hydrogels but also highlight that it can be a challenge to obtain sufficient concentrations and overall quantities of the required fusion proteins. Despite the clear need for optimization of sequences and procedures, the building blocks introduced and tested will aid the future design of novel molecularly controlled hydrogels. Protein-based hydrogels are powerful candidates to serve as extracellular matrix mimicking, mechano-responsive networks with tunable mechanical properties.

Zusammenfassung

Hydrogele als Biomaterialien finden eine breite Anwendung in der Zellkultur und der Gewebezüchtung. Sie können aus natürlichen Biopolymeren (z. B. Kollagen, Elastin, Hyaluronsäure) oder synthetischen Polymeren (z. B. Polyethylenglykol, Polylactiden, Polyacrylamid) bestehen. Die mechanischen Eigenschaften der Hydrogele, wie beispielsweise Steifigkeit, Zähigkeit und Relaxation, hängen hauptsächlich von den Molekülbausteinen sowie der räumlichen Organisation der Netzwerkketten und ihrer Vernetzer ab (Netzwerktopologie). Das sternförmige, vierarmige Polyethylenglykol (sPEG) wird oft als Baustein für Hydrogele verwendet. sPEG weist eine geringe Polydispersität auf und besitzt genau einen Vernetzungspunkt pro Terminus. Unter bestimmten Bedingungen erlaubt dies die Synthese nahezu ideal vernetzter Hydrogele. Ziel dieser Arbeit war es, sPEG mit einem rein proteinbasierten, vierarmigen Baustein zu ersetzen. Dieser besteht aus dem tetrameren fluoreszierenden Protein DsRed sowie aus Polypeptiden ohne Sekundärstruktur (*random coil polypeptides* - RCPPs). Diese Strategie ermöglichte die rekombinante Herstellung von Fusionsproteinen, welche aus DsRed, RCPPs und kovalenten oder dynamischen Vernetzern bestanden, wodurch rein proteinbasierte Hydrogele realisiert werden konnten. Diese Vorgehensweise erlaubt die Herstellung monodisperser RCPP-Sequenzen mit modular Länge. Darüber hinaus können Polymerlängen erreicht werden, die über die von typischerweise verfügbaren sPEGs hinausgehen.

In einer Reihe von Experimenten wurden anfänglich drei verschiedene DsRed Varianten auf ihre Tauglichkeit getestet, als Tetramer im Kern der Fusionsproteine zu fungieren. Das Schlüsselkriterium hierfür war die Ausbeute in einem *E. coli* Expressionssystem sowie die Stabilität in einem Hydrogelnetzwerk. Die unterschiedlichen DsRed Varianten wurden so konstruiert, dass sie genau ein Cystein pro Monomer besitzen. Das Cystein wurde benutzt, um das DsRed-Protein an Maleimid-funktionalisiertes sPEG zu koppeln und somit die Vernetzung zwischen DsRed und sPEG herzustellen. Diese kovalente

Vernetzung macht die DsRed Tetramere zum mechanisch schwächsten Bindeglied im Netzwerk. Es wird daher erwartet, dass DsRed eine kraftinduzierte Dissoziation erfährt, wenn das Hydrogel einer mechanischen Spannung ausgesetzt wird. Um die Auswirkungen verschiedener Kraftangriffspunkte zu untersuchen, wurde das Cystein entweder am C-Terminus oder an einer internen, an der Oberfläche liegenden Position eingefügt. Mit allen getesteten DsRed Varianten konnten Hydrogele erhalten werden, während keine Vernetzung stattfand, wenn eine Cystein-freie Mutante verwendet wurde. Zusätzlich wurde ein einfaches Spannungs-Dehnungs-Experiment durchgeführt während das Fluoreszenzsignal von DsRed verfolgt wurde. Aufgrund der Struktur von DsRed wurde angenommen, dass bei der mechanisch-induzierten Dissoziation von DsRed Tetrameren eine Verschiebung der Fluoreszenz von Rot zu Grün stattfinden kann. Jedoch wurde eine solche Verschiebung auch bei großen Spannungen nicht beobachtet. Die Ergebnisse dieser beiden Experimente geben Grund zur Annahme, dass DsRed eine hohe Stabilität besitzt und deshalb als Kern für die Herstellung sternförmiger, protein-basierter RCPPs geeignet ist.

Anschließend wurde eine der DsRed Varianten benutzt, um diese gentechnisch mit einem Elastin-ähnlichem Polypeptid (*elastin-like polypeptide* - ELP) zu fusionieren. Dabei wurde das ELP mit genau kontrollierbarer Polymerlänge an den C-Terminus von DsRed angehängt. Das resultierende Fusionsprotein wurde entweder durch die SpyCatcher oder SpyTag Sequenz erweitert, um dieses System der Proteinligation als kovalenten Vernetzer zu etablieren. Die Länge der ELP-Ketten wurde systematisch variiert, um den Einfluss dieses Parameters auf die resultierenden Hydrogeleigenschaften zu untersuchen. Dabei wurde gleichzeitig auch die Gesamtkonzentration der Fusionsproteine verändert. Rheologieexperimente zeigten rein elastisches Verhalten mit einer Steifigkeit von ca. 10.000 Pa für das beste Hydrogel mit einer ELP-Länge von 132 nm und einer Proteinkonzentration von 2 mM. Dies ist eine deutliche Verbesserung im Vergleich zu anderen proteinbasierten Hydrogelen, die oft eine geringere

Steifigkeit als 1000 Pa aufweisen. Der Bereich der linearen Viskoelastizität hing von der ELP-Länge ab. Dieses Ergebnis ist ein deutlicher Indikator dafür, dass die Hydrogele tatsächlich über die SpyCatcher/SpyTag-Reaktion vernetzt sind. Insgesamt zeigen diese Experimente, dass ein rein proteinbasiertes Hydrogel mit einem hohen Maß an molekularer Kontrolle synthetisiert werden kann, ähnlich wie es schon mit sPEG realisiert wurde.

Für die meisten Zellkulturanwendungen sind dynamische Vernetzer von Vorteil. Zellen reagieren auf die viskoelastischen Eigenschaften von Hydrogelen und die Zellmigration und Proliferation wird entsprechend begünstigt. Demzufolge wurde im nächsten Arbeitsschritt das SpyCatcher/SpyTag-System mit reversiblen Coiled Coil (CC)-basierten Vernetzern ersetzt. Um während der rekombinanten Proteinexpression eine Gelbildung zu verhindern, wurde ein heterodimeres CC (AB) benutzt. Im Gegensatz zum SpyCatcher/SpyTag-System war jedoch die Ausbeute der Fusionsproteine nach Expression und Aufreinigung viel geringer. Das Fusionsprotein DsRed-ELP-A konnte nur in geringer Menge gewonnen werden. DsRed-ELP-B hatte eine starke Neigung zur Aggregation. Dies ist auf die Tendenz der B-Sequenz, Homodimere zu formen, zurückzuführen. Auch ein modifiziertes B-Peptid mit geringerer Homodimerstabilität brachte keine maßgeblichen Verbesserungen. Deshalb ist eine weitere Optimierung der Proteinsequenzen notwendig, damit zukünftig eine ausreichende Proteinmenge für die Hydrogelsynthese gewonnen werden kann.

Die obigen Ergebnisse haben gezeigt, dass ELPs exzellente RCPP-Bausteine für die Hydrogelsynthese darstellen. Abhängig von der Salzkonzentration und der Temperatur unterziehen sich ELPs jedoch einem Phasenübergang. Als möglichen Ersatz für die ELPs wurde deshalb eine weitere proteinbasierte, repetitive Sequenz bestehend aus Prolin, Alanin und Serin (PAS) getestet. Obwohl diese PAS-Sequenz bereits als PEG-Ersatz bei Proteintherapeutika verwendet wird, ist der geplante Einsatz als Hydrogelbaustein neu. Erste Expressions- und Aufreinigungsversuche der Fusionsproteine DsRed-PAS-A

und DsRed-PAS-B zeigen jedoch eine noch geringere Ausbeute als bei den ELP-basierten Fusionsproteinen.

Zusammenfassend wurden in dieser Arbeit verschiedene proteinbasierte Module getestet, die als Tetramerkern, Zufallsknäuelpolymer und Vernetzer für die Synthese von proteinbasierten Hydrogelen benutzt werden können. Die erzielten Resultate zeigen das Potential proteinbasierter Hydrogele auf, heben jedoch auch hervor, dass die Gewinnung einer ausreichenden Konzentration und Menge der erwünschten Fusionsproteine eine Herausforderung darstellen kann. Trotz des deutlichen Optimierungsbedarfs der Sequenzen und Methoden sind die hier eingeführten und getesteten Molekülbausteine eine vielversprechende Grundlage für die zukünftige Herstellung von proteinbasierten Hydrogelen.

1. Introduction

A hydrogel is a network of macromolecules, constructed of cross-linked polymer chains. These cross-links can either be chemical (i.e., covalent bonds) or physical (e.g., making use of hydrogen bonds, metal-coordination bonds or specific biological interactions). Hydrogels can absorb large amounts of water without dissolving. The first hydrogels, synthesized by Wichterle et al.¹ in 1960, were composed of a copolymer of 2-hydroxyethyl methacrylate and ethylene dimethacrylate. They were the first biomaterials created specifically for use in the human body.¹ Until now, there are more than 65,000 papers published related to hydrogels. An overview of different hydrogels in use today is shown in **Figure 1**.

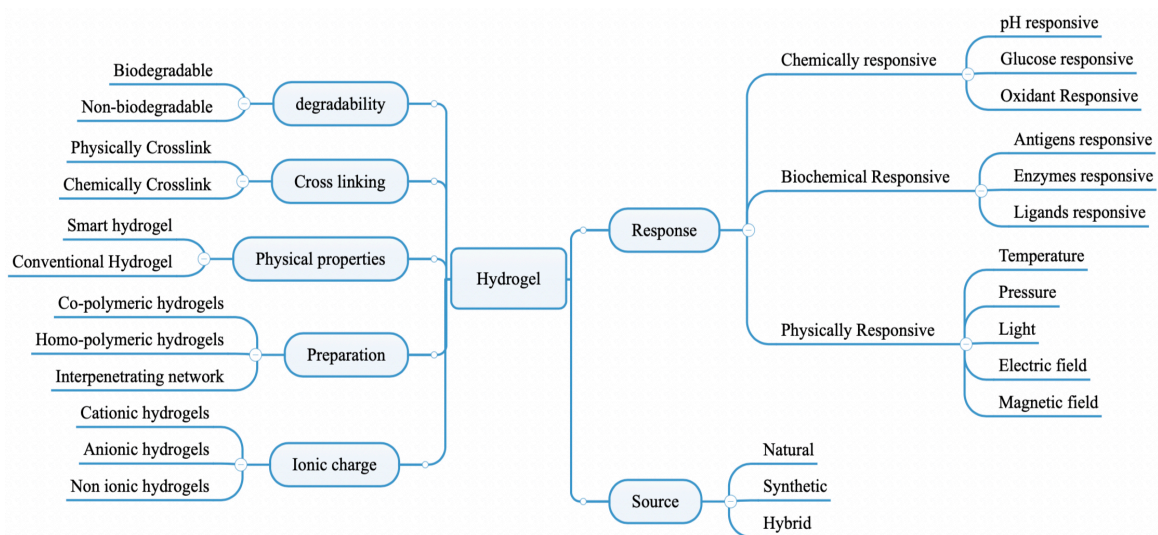


Figure 1. Classification of hydrogels based on different properties. Adapted from Ullah et al.² and redrawn in this thesis.

1.1 Classification of hydrogels based on their source

1.1.1 Natural hydrogels

Natural hydrogels are mainly made from natural sources, like collagen, hyaluronic acid, cellulose, chondroitin sulfate, starch and soy protein. Focusing on biomedical applications, natural hydrogels have a significant advantage for drug

delivery and tissue engineering applications.³⁻⁷ Natural hydrogels are biocompatible and biodegradable, and often inexpensive. At the same time, their relatively poor mechanical properties limit their range of applications. Purified from natural sources, the exact sequences and structures are often not defined. Especially the stochastic distribution of molecular weights restricts the capacity to link polymer structure, network properties and function. Natural hydrogels are also limited in their application due to their possible pathogen transmission and immunogenicity.

1.1.2 Synthetic hydrogels

Synthetic hydrogels were developed as a promising substitution of natural hydrogels. Polyethyleneglycol (PEG) and its copolymers, polyvinylpyrrolidone (PVP), polyacrylic acid (PAA) and its derivatives, polyvinyl alcohol (PVA), are examples of polymers usually used as the backbone of synthetic hydrogel networks. These chemically synthesized polymers are generally functionalized with reactive groups, which can be used for building covalent and/or non-covalent cross-links. The advantages of synthetic hydrogels are their ease of industrial manufacturing, chemical manipulation, and precisely regulated characteristics. This allows for the rational design of chemically synthesized polymer networks with specific physical properties. However, significant challenges also exist with chemically synthesized hydrogels. For example, synthetic polymers do not contain natural biological ligands, making it necessary to add bioactive peptides and biodegradable cross-links to allow for cell responsiveness. Synthetic hydrogels may further be toxic to cells due to the presence of residual monomers and non-reacted cross-links. To solve the existing challenges of synthetic hydrogels, recombinant protein-based hydrogels could be a promising substitution, as protein-based hydrogels can combine the advantages of both natural and synthetic materials,⁸ and avoiding most of the limitations.

1.1.3 Genetically engineered protein-based hydrogels

Protein-based hydrogels, consisting of genetically engineered proteins, represent novel biomaterials with a vast potential for biological applications.⁸ Through genetic engineering, exquisitely tailored protein/peptide molecules can be obtained. For example, Lapenta et al.⁹ designed origami CC proteins that fold into various, preprogrammed shapes. Zhang et al.¹⁰ successfully rewired the SpyTag-SpyCatcher protein ligation system¹¹ in order to generate rationally planned circular proteins and branched topologies.

The above examples show that recombinant DNA technology can be employed to engineer multifunctional proteins for use as material building blocks. Protein building blocks that equip a material with desired functionalities include tailored physical cross-links, bio-instructional ligands (e.g., RGDS sequence), and fluorescent proteins. Also, stimuli-responsive proteins are attractive building blocks. Typical examples are elastin, which is sensitive to temperature and ion concentration, or light- and pH-sensitive fluorescent proteins.

Depending on the structure of protein-based material building blocks, they can fulfill different functions in protein-based hydrogels. Random coil-like proteins, such as ELPs, can serve as the polymer backbone of a hydrogel network that is then appended with other functional units. Proteins that self-assemble into oligomers can act as cross-links with tunable stability and thermally switchable dynamic properties. Depending on the type of cross-link, the cross-link assembly state and the thermodynamic, kinetic and mechanical stability, a wide range of material properties can be obtained.¹²⁻¹⁹ The molecular mechanical properties of hydrogel building blocks also determine the macroscopic mechanical response to deformation.²⁰

Compared to the overall large number of publications on hydrogels, the number of genetically engineered protein-based materials is still small. Examples include hydrogels with tunable viscoelastic properties,²¹ ion sensitivity or light-responsiveness.²² Considering their potential, it is expected that the area of recombinant protein-based hydrogels will grow in coming years. Just as natural hydrogels, protein-based hydrogels have the potential to better mimic the *in vivo* extracellular matrix, which controls cell behavior,²³ e.g., cell adhesion, proliferation, and differentiation. Thanks to the high precision of recombinant protein synthesis, protein-based hydrogels can be designed to incorporate a variety of bio-instructional ligands. Exploring the wide range of possible material building blocks, these hydrogels can further be engineered to exhibit mechanically adaptable properties similar to native tissues and can contain proteolytic target sites for cell-triggered scaffold modification.

1.2 Rationally designed, recombinant protein-based hydrogels

Currently, most reported protein-based hydrogels are soft or brittle. Their rupture stress is often below 1 kPa and the yield strain is less than 100%. These mechanical properties are inferior when compared to natural and hybrid hydrogels. The poor mechanical properties of protein-based hydrogels typically originate from an inhomogeneous network, weak cross-links, and the absence of material building blocks that facilitate energy dissipation. In defective networks, stress is quickly transmitted and concentrates at the weakest cross-links. Subsequently, the defects grow and the hydrogel cracks. In order to develop extensible and tough protein-based hydrogels, it is crucial to develop strategies for the synthesis of more homogeneous networks,²⁴ to utilize and engineer the dynamic properties of the cross-links,²⁵ and to include elements with hidden

length (e.g. folded protein domains) that can reversibly unfold for energy dissipation.

The available literature on protein-based hydrogels mentions a still relatively small number of different protein and peptide building blocks that are suitable for the assembly of protein hydrogels. These include RCPPs, chemical and physical cross-linking units as well as folded protein domains. RCPPs are ideally suited as monodisperse random coil mimics of synthetic polymers. RCPPs can be fused to terminal or internal cross-linking units, based on oligomeric proteins or protein-ligation systems. Folded protein domains can further be inserted into the recombinant construct to provide hidden length. A selection of possible RCPPs and cross-linking units is introduced in the following, with a special focus on those relevant for this thesis.

1.2.1 Random coil polypeptides

Frequently used RCPPs are ELPs,^{26–31} XTEN^{32,33} and PAS polypeptides,^{34–36} gelatin-like polypeptides (GLKs),³⁷ as well as resilin-like polypeptides.³⁸ ELP is a polypeptide derived from the mammalian ECM. It is made up of consistent repeat units with the sequence (VPGXG)_n. The guest residue, denoted by the letter 'X', is frequently valine (Val, V). The X position can, however, accommodate any amino acid, except proline. Changing the guest residue significantly affects the physicochemical characteristics of the resultant protein, making it a critical parameter for ELP design.^{39,40} Other substitutions, in addition to the guest residue, cause significant changes in macromolecular characteristics. One possible modification is the substitution of glycine (Gly, G) in the third position of the repeat sequence for alanine (Ala, A) to yield (VPAXG).⁴¹ Tarakanova et al.⁴² reported a virtual library of ELPs. All-atom replica exchange molecular dynamics simulations were used to investigate the connection between atomic and macroscopic

characteristics of an ELP-based hydrogel. This computer methodology can discover empirically relevant sequences. The basic unit of the used ELP was VPGXG. The molecular structure was identified by Urry et al.²⁷ and is shown in **Figure 2**.

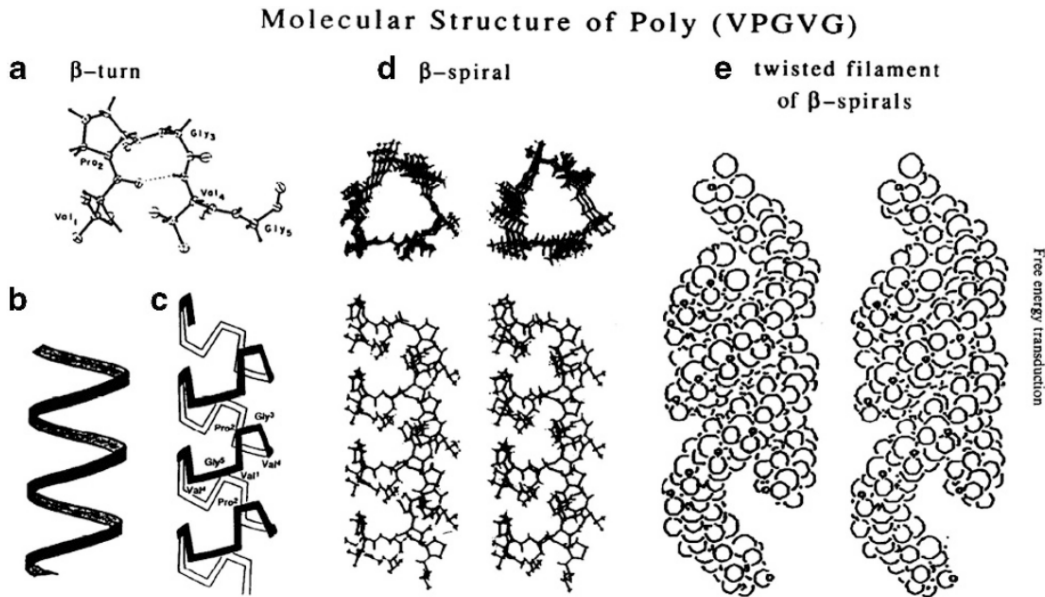


Figure 2. Structure of elastin-like polypeptides (ELPs). The basic repeat unit was VPGXG. At different temperatures, the helical structure can twist into filaments of several β -spirals. Reproduced with the permission from Urry et al.²⁷ Copyright (1992) Elsevier.

The PAS and XTEN polypeptides are closely related. XTEN sequences were originally introduced by Schellenberger et al.³² in 2009. They contain a random, non-repetitive sequence of the amino acids alanine, glutamic acid, glycine, proline, serine and threonine and were optimized for high expression yields in *E. coli*. XTENS were developed as a novel non-structured polypeptide with the goal of replacing PEGylated proteins in pharmaceutical applications.³³ In the meantime, a range of XTENS with different lengths and amino acid sequences are available.

PAS sequences only contain proline, alanine and serine, after elimination of negatively charged glutamic acids, β -sheet preferring threonine and poorly soluble glycine. These three amino acids can be arbitrarily dispersed within a 20- or 24-amino acid repeat sequence to create PAS polypeptide with lengths over 200 amino acid residues.⁴³ Depending on the fraction of proline, structures with varying α -helix, polyproline-II helix or random coil content can be obtained. PAS polypeptides are extremely hydrophilic and conformationally disordered, resulting in a large hydrodynamic volume. As a result, PAS sequences are considered to be an excellent replacement for PEG. Because of its uncharged, random coil structure, it displays comparable biophysical activity. PASylation endows pharmacologically active proteins and peptides with the same favorable properties as PEGylation with the added benefit of traceless metabolization of its natural amino acid constituents.³⁴ PAS-fused proteins were shown to be highly soluble, and have the potential to improve the yield of synthesized fusion proteins. Until now, PAS polypeptides have never been used to form a hydrogel.

GLK polypeptides were constructed by exchanging all hydrophobic residues in collagen while keeping the (Gly-Xaa-Yaa)_n repeat sequence.³⁷ As GLKs have a more open and unfolded structure than collagen, they can also be used as a PEG alternative for the modification of pharmaceutically active proteins.

Natural resilins are rubber-like proteins that are found in various body parts of arthropods. Resilin has advantageous mechanical properties like high resilience, low stiffness and effectual energy storage.³⁸ Genetically synthesized resilin-like polypeptides (RLPs) possess similar properties as native resilin. RLPs are also attractive candidates for designing mechanically engineered biomaterials.

1.2.2 Chemical and physical cross-links

Both chemical and physical cross-links have been implemented in recombinant protein-based hydrogels. Chemical cross-links form a permanent covalent bond and the resulting network is elastic. In contrast, physical cross-links form a dynamically reversible non-covalent bond. These bonds open and close on the timescale of a typical experiment and the hydrogel is viscoelastic, displaying stress relaxation. The relaxation timescale depends on the thermodynamic and kinetic properties of the cross-links and on network topology. When a shearing or compression force is applied to a hydrogel network, it is transmitted along the polymer chains to the cross-links. In the case of a physically cross-linked network, the cross-links are the weakest mechanical link in the network and may respond to the applied force first. Engineering cross-link properties is thus a highly powerful strategy to tune the linear and non-linear viscoelastic properties of hydrogels. In the following the cross-links used in this thesis will be introduced. These include the SpyCatcher/SpyTag protein ligation system that forms a chemical cross-link.^{11,44–48} As physical cross-links, two different proteins with either a heterodimeric or tetrameric assembly state are used.

Howarth and coworkers^{11,44,45,47} have designed a glue-like protein-peptide pair (SpyCatcher and SpyTag) that is increasingly employed for protein labelling and immobilization. The SpyCatcher-SpyTag pair originates from the fibronectin-binding protein (FbaB) of *Streptococcus pyogenes*. One domain of this bacterial adhesin forms a naturally occurring isopeptide bond between Lys₃₁ and Asp₁₁₇.⁴⁹ Splitting this domain into SpyCatcher (Lys₃₁) and the short peptide SpyTag (Asp₁₁₇) has generated a highly powerful, specific protein-ligation system where the two components spontaneously bind and create an intermolecular isopeptide bond during the process. SpyCatcher and SpyTag technology is a powerful means to covalently link two fusion proteins and also allows for the easy synthesis

of branched proteins.¹⁰ Recently, also the mechanical stability of the covalently connected SpyCatcher-SpyTag pair has been characterized by single-molecule force spectroscopy, using different force applications points.⁵⁰ In recent years, the SpyCatcher-SpyTag pair has also become a frequently employed chemical cross-link in recombinant protein-based hydrogels.^{21,22,31,31,51–53}

To obtain physical cross-links, oligomeric proteins are desired that self-assemble into a defined structure stabilized by hydrogen bonds, ionic bonds, and hydrophobic interactions. The reversible association and dissociation of protein-protein interactions determines network stress relaxation and allows self-healing and energy dissipation. The properties are important for the development of *in vitro* cell culture systems and tissue engineering applications. In this work, coiled coil (CC) heterodimers and the tetrameric fluorescent protein DsRed were used as physical cross-links.

CCs are common protein motifs found in natural proteins that frequently play a mechanical role, such as in myosin or fibrin. CCs are frequently employed as programmable hydrogel cross-links and as fiber forming peptide building blocks. CCs are superhelices composed of two or more α -helices wrapped around each another.⁵⁴ Self-assembly is based on a repeating sequence of seven amino acids $(abcdefg)_n$, known as heptad. The oligomerization interface of the CC consists of hydrophobic amino acids located in the *a* and *d* positions of each heptad. Charged amino acids, placed in the *e* and *g* positions, contribute electrostatic interactions. Because they are interchangeable, the solvent-exposed locations *b*, *c*, and *f* are ideal targets for modifications (**Figure 3**).

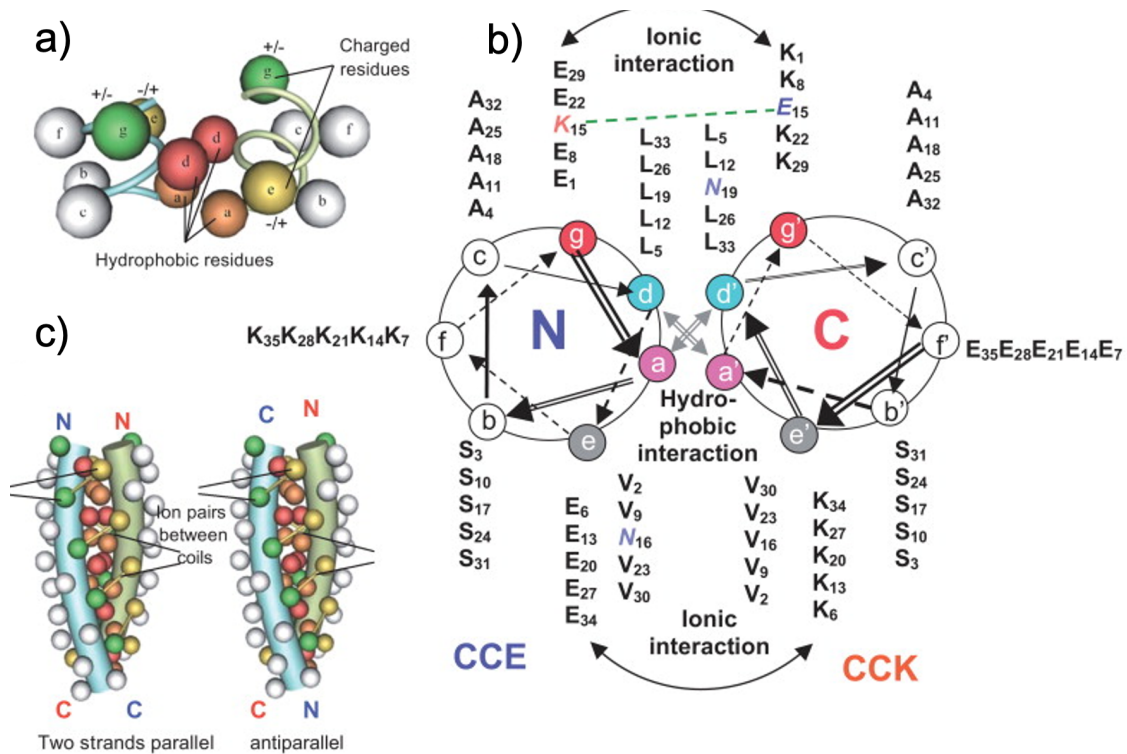


Figure 3. Coiled coil structure. a) Position of amino acids in the hydrophobic core of a CC dimer. b) Helical wheel representation of an exemplary antiparallel CC heterodimer. c) Diagram depicting the parallel or antiparallel orientation of the two helices in a CC dimer. The cartoons are adapted from www.ocw.mit.edu/NR/rdonlyres/Biology.

The DsRed protein^{55–57} is a tetrameric red fluorescent protein derived from *Discosoma genus* corals (**Figure 4**). In these tetramers, two types of interfaces were discovered: the first is characteristic of many high-affinity protein-protein interaction surfaces (AC interface) and is comprised of hydrophobic residues surrounded by polar residues; the second is almost entirely composed of polar and charged residues (AB interface). The interfaces between the tetramer subunits are symmetrical. Contacts between the same amino acid sequences of two subunits constitute each interface. The overall tetramer structure resembles a dimer made up of dimers. Dimers first establish a hydrophobic AC interface and then two dimers connect to generate a highly charged AB(CD) interface. As a

result, changes in the hydrophobic AC interface improve tetramer assembly.⁵⁸ It is assumed that the DsRed tetramer is more stable than the other physical CC cross-link used in this work.^{59,60} This assumption is based on single-molecule force spectroscopy experiments of the streptavidin tetramer, which showed that forces of ~300 pN were required for the unfolding of this tetramer.⁶¹

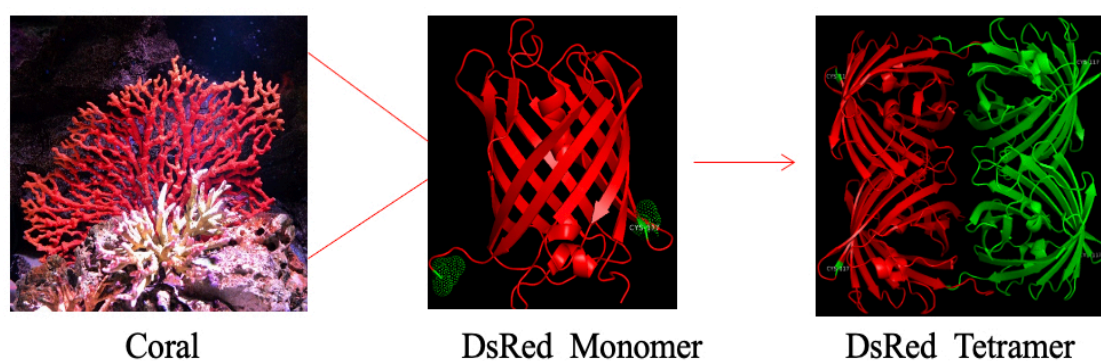


Figure 4. Structure of the fluorescent protein DsRed. The tetrameric protein originates from *Discosoma genus* coral. The monomer is a GFP-like protein, consisting of 11 β -strands. Four monomers assemble into a dimer of dimers. The DsRed tetramer (PDB ID: 1GGX) frequently contains of a mixture of green- and red-fluorescent chromophores. Due to intermonomer FRET, only red fluorescence is usually measured. The picture of the coral is taken from <https://www.alamy.de/blume-sea-living-red-coral-reef-wachst-an-den-felsen-unterwasserwelt-unterwasser-ocean-image255271179.html>

DsRed is a red fluorescent protein that has been studied as a reporter for *in vivo* and *in vitro* imaging applications. It has been shown that the DsRed tetramer consists of a mixture of monomers with different chromophores with absorbance at 450 nm and 580 nm.⁶² Both chromophores are fluorescent and the distance between them allows Förster resonance energy transfer (FRET). It is thus likely that detectable fluorescence is only emitted from the chromophore with the longer absorbance and emission maximum. When the DsRed structure dissociates into dimers or monomers, a “color change” may be observed as FRET is no longer possible. One may speculate that DsRed disassembly, e.g., induced by

mechanical rupture, may be detectable when recording the relative number of photons emitted from the two chromophores. DsRed may thus be developed into a mechanosensitive molecule that can report on its assembly state.

1.2.3 Network structure and topology

The macroscale characteristics of hydrogel networks are determined by the properties of their molecular building blocks, e.g., the architecture and length of polymer chains between cross-links and the stability of their physical cross-links. These properties directly and indirectly affect network structure and topology. In addition, also defects play an important role. The significance of network topology was demonstrated for the first time by Flory in his theory of rubber elasticity.⁶³ The developed theory was based on the assumption of an idealized, defect-free network. The complexity of real networks is shown in **Figure 5**.

In the past two decades, tremendous effort has been made to control network synthesis and to eliminate defects. In 2008, Sakai et al.⁶³ created a covalently cross-linked hydrogel, composed of sPEG. Two different sPEG macromonomers were used as building blocks. One sPEG was amine-terminated while the second one carried N-hydroxysuccinimide-glutarate functional groups. Mixing the two building blocks in a 1:1 molar ratio under optimized conditions yielded a nearly ideal network structure with impressive homogeneity, as proven with small-angle neutron scattering. The hydrogel also showed excellent mechanical stiffness up to 2.5 MPa.

Until now, only a very small number of structurally similar, highly ordered networks based on tetrameric protein building blocks have been fabricated. For example, the tetrameric ubiquitin-like domain (ULD) from the special AT-rich sequence binding protein was used as a tetrameric hub-like-core.^{64,65} To allow cross-linking, the core protein was appended with the PDZ domain protein TIP-1

and a PDZ-binding peptide.⁶⁴ As no RCPP linkers were used between the tetrameric core and the TIP-1 – peptide cross-links, the hydrogel showed poor stiffness (~10 Pa).

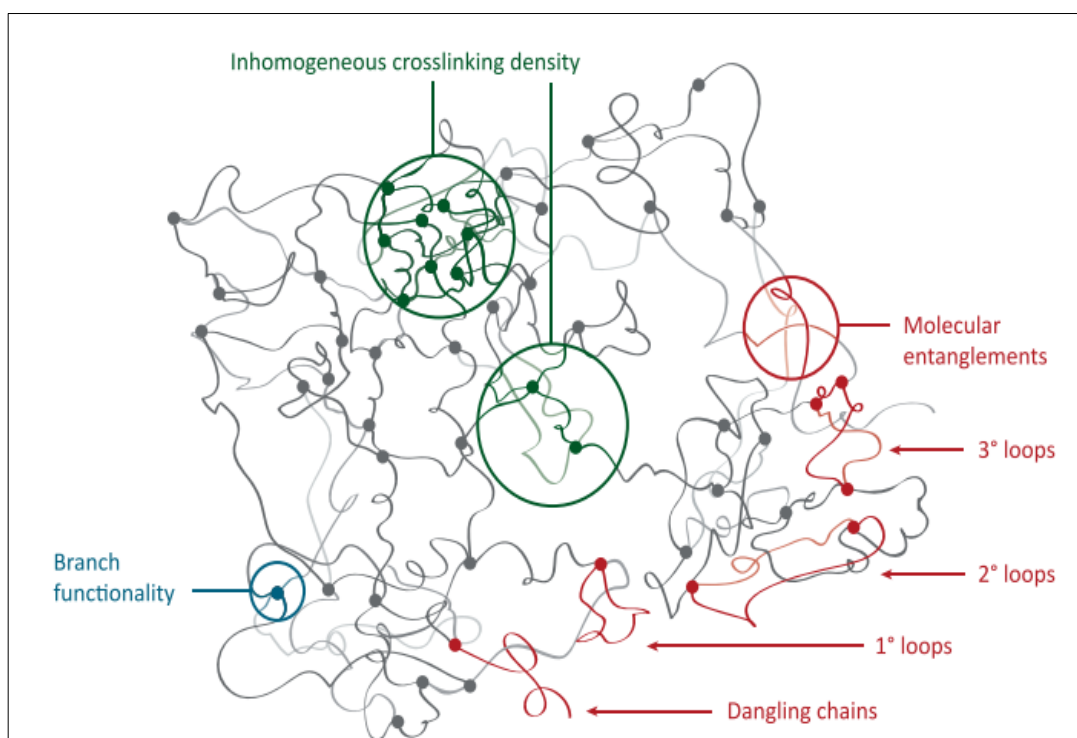


Figure 5. Network structure with defects. The topological structure of a polymer network is described as linking points (junctions) and connections (chains). Inhomogeneities exist on the 10 to 100 nm length scale (shown in green). These are caused by concentration fluctuation during network synthesis. At the 1 to 10 nm length scale, defects are introduced at the macromolecular level (shown in red). Unreacted functional groups cause dangling network chains and loops act as mechanically inactive network chains. Branch functionality (shown in blue) is the primary topological structure of importance below 1 nm, describing the maximum number of network chains linked to a network junction. Reproduced with permission from Gu et al.⁶⁶ Copyright (2019) Elsevier.

Another tetrameric core design is making use of the spontaneous self-assembly of split-GFP.²² Using split-GFP, two N-termini and two C-termini are available that

were fused to SpyCatcher to obtain (SpyCatcher)₄GFP. In this case, an ELP sequence with 15 pentapeptide repeats was inserted between GFP and the SpyCatcher domains. As the second component, the bifunctional protein SpyTag-ELP-RGD-ELP-SpyTag or the trifunctional protein SpyTag-ELP-SpyTag-ELP-SpyTag were used. The resulting hydrogel networks displayed a storage modulus between 200 and 500 Pa when using the bifunctional protein. The storage modulus increased to values between 500 and 800 Pa for the trifunctional protein.

Instead of making use of splitGFP, the tetrameric fluorescent protein DsRed can also serve as a core protein.⁶⁷ It was fused to the RCPP sequence (AGAGPEG)₁₀ and appended with a CC to achieve cross-linking. The resulting hydrogels had a storage modulus slightly above 1000 Pa. A possible drawback of this design is the use of a CC homodimer, which may already assemble on the same DsRed core and thus not contribute to cross-linking.

Again making use of the RCPP sequence (AGAGPEG)₁₀, a streptavidin-based tetrameric core protein was engineered and different cross-linking units were compared.⁶⁸ These included the SpyCatcher-SpyTag system, a homodimeric CC or tyrosine for photo-cross-linking. Depending on the cross-link used different storage moduli were obtained. While the CC and photo-cross-linked networks displayed storage moduli >1000 Pa, a very weak hydrogel (<10 Pa) was obtained for the SpyCatcher-SpyTag cross-linked network. This has been explained with fast cross-linking kinetics, which causes highly inhomogeneous hydrogels.

The above proteins have a thermodynamically stable tetrameric structure. In another example, a stimulus-responsive tetrameric protein was used.⁶⁹ The protein CarH_C is a light-responsive protein that is derived from a bacterial transcriptional regulator. CarH_C is initially monomeric but assembles into

tetramers when binding its cofactor AdoB₁₂ in the dark. AdoB₁₂ contains a cobalt cofactor that is sensitive to green light. When exposed to green light, cleavage of the photolabile C-Co bond causes disassembly into monomers. CarH_C was C-terminally fused to an ELP sequence (15 pentapeptide repeats) and a histag. The histag was used for cross-linking with the transition metal ions Cu²⁺, Ni²⁺, Zn²⁺ and Co²⁺. In all cases, storage moduli of approximately 1000 Pa were obtained. The hydrogels were used to encapsulate cells, which could be released upon light exposure to disassemble the hydrogel.

The above examples highlight a number of possible building blocks that partially also inspired this work. At the same time, the examples also show that highly similar networks (e.g., using the same cross-linking modules) can yield hydrogels with very different viscoelastic properties. This suggests that the parameters that determine the formation of well-controlled networks are not always controlled and may also not always be known. A more systematic approach is thus necessary to identify which molecular properties need to be controlled to achieve desired network properties.

1.3 Bottom-up control of hydrogel properties

One key goal of current hydrogel research is to link molecular properties, network topology and macroscopic properties with the ultimate goal to achieve the controlled bottom-up design of hydrogels with controlled linear and non-linear viscoelastic properties. This includes stiffness, toughness, relaxation time and failure properties. Reaching this goal requires building blocks with controlled structure (e.g., polymer length, cross-link assembly state) and known thermodynamic, kinetic and mechanical properties. In the case of physical cross-links, their thermodynamic and kinetic parameters affect material properties in the LVE range. At the same time, non-linear properties, e.g., failure, are determined

by the mechanical properties of the building blocks. Mechanical engineering of proteins with customized nanomechanical characteristics has made significant progress due to the development of single-molecule force spectroscopy (SMFS). For example, Wu et al.²⁰ calibrated three individual proteins (soft, rigid, strong) using SMFS. When incorporated into a hydrogel, the bulk hydrogel behavior could be related to the mechanical properties of the building blocks (**Figure 6**).

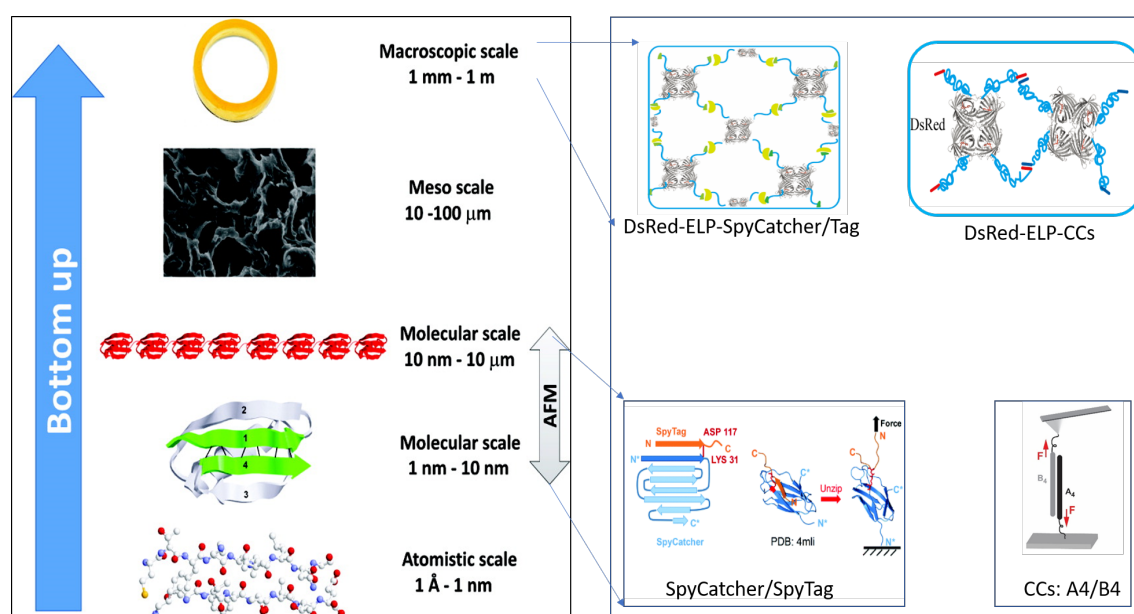


Figure 6. Bottom-up strategy for the design of hydrogels with controlled properties. **Left:** A protein-based hydrogel building block was designed at the genetically level. The bio-synthesized protein was mechanically characterized using AFM-based single-molecule force spectroscopy. The resulting mechanical properties of the hydrogel can be determined at the macro-level, e.g., using rheology or tensile testing. **Right:** The mechanical properties of the SpyCatcher-SpyTag pair as well as the heterodimeric CC A4B4 were studied at the molecular level and are employed here as hydrogel building blocks. The left figure is adapted from Li et al.⁷⁰ Copyright © 2010, American Chemical Society. The right figure (SMFS of SpyCatcher/SpyTag and A4B4) was adapted from Guo et al.⁵⁰ Copyright. 2021, RSC Pub and Lopez-Garcia et al.⁷¹ (CC BY-NC 4.0).

Within a hydrogel network, each polymer chain plays a significant role in averaging, transmitting, and distributing local fluctuations. Network properties depend on chain length and architecture, polymer concentration as well as cross-link properties and density. These in turn affect network connectivity and the presence and number of entanglements. For example, Norioka et al.⁷² demonstrated that lowering the concentration of cross-links while increasing the mass of polymer in the network increased the number of entanglements and, as a result, the toughness. Grindy et al.⁷³ synthesized sPEG networks with terminal imidazole functional groups. Cross-linked with different transition metal ions, they showed that the binding strength of the imidazole-metal coordination bond directly affected the viscoelastic network properties. This is only the case, however, as long as the network topology is not altered. This was subsequently demonstrated with 3,4-dihydroxyphenylalanine (DOPA)-terminated sPEG, which was either cross-linked with Fe³⁺ ions or iron oxide nanoparticles.¹⁷ In the case of Fe³⁺ ions (low cross-link functionality), much faster network relaxation was observed than in the case of the nanoparticles (high cross-link functionality).

Our group is primarily focusing on protein and peptide-based cross-links with controlled molecular properties. Using a library of thermodynamically, kinetically and mechanically characterized heterodimeric CCs,^{18,59,60,71,74} it has been shown that the network relaxation time scales with the thermodynamic stability of the CCs. Cross-links with a higher thermodynamic stability yield hydrogels with a longer relaxation time,¹⁸ similar to the results described above for metal coordination cross-links.⁷³ Also in the case of CC cross-links, this correlation is only true as long as the network topology is not affected.

Even though progress is made with establishing such correlations, the field still lacks highly defined, monodisperse polymer building blocks, tunable cross-links as well as methods to determine and visualize the network topology. Also,

building blocks with known and tunable dynamic mechanical properties are still rare. Engineered protein building blocks fulfil all these criteria. Their potential as hydrogel building blocks is increasingly recognized, especially when considering that these proteins might also be used as new mechanical elements, such as fluorescence-based force sensors,⁷⁵ or mechanically tunable biocatalysts.^{76,77}

1.4. Aims of this thesis

Tuning the linear and non-linear viscoelastic properties of hydrogels is key to using these materials as ECM mimics for cell culture and tissue engineering applications. Current research mostly focuses on natural hydrogels or hybrids made from synthetic and natural building blocks. Recombinant protein-based hydrogels are rarely studied even though first examples highlight the potential of these materials. In this thesis, I am introducing a tetrameric protein building block that is intended to mimic and replace sPEG, thus principally allowing the synthesis of ideal protein-based hydrogels. This building block consists of the tetrameric fluorescent protein DsRed, genetically fused to either ELP or PAS sequences of different length. These RCPPs are further equipped with a chemical cross-link (SpyCatcher-SpyTag) or physical cross-link (heterodimeric CC A4B4). Using this combination of building blocks, my goal was to answer the following questions:

i. Is DsRed a suitable tetrameric core for protein-based star-polymers?

DsRed is an excellent candidate to serve as a tetrameric core unit for protein-based star-polymers. To be a suitable building block, the protein needs to express in a high yield in a suitable expression system (*E. coli*). It further needs to remain functional when coupled or fused to random coil polymers and the structure needs to be thermodynamically, kinetically and mechanically stable in the hydrogel network. Different variants of DsRed were expressed with one Cys per monomer and tested for their suitability to serve as a hydrogel building block. They were reacted with Mal-terminated sPEG and the properties of the resulting hydrogel networks were determined.

ii. Can the elastic properties of protein-based hydrogels be rationally tuned when using DsRed-ELP star-polymers?

Chemically synthesized sPEGs have inherent polydispersity. In contrast, recombinantly produced protein-based polymers are monodisperse. The DsRed core was thus fused to ELP to obtain a DsRed-ELP star protein. These protein stars were chemically cross-linked using the SpyCatcher-SpyTag protein ligation system. The possibility to tune network properties was explored using ELPs of different length as well as different protein concentrations. After cross-linking, the stiffness as well as the LVE range were determined with rheology to correlate the molecular characteristics with the material properties. In addition, an attempt was made to quantify the cross-linking efficiency via SDS-PAGE.

iii. Can the viscoelastic properties of protein-based hydrogels be rationally tuned when using DsRed-ELP star proteins?

To switch from chemically cross-linked networks to physically cross-linked networks, the SpyCatcher-SpyTag protein ligation system was replaced with a heterodimeric CC. CC-based physical cross-links provide additional tunability when making use of the wide range of available CC sequences with different thermodynamic, kinetic and mechanical properties as well as oligomerization states. The CC A4B4 has already been extensively characterized. Different derivatives exist that have also already been used to cross-link sPEG. Here, the first goal was to establish an expression and purification protocol for the respective fusion proteins, followed by characterization with rheology to determine the relaxation time and self-healing properties of the hydrogel network.

iv. Can the ELP sequence in the DsRed star proteins be replaced with a PAS polypeptide?

PAS sequences were designed to replace PEG in PEGylated protein therapeutics. PAS polypeptides have been optimized for high solubility in aqueous environments and for high-level expression in *E. coli*. However, PAS has never

been investigated as an RCPP for hydrogel synthesis. This inspired me to test the PAS sequence as an ELP replacement for the recombinant production of DsRed-based star proteins. The last goal of this work was thus to test if replacing ELP with PAS improves the protein yield or alters hydrogel properties.

Overall, focusing on the above questions, I aim to expand the range of building blocks for the fabrication of recombinant protein hydrogels. With the ultimate goal of correlating and predicting network properties in a bottom-up approach, a library of characterized and tunable molecular building blocks is needed. Such a modular toolkit will ultimately also allow the recombinant expression of bioactive, self-healing and stimuli-responsive hydrogels for applications in cell biology and tissue engineering.

2. Materials and Methods

2.1 Gene design and cloning

2.1.1 DsRed variants

Goal of the first series of experiments was to test the expression level of two variants of DsRed. The DsRed.T3 variant^{55,56} has one Cys per monomer that I intended to use for site-specific coupling to Mal-terminated sPEG. A histag for purification purposes was C-terminally fused to this variant, which is termed 3CY in the following. In the second variant to be tested, DsRed-Express2,⁵⁷ this Cys is mutated to threonine (TH2). To compare this variant to 3CY, a mutant was generated that contained Cys in the respective position (2CH). To additionally test the influence of the position of the Cys residues on protein expression and coupling efficiency, another mutant was generated where Cys was located at the C-terminus after the histag instead. The protein sequences are shown in the **appendix S1**. The corresponding DNA sequences were optimized for *E. coli* codon usage and appended with a 5' NcoI and a 3' HindIII restriction site for cloning into the expression vector pET28a (Merck Millipore). Gene synthesis was performed by Eurofins Genomics. The genes were received in a pEX cloning vector and subcloned into pET28a via the above-mentioned restriction sites. Standard restriction cloning protocols were followed. *E. coli* XL1-blue (Agilent Technologies) was used for all transformations.

2.1.2 DsRed-ELP_n-SpyCatcher-His and DsRed-ELP_n-SpyTag-His

To obtain gene constructs coding for DsRed-ELP_n-SpyCatcher-His and DsRed-ELP_n-SpyTag-His star proteins, two master plasmids were prepared first. The master plasmids contained the DsRed(3CY) sequence, followed by a short linker and the SpyCatcher or SpyTag sequence. The corresponding protein sequences

DsRed-linker-SpyCatcher-His and DsRed-linker-ST-His are shown in **appendix S1.2**. The codon optimized genes were again obtained from Eurofins Genomics and subsequently cloned into BglI-free pET28a (see below). The linker contains the restriction sites BamHI and BglI that allow for the insertion of four different ELP sequences (see **appendix S1.2** for details). The shortest ELP₃ sequence was obtained via gene synthesis (BioCat GmbH). The longer sequences, ELP₅, ELP₉ and ELP₁₂, were a gift from Prof. Dr. Michael Nash (University of Basel).⁷⁸ Correct insertion of the ELP_n sequences was confirmed by sequencing, using the primers T7 and T7term (see **appendix S2**).

As the plasmid pET28a contains a BglI site, this restriction site was removed to avoid the need for performing a three-fragment ligation. To do so, pET28a was cut with BglI and the linearized fragments were purified. Single strand overhangs were digested with mung bean nuclease (New England Biolabs), following the protocol provided by the manufacturer. The resulting DNA with blunt ends was re-ligated and transformed into *E. coli* XL1-blue. The plasmid was purified and the removal of the restriction site was confirmed with DNA sequencing (Eurofins Genomics), using the primers Removal-BglI-forw and Removal-BglI-rev (see **appendix S2**).

2.1.3 DsRed-ELP_n/PAS_n-A4 and DsRed-ELP_n/PAS_n-B4

Master plasmids were also prepared for cloning the plasmids His-DsRed(3CY)-ELP_n-A4 and B4-ELP_n-DsRed(3CY)-His. The genes were obtained from Eurofins Genomics and cloned as described in **2.1.2**. The plasmids for the second-generation CC star proteins DsRed_C117T-ELP₃/PAS₈-A4-His, DsRed_C117T-ELP₃/PAS₈-B4 and DsRed_C117T-ELP₃/PAS₈-B4S-His were purchased from Biocat GmbH (already cloned into the expression vector pET28a).

2.2 Protein expression and purification

2.2.1 DsRed variants

All plasmids were transformed into *E. coli* BL21(DE3) (Merck Millipore) and plated on LB agar (10 g L⁻¹ tryptone, 5 g L⁻¹ yeast extract, 10 g L⁻¹ NaCl, 20 g L⁻¹ agar, 50 µg mL⁻¹ kanamycin). Precultures were inoculated from single colonies and grown in LB medium (10 g L⁻¹ tryptone, 5 g L⁻¹ yeast extract, 10 g L⁻¹ NaCl, 50 µg mL⁻¹ kanamycin) at 37 °C and 250 rpm overnight. The precultured cells were used to inoculate the expression culture in LB medium with an OD₆₀₀ of 0.2. The cells were grown in LB medium at 37 °C and 250 rpm until OD₆₀₀ reached a value between 0.6 and 0.8. The temperature was lowered to 25 °C and 1 mM isopropyl β-D-1-thiogalactopyranoside (IPTG) was added. After 6 h, the cells were harvested by centrifugation at 5,000 g, 4 °C for 15 min. The cell pellets were frozen at -80 °C for at least 2 h before proceeding with cell lysis. The cell pellets were resuspended in lysis buffer (20 mM sodium phosphate pH 7.4, 300 mM NaCl, 10 mM imidazole, 1 mg mL⁻¹ lysozyme, DNase) for 30 min on ice. Cell lysis was performed with a high-pressure homogenizer (Emulsiflex B15, Avestin) in 3 cycles. After cell lysis, the sample was cleared by centrifugation at 53,300 g for 30 min at 4 °C. The supernatant contains all soluble proteins. Samples (10 µL) were usually kept for SDS-PAGE.

After passing the supernatant through a 0.22 µm syringe filter, it was loaded onto a gravity flow His-Trap Ni²⁺-NTA column (1 ml column volume; Cytiva). To reduce possible disulfide bonds, 10 mM TCEP was added in all subsequent steps. The column was washed with 10 column volumes of loading buffer (20 mM sodium phosphate pH 7.4, 0.5 M NaCl, 10 mM imidazole). Proteins were eluted with 10 column volumes of elution buffer (20 mM sodium phosphate pH 7.4, 0.5 M NaCl, 400 mM imidazole). The eluted protein was dialyzed against ultrapure

water (5 L, 7 times) at 4°C. The sample was centrifuged at 5,000 g for 30 min to remove insoluble protein. The resulting supernatants were flash-frozen in liquid nitrogen and lyophilized for 2 days. Lyophilized protein powders were aliquoted and stored at -80°C until use.

2.2.2 Expression of DsRed star proteins

Initially, the DsRed star proteins were expressed and purified with a similar protocol (37°C) as described above for the DsRed variants while modifications were made to improve the expression yields of some proteins. Modifications include the use of *E. coli* BLR(DE3) (Merck Millipore) for plasmids containing ELP or PAS sequences. As a *recA* derivative of BL21(DE3), BLR(DE3) is known to stabilize target plasmids containing repetitive sequences. In addition, LB medium was replaced with terrific broth (24 g L⁻¹ yeast extract, 12 g L⁻¹ tryptone, 0.4% glycerol, 72 mM K₂HPO₄, 17 mM KH₂PO₄), the temperature was lowered to 16°C and the IPTG concentration was reduced to 0.5 mM. It should be noted that these well-known modifications were made with the goal of improving the expression level; however, no systematic comparison of these conditions was performed.

2.2.3 Purification of ELP-containing fusion proteins

Considering that relative large amounts of DsRed star proteins are needed, it was tested if the DsRed-ELP star proteins can be purified based on the reversible phase transition of ELPs, which depends on temperature, pH and ionic strength.^{79,80} ELPs are highly soluble at low temperature and low salt concentration, but form coacervates at high temperature and high salt concentration. This phase transition is not affected when fusion partners are present. In fact, this ELP phase transition has been utilized to separate

recombinant ELP fusion proteins from other proteins in a cell lysate, using a method called inverse transition cycle (ITC; **Figure 7**).

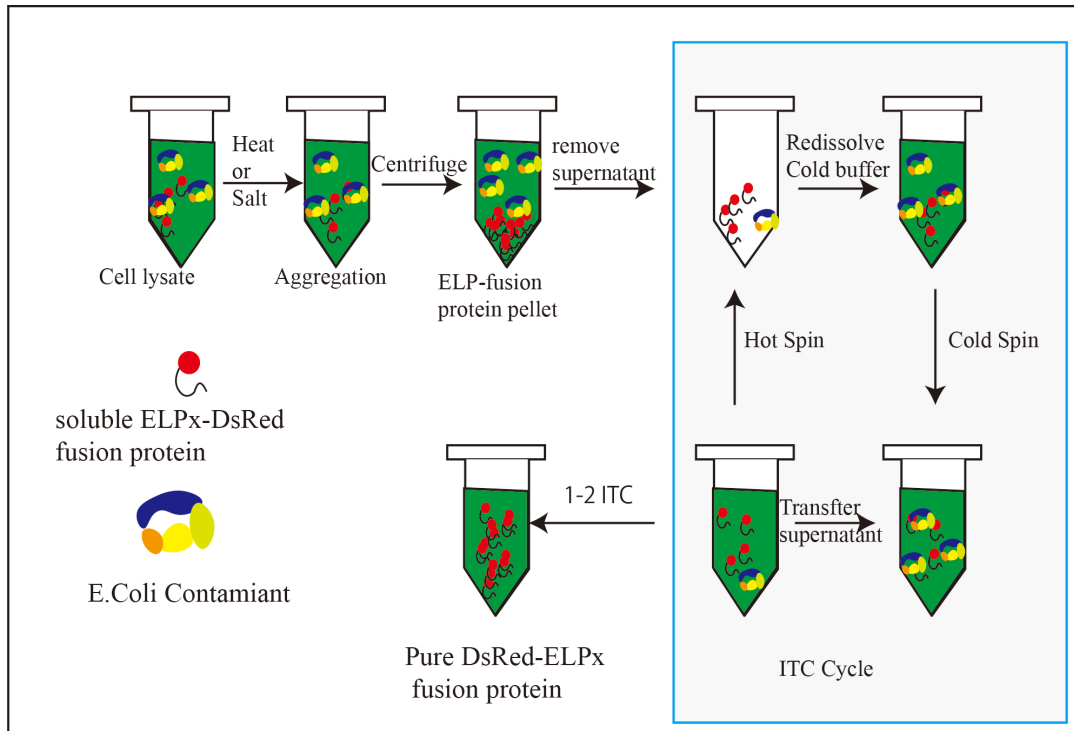


Figure 7. Schematic diagram illustrating the inverse transition cycle (ITC) method used for the purification of ELP-fusion proteins.

The ITC methods was applied as follows. The cell lysate was diluted with pre-cooled ultrapure water to a total volume of 20 mL. The sample was centrifuged at 38,071 g, 4°C for 15 min. The supernatant (20 mL) was mixed with an equal volume of 0.8 M $(\text{NH}_4)_2\text{SO}_4$ to yield a final concentration of 0.4 M $(\text{NH}_4)_2\text{SO}_4$. The sample was incubated at 37°C in a water bath for 15 min and centrifuged at 38,071 g, 37 °C for 15 min. The ELP-fusion protein is now in the pellet and the supernatant was discard. The pelleted protein was then dissolved in pre-cooled ultrapure water and centrifuged. $(\text{NH}_4)_2\text{SO}_4$ was added to the supernatant. The supernatant was warmed up to 37°C and the protein was pelleted again. After a total amount of 2 to 4 cycles, pure ELP fusion protein was obtained. To remove

residual $(\text{NH}_4)_2\text{SO}_4$, the sample was dialyzed against ultrapure water. The final product was lyophilized. Protein purity was assessed by SDS-PAGE.

2.3 Protein characterization

2.3.1 SDS-PAGE

Crude extracts and purified proteins were analyzed with SDS-PAGE (12% acrylamide unless otherwise stated) to estimate the molecular weight of the proteins and to determine their purity. Standard protocols for gel preparation were used. The gels were stained with Coomassie Brilliant Blue or SimplyBlue™ SafeStain (ThermoFisher Scientific).

2.3.2 MALDI-TOF

MALDI-TOF is a mass spectrometry method suited for the analysis of proteins without fragmentation. It serves as a method for determining the molecular weight of proteins. It can also provide information about the purity of a protein sample in a semiquantitative manner. The protein samples were dissolved in 1% trifluoroacetic acid, mixed with the matrix 2',4'-dihydroxyacetophenone (DHAP) and spotted onto the MALDI target plate. The measurement was performed on an Autoflex Speed mass spectrometer (Bruker) in positive, long-pass mode.

2.3.3 Dynamic light scattering

The purified and lyophilized proteins were dissolved in ultrapure water to a concentration of 100 μM . The protein samples were centrifuged to remove insoluble material. The supernatant was further passed through the 0.22 μm syringe filter and kept at 4°C until the measurement. A Zetasizer Nano Series instrument (Malvern Instruments) was used. Samples were measured in polystyrene cuvettes. The data was analyzed with the instrument software.

2.4 Hydrogel synthesis

2.4.1 DsRed-sPEG hybrid hydrogels

The lyophilized DsRed variants and sPEG-Mal (40 kDa, Jenkem) were dissolved in 30 μL ultrapure water. The concentration of DsRed and sPEG-Mal was 1.5 mM (**Figure 8a**). The two components were mixed in a metal-based mold with 8 mm diameter, which exactly fits to the diameter of the rheometer measuring system. The height of mold is 1 mm and fits a volume of 50 μL . The mold was covered with glass that was treated with trichlorosilane to obtain a hydrophobic surface. The hydrogel sample was left to gel in the fridge at 4°C overnight. The sample was removed from the mold (**Figure 8b**) and used for rheology immediately.

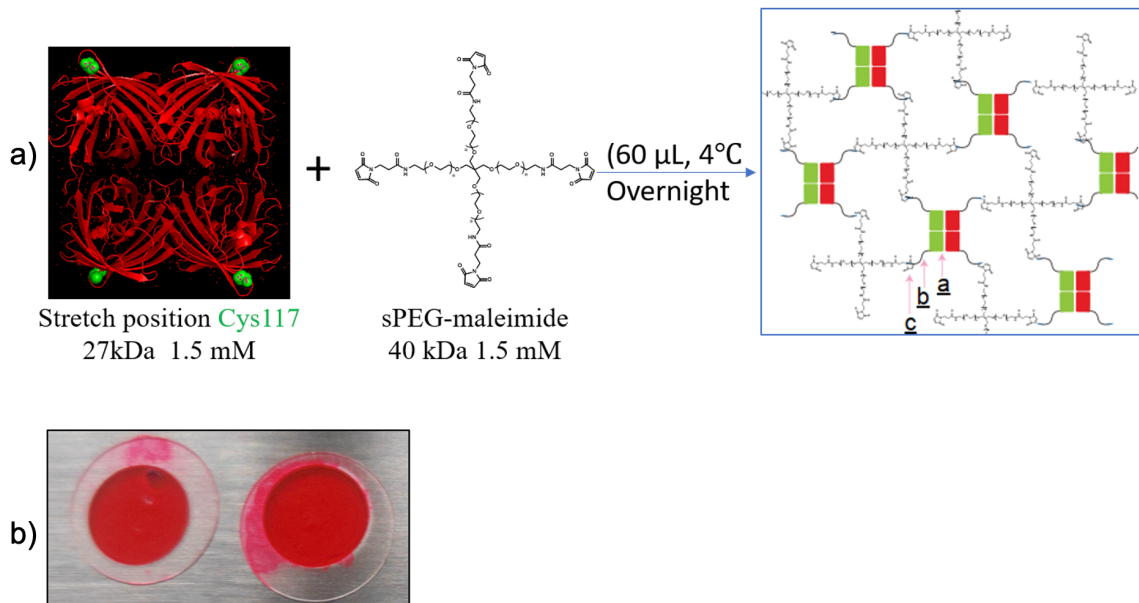


Figure 8. Preparation of DsRed-sPEG hydrogels based on the thiol-maleimide reaction.

a) An aqueous protein solution (1.5 mM) was mixed with sPEG-Mal (1.5 mM) in a 1:1 molar ratio. b) The hydrogel was fabricated in a metal-made mold, covered with a glass cover slip. The surface of the glass was silanized to make it hydrophobic.

2.4.2 Hydrogels based on DsRed-ELP star proteins

The lyophilized protein powders of DsRed(3CY)-ELP_n-SpyCatcher-His and DsRed(3CY)-ELP_n-SpyTag-His were dissolved in 30 μ L of ultrapure water to obtain concentrations of 0.5 mM, 1 mM, 1.5 mM and 2 mM, respectively. These values refer to the concentration of SpyCatcher or SpyTag, which is equal to the concentration of DsRed monomers. The weighted mass used for each protein is given in **Table 1**. The resulting protein solutions were mixed in a 1:1 molar ratio, yielding stoichiometric molar concentrations of the two components. Gelation occurred rapidly and a solid gel was obtained after 30 min of incubation at 4°C.

Table 1. Preparation of SpyCatcher-SpyTag cross-linked hydrogels. The table shows the weighted mass of protein to obtain the indicated concentration of SpyCatcher-SpyTag cross-links (CC) for each respective protein.

Protein	x=	Mw monomer	CC-0.5mM	CC-1mM	CC-1.5mM	CC- 2.2 mM
			mg	mg	mg	mg
3CY-ELPx-SpyCatcher	0	40271.02	1.2	2.4	3.6	4.8
	3	54043.1	1.6	3.2	4.9	6.5
	5	63235.84	1.9	3.8	5.7	7.6
	9	81621.31	2.4	4.9	7.3	9.8
	12	95410.42	2.9	5.7	8.6	11.4
3CY-ELPx-SpyTag	0	28749.63	0.9	1.7	2.6	3.4
	3	42521.71	1.3	2.6	3.8	5.1
	5	51714.45	1.6	3.1	4.7	6.2
	9	70099.92	2.1	4.2	6.3	8.4
	12	83889.03	2.5	5.0	7.6	10.1

2.5 Rheology

Rheology is a valuable technique for the characterization of hydrogels. It provides information on the linear and non-linear viscoelastic properties of these materials. Rheological measurements report the response of hydrogels to deformation, such as rotational or oscillating shear forces. When applying oscillating forces,

both the frequency and strain amplitude of the deformation can be varied and different aspects of the hydrogel's mechanical behavior can be assessed, as will be explained in more detail in the following. Measurements with oscillating deformation provide time-, strain- and frequency-dependent viscoelastic moduli, G' and G'' , where the storage modulus G' represents the elastic and the loss modulus G'' the viscous component of the material response.

The hydrogel samples were measured with an oscillatory shear rheometer (MCR302, Anton Paar GmbH). The measurement was performed with parallel-plate geometry, using a plate diameter of 8 mm (PP-8, Anton Paar GmbH). The gap size was 200 μm unless otherwise stated. The temperature of the sample table was equipped with Peltier thermoelectric cooling and the temperature was set to a temperature between 20 and 25°C unless stated otherwise. The sample was loaded onto the sample table and water was filled into a trough around the sample to maintain a humid environment during the measurement. A temperature-controlled hood was lowered onto the sample table to slow down evaporation.

2.5.1 Time sweeps to measure hydrogel gelation time

In a time sweep experiment, the strain amplitude and angular frequency of the oscillation are kept constant and G' and G'' are monitored as a function of time. In this way, network cross-linking can be monitored as an increase in G' , which reports on the growing elastic (i.e., solid) contribution during gelation. For this experiment, the two components of the sample (i.e., DsRed-Cys and sPEG-Mal) were directly mixed on the sample table of the rheometer and the measurement was started immediately. The strain amplitude was set to 5% and the angular frequency was 10 rad s^{-1} .

2.5.2 Strain amplitude sweeps to determine the linear viscoelastic range

Strain amplitude sweeps were carried out to determine the LVE range. During the measurement, the deflection of the measuring system was increased step-wise while keeping the angular frequency at a constant value. The samples, as prepared in 2.4, were placed onto the sample table and mildly homogenized during a 10 min oscillation at a strain amplitude of 5% and an angular frequency of 5 rad s⁻¹. For the following amplitude sweep, the angular frequency was set to 10 rad s⁻¹ and the strain amplitude was increased from 0.1 to 1000%.

2.5.3 Rotational stress-strain experiment

Additional information about hydrogel failure can be obtained from rotational stress-strain experiments where the measuring system is continuously rotated in one direction so that the shear strain increases gradually. The samples were placed onto the sample table and the strain was increased up to 10,000% while recording the stress. The strain rate was 0.1 s⁻¹.

2.5.4 Oscillatory frequency sweep test on the network property

Frequency sweeps were used to determine the time-dependent behavior of the samples in the LVE range. During the measurement, the angular frequency was increased step-wise while keeping the deflection of the measuring system at a constant value. The samples were prepared and placed onto the sample table as described. The strain amplitude was set to 5% and the angular frequency was varied from 0.01 to 100 rad s⁻¹.

2.5.5 Step-strain experiment to probe self-healing

Step-strain experiments, where the strain amplitude is repeatedly switched between very small and very large values can be used to test the ability of a

hydrogel to self-heal. When the strain amplitude is suddenly increased, bonds are broken. These bonds eventually reform (i.e., heal) when the strain amplitude is decreased again. Such experiments are particularly interesting for physically cross-linked materials. Here, the angular frequency was kept constant at 10 rad s^{-1} while the strain amplitude was switched back and forth between 5% and 2000%.

2.5.6 Rheo-optical measurements

The MCR302 rheometer was integrated with a basic fluorescence microscope, consisting of a LED light source and a CCD camera with RGB chip. This setup was designed to allow for monitoring changes in the fluorescent properties of a hydrogel sample during a rheology experiment. The setup was equipped with excitation and emission filters for fluorescein and tetramethylrhodamine as well as a multiband dichroic mirror. In principle, this configuration should be able to discriminate the “green” and the “red” chromophores present in DsRed. Within this work, fluorescence at both wavelengths was monitored during an amplitude sweep and a rotational stress-strain experiment to probe possible changes in DsRed fluorescence as a function of strain.

2.6 Determination of SpyCatcher-SpyTag coupling efficiency

After covalent SpyCatcher-SpyTag cross-links have formed, the only non-covalent bond in the hydrogel is within the DsRed tetramer. This provides the unique opportunity to disassemble DsRed and thus the hydrogel into its network chains and to estimate the fraction of cross-links. SDS-PAGE was employed to separate cross-linked from unreacted chains. The hydrogel was fabricated as described under **2.4.2**. Afterwards, 20% SDS (200 μL) was added to the hydrogel sample (50 μL), resulting in a final SDS concentration of 16%. The samples were

incubated overnight at 4°C. After this treatment, the red fluorescence disappeared, indicating that DsRed was denatured. The denatured sample (20 µL) was mixed with reducing SDS-PAGE loading buffer (5 µL) and incubated at 95 °C for 10 min. The samples were then run on SDS-PAGE.

3. Results

3.1 Suitability of DsRed as a tetrameric core for protein-based star-polymers

3.1.1 Experimental setup and design

Highly ordered tetrameric networks attract the attention of scientists because of their unique structural and mechanical properties. These ordered tetrameric networks are also an important platform for correlating molecular with material properties.⁶³ While sPEG networks are widely studied, there is still a very small number of related papers published on recombinant protein-based hydrogels with tetrameric building blocks.^{22,64,65,67–69}

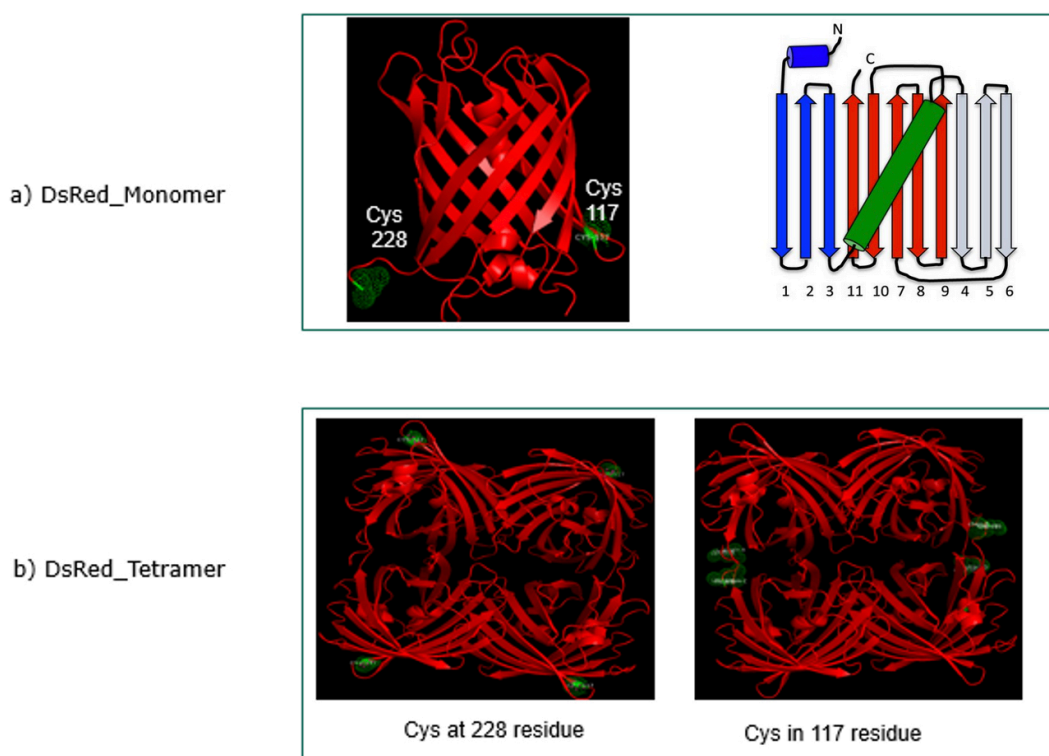


Figure 9. DsRed variants used in this project. a) DsRed monomers either possess an internal Cys at position 117 or a C-terminal Cys at position 228. b) Location of the Cys residues in the folded DsRed tetramer. The structures are based on PDB ID 1GGX.

In this project, two different variants of DsRed were tested for their suitability to serve as the tetrameric core of star-shaped fusion proteins. These are DsRed.T3^{55,56} and DsRed-Express2.⁵⁷ Optimization of these two DsRed derivatives was performed in an *E. coli* expression system, suggesting that they show high-level expression in *E. coli*. The maturation kinetics of the chromophore was improved for DsRed.T3 compared to the wildtype protein; however, at the cost of a higher fraction of “green” chromophores. DsRed.T3 may thus be an ideal candidate to display an increase in green fluorescence upon tetramer dissociation. Besides serving as a tetrameric core, it may also become a marker that reports on the force-induced disassembly of the protein in DsRed-containing hydrogels. Maturation kinetics was also improved for DsRed-Express2. It displays a lower fraction of “green” chromophores than DsRed.T3.

Different variants were engineered so that they carry exactly one Cys residue per monomer (**Figure 9**). The Cys residues are required to cross-link the DsRed proteins with sPEG-Mal for obtaining a hydrogel network. The published sequence of DsRed.T3 comes with exactly one Cys per monomer (Cys117; **Figure 9b**). In DsRed-Express2, this Cys has been replaced with threonine (Thr). Two mutants were cloned where Thr was replaced with Cys or where Cys has been added to the C-terminus (Cys228; **Figure 9b**). The published sequence of DsRed-Express2 was also cloned as a Cys-free control.

After the network has been cross-linked via the Cys-Mal reaction, the oligomerization interfaces between the monomeric units of DsRed are expected to be the weakest bonds in the otherwise covalently cross-linked hydrogel. The thermodynamic and kinetic stability of DsRed is thus a key factor to determine the viscoelastic properties of the hydrogel. Slow dissociation (and re-association) is expected to yield purely elastic networks. In contrast, dissociation on the timescale of the planned rheology experiments will yield viscoelastic behavior.

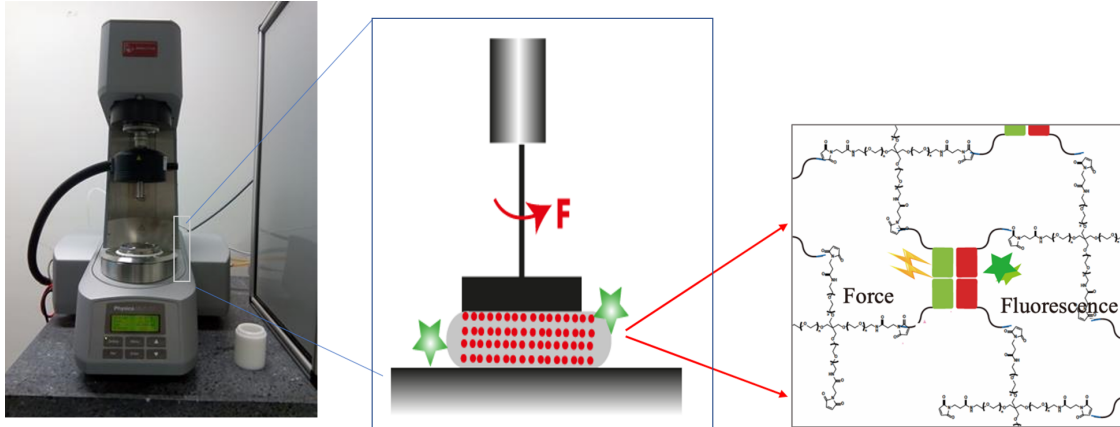


Figure 10. Experimental setup intended to probe a possible color change when DsRed tetramers dissociate as a result of the applied shear force.

In addition, force-induced dissociation of DsRed may occur when the hydrogel experiences large shear strains. It has been proposed that a shift from red to green fluorescence may occur upon tetramer dissociation. In this non-linear viscoelastic regime, it may thus become possible to monitor color changes by fluorescence spectroscopy (**Figure 10**).

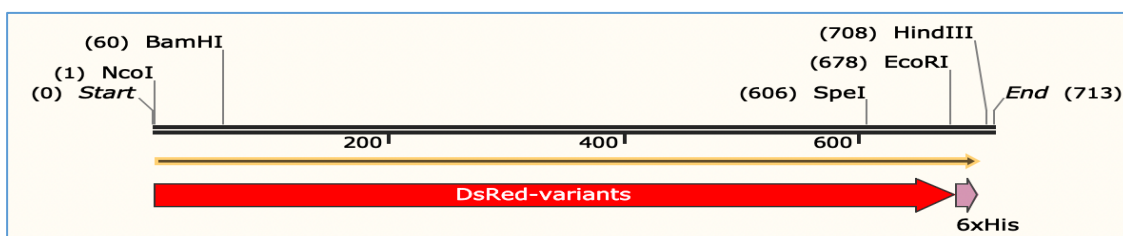
3.1.2 Protein design, expression and purification

In order to obtain DsRed-sPEG hybrid hydrogels, four main aspects need to be considered: 1) The protein expression yield of DsRed needs to be high enough to obtain a sufficient amount of material for hydrogel synthesis. 2) The proteins need to be soluble in the concentration range required for hydrogel synthesis. 3) Exactly one Cys residue per monomer is necessary to achieve site-specific cross-linking with sPEG-Mal. 4) The Cys residue has to be accessible and reactive on the protein surface.

Table 2. Overview of DsRed mutants.

Protein	Molecular weight	Properties
3CY	27007.65	DsRed.T3 - Cys ₁₁₇
2TH	26802.32	DsRedExpress2 - Thr ₁₁₇
2CH	26804.35	DsRedExpress2 - Thr ₁₁₇ Cys
2THG	27019.56	DsRedExpress2 - Thr ₁₁₇ with C-term Cys

Here, a total number of 4 mutants of DsRed.T3 and DsRed-Express2 were used. The protein 3CY is based on DsRed.T3 and has one internal Cys per monomer (**Figure 9**). The protein 2CH originates from DsRed Express2 and carries a Thr₁₁₇Cys mutation. To obtain the protein 2THG, a Cys residue was added at the C-terminus. The original DsRed-Express2 protein without Cys is termed 2TH. All DsRed mutants were designed with a C-terminal histag to allow purification via IMAC. The mutants are summarized in **Table 2** and the corresponding amino acid sequences are shown in **appendix S1**.

**Figure 11.** Protein expression cassettes for the DsRed variants 3CY, 2CH, 2TH, 2THG. All genes were cloned using the restriction enzymes NcoI and HindIII.

All DsRed genes were cloned into the plasmid pET28a using NcoI and HindIII restriction sites, following standard protocols. The expression cassette is identical for all 4 mutants (**Figure 11**). The plasmids were transformed into *E. coli* BL21(DE3). Expression and purification were performed as described in **2.2.1**.

3.1.3 Protein characterization by SDS-PAGE and MALDI-TOF

The cell lysates as well as the purified proteins were run on SDS-PAGE (Figure 12). Already the cell lysates show a very strong band with a molecular weight of ~27 kDa, which corresponds well with the calculated molecular weight of the monomers (Table 2). This clearly indicates that the expression level of all 4 mutants is very high.

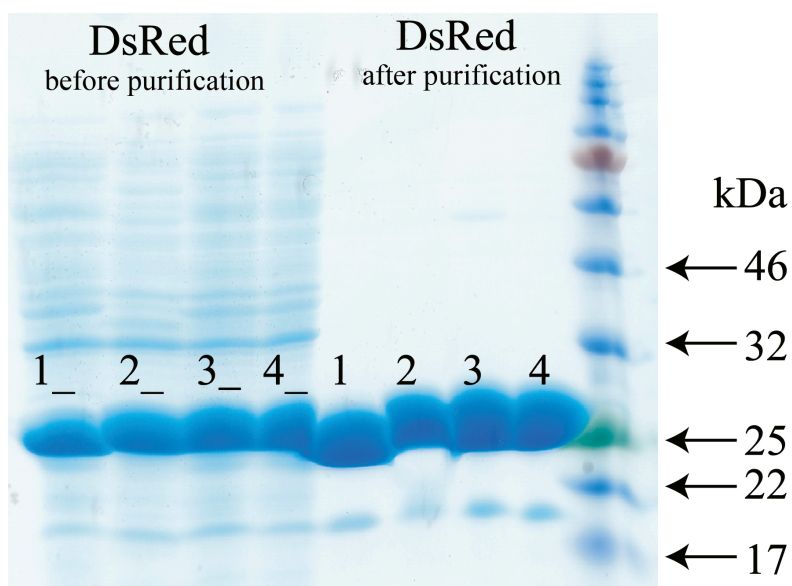


Figure 12. SDS-PAGE analysis of the expressed and purified DsRed mutants (1: 2TH; 2: THG; 3: 2CH; 4: 3CY).

The samples of purified protein again show one strong band at ~27 kDa as well as a less dominant second band of smaller molecular weight. This band has been observed in other preparations of DsRed before and is thus not considered to be a contamination. During sample preparation for SDS-PAGE, the chromophore in the denatured protein becomes hydrated and can further be hydrolyzed. This results in fragmentation of the denatured protein. One fragment is expected to have a size between 18 and 20 kDa while the other band is too small to be visible in a 12% gel.⁸¹

The amount of purified protein was determined and related to the culture volume to obtain the yield of purified protein (**Table 2**). The yield appears to be higher for the protein 3CY (i.e., DsRed.T3). The results further suggest that the presence of Cys does not have a negative effect on the yield of purified protein. The purified proteins were further characterized with MALDI-TOF. The mass spectra are shown in the **appendix S3.1** and are summarized in **Table 3**. The relative difference in measured and calculated molecular weight is less than 1%, confirming that the purified proteins are indeed DsRed.

Table 3. Yield and measured molecular weight (MW_{meas}) of the purified DsRed derivatives. The calculated molecular weight (MW_{calc}) and the relative difference is also shown. For MW_{calc} , chromophore maturation is not considered.

Protein	Yield (mg L ⁻¹)	MW_{meas} (Da)	MW_{calc} (Da)	Difference (%)
3CY	200	26831.1	27007.65	0.65
2TH	56	26740.1	26802.32	0.23
2CH	120	26739.2	26804.35	0.24
2THG	80	26960.8	27019.56	0.22

3.1.4 Fluorescence spectroscopy

To further characterize the proteins, their fluorescence excitation spectrum was measured (**Figure 13**). The spectra provide information about the ratio of the “green” and “red” chromophores.

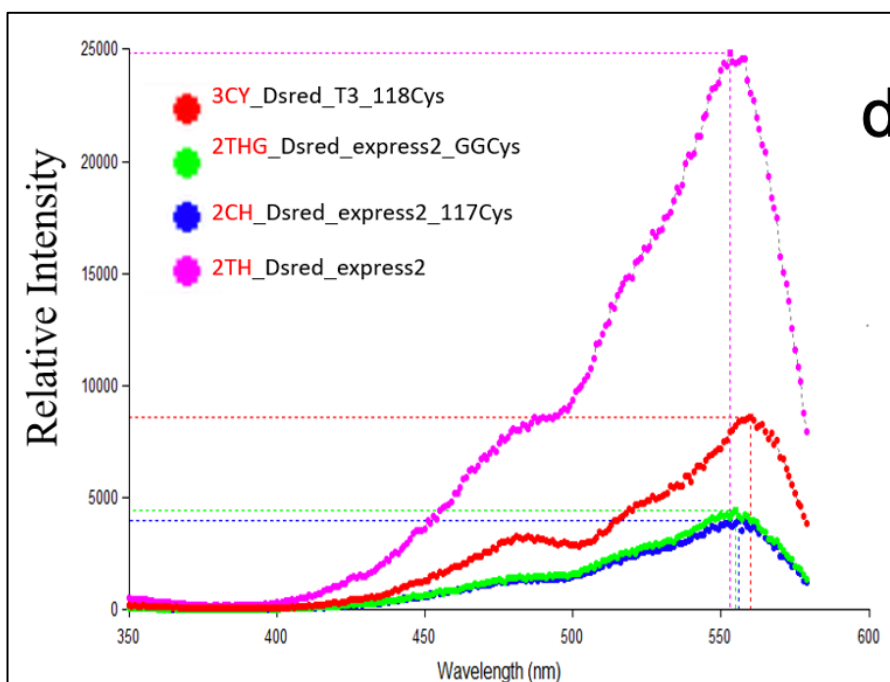


Figure 13. Fluorescence excitation spectrum of the DsRed mutants, recorded at an emission wavelength of 620 nm.

3.1.5 Hydrogel characterization

The protein with the highest yield (3CY) was chosen to establish if a hydrogel forms upon cross-linking via the Cys-Mal reaction, which yields a covalent thioester-based cross-link. Hydrogel formation was monitored on the rheometer, performing a time sweep as described in **2.5.1**. The DsRed-Cys and sPEG-Mal solutions were mixed on the sample table of the rheometer and the time sweep was started (**Figure 14**). After a short lag phase of approximately 40 s, G' steadily increased, indicating a transition from a liquid to a solid-like gel. After around 150 s, the increase of G' slowed down and a plateau was gradually reached.

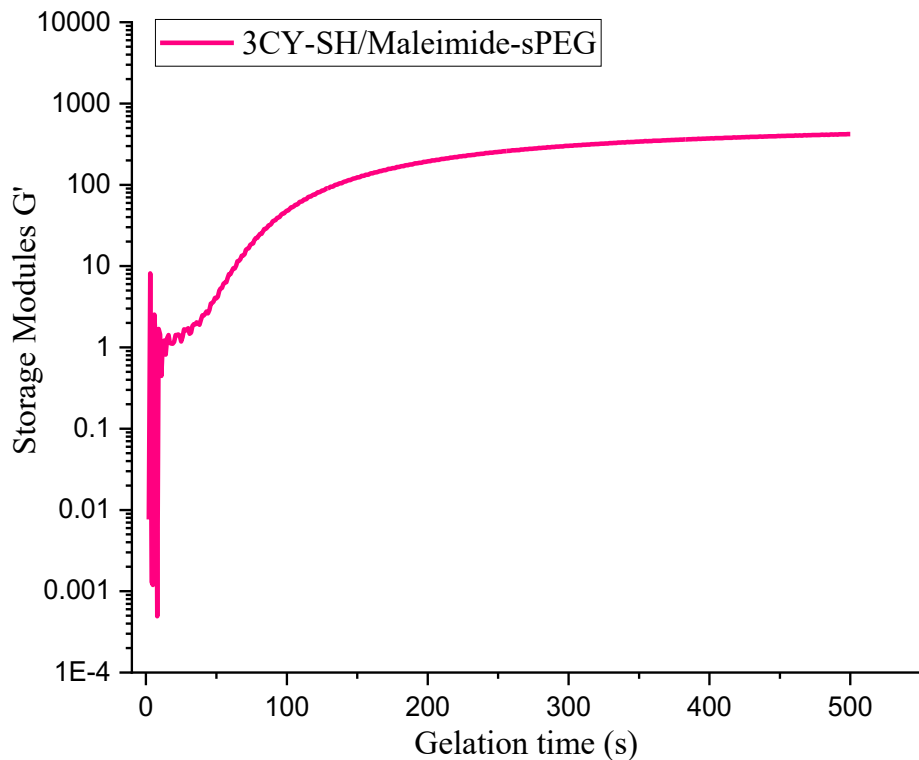


Figure 14. Time sweep performed to monitor gelation after mixing DsRed(3CY) and sPEG-Mal. The two solutions, each with a concentration of 1.5 mM, were mixed on the sample table of the rheometer. The time sweep was performed at a constant strain amplitude of 5% angular frequency 10 rad s^{-1} .

Hydrogels based on the protein 3CY were further characterized with three consecutive rounds of ascending and descending amplitude sweeps to determine the LVE range (**Figure 15**). In the first ascending amplitude sweep, both the storage modulus G' and the loss modulus G'' are nearly constant up to a strain of approximately 10%. G' is at least 10x higher than G'' , indicating that the elastic properties dominate and a hydrogel has been formed. The LVE range ends at approximately 10% where G' begins to gradually decrease while G'' increases. At a strain of approximately 1000%, G' and G'' cross and the liquid properties

begin to dominate. Both moduli are lower in the second and third ascending amplitude sweeps, suggesting that part of the hydrogel structure was destroyed in the first amplitude sweep.

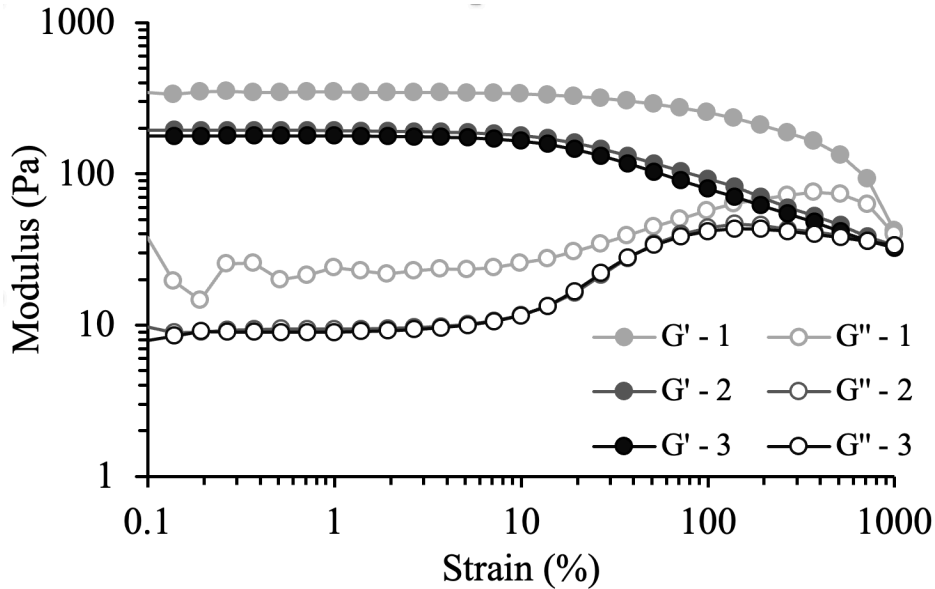


Figure 15. Amplitude sweeps of the DsRed(3CY)-Cys/sPEG-Mal hydrogel. The hydrogel was fabricated from 1.5 mM protein and sPEG, respectively. Three consecutive rounds of ascending and descending amplitude sweep were performed at an angular frequency of 10 rad s^{-1} . The gap size was $100 \text{ }\mu\text{m}$ and the temperature was set to 25°C . The plot shows the ascending amplitude sweeps only.

In addition to the amplitude sweeps, also a rotational stress-strain experiment was performed to determine the yield strain of the hydrogel. In this experiment, the measurement system was continuously rotated in one direction so that the shear strain acting on the sample increased continuously (**Figure 16**). The hydrogel displays a yield point at around 800% strain. Rupture of load bearing structures in the hydrogel thus occurs at a similar strain value in the amplitude sweep and in this stress-strain experiment.

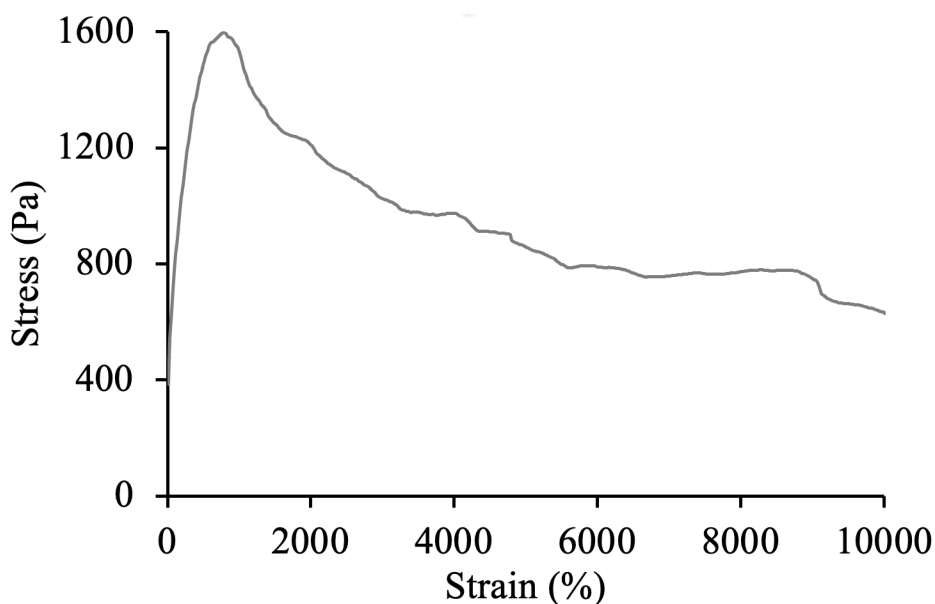


Figure 16. Rotational stress-strain experiment of the DsRed(3CY)-Cys/sPEG-Mal hydrogel. The hydrogel was fabricated from 1.5 mM protein and sPEG, respectively. The measurement system was continuously rotated into the same direction so that the shear strain acting on the sample increased continuously. The gap size was 200 μm and the temperature was set to 22°C.

Visual inspection of the hydrogel after the amplitude sweep and the stress-strain experiment, showed that the hydrogel maintained its bright pink color, suggesting that the number of green monomers is too low to observe a visible color change. No or very little DsRed tetramers have ruptured or the ruptured DsRed tetramers are able to reassemble quickly after the shear strain is removed. An attempt was subsequently made to monitor a possible color change while the shear strain was applied. The rheometer is equipped with a simple fluorescence microscope that allows for detecting fluorescence emission from the “red” and “green” chromophores (**Figure 10** and **Figure 17**). The original metal sample table was replaced with glass plate that allows for placing a camera below the sample. Images were captured every second during a rotational stress-strain experiment.

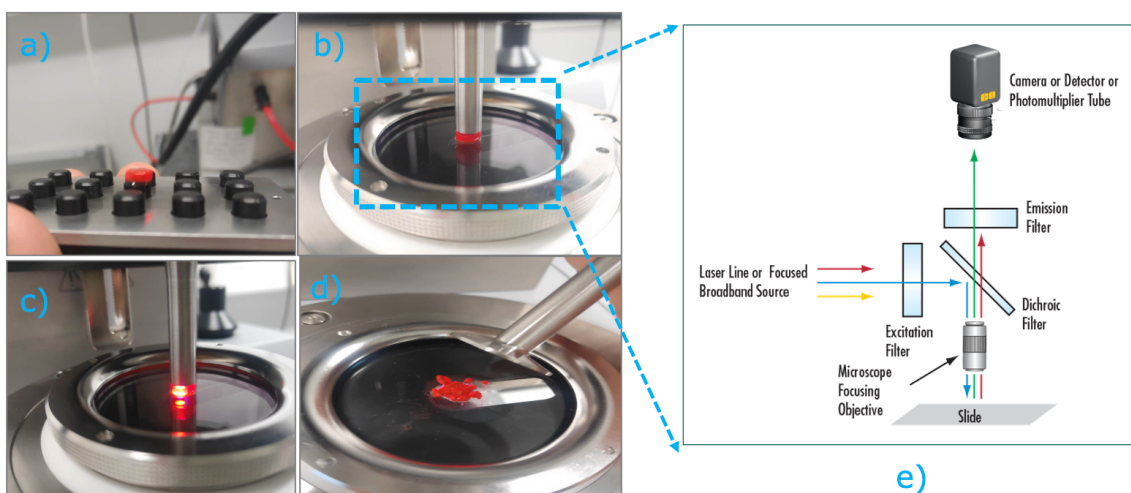


Figure 17. Rheo-fluorescence setup. a) Hydrogel sample prepared in the mold. The gel can stand alone after it has been removed from the mold. b) Hydrogel sample loaded between the glass plate and the PP-8 measuring system. c) Fluorescence excited in the hydrogel sample. d) Hydrogel after the stress-strain experiment. e) Simplified cartoon of the fluorescence microscope taken from <https://www.edmundoptics.com/knowledge-center/application-notes/microscopy/understanding-microscopes-and-objectives/>

The combined rheo-fluorescence experiment also did not unambiguously prove a color change. No clear increase in green fluorescence was observed around the yield point and also not at larger strains. At this moment, no clear conclusions can be drawn if DsRed is mechanically dissociated and if this results in a color change. If so, the number of broken tetramers must be small or it may not be possible to detect them with the setup used. At this stage, it was concluded that DsRed is sufficiently stable to serve as a tetrameric core to produce protein-based star polymers.

3.2 Chemically cross-linked DsRed-ELP star polymers

3.2.1 Experimental setup and design

The goal of this chapter was to construct a series of recombinant protein-based hydrogels cross-linked via the SpyCatcher-Spytag protein ligation system. The hydrogel building blocks consisted of two DsRed-ELP star proteins, fused to either SpyCatcher or SpyTag. Specifically, I aimed to investigate how the mass fraction of protein in the hydrogel as well as the ELP length affect the mechanical properties of the bulk hydrogel. The resulting hydrogels were characterized with oscillatory shear rheology (amplitude and frequency sweeps) and the fraction of formed cross-links was determined after denaturing the hydrogel in a concentrated SDS solution.

A series of constructs was designed that consisted of the tetrameric core protein DsRed.T3 (3CY), an ELP sequence and either the SpyCatcher domain or the SpyTag peptide (from N-terminus to C-terminus; **Figure 18a**). To facilitate cloning of these constructs, two master plasmids (DsRed-linker-SpyCatcher-His and DsRed-linker-SpyTag-His) were cloned first. These master plasmids contained a short linker instead of an ELP sequence (see **appendix S1.2**). The linker allowed cloning of 4 different ELP sequences via BamHI and BglI. These ELP sequences consisted of 3, 5, 9 or 12 repeats of the same basic building block (**Figure 18b**). The amino acids in the X position of the VPGXG repeat sequence were chosen such that the LCST is significantly above room temperature.⁷⁸ The resulting proteins are listed in **Table 3** and the full sequence of DsRed-ELP₃-SpyCatcher-His and DsRed-ELP₃-SpyTag-His is given in **appendix S1.2**. For protein purification, a histag was fused at the C-terminus of all constructs. Alternatively, it was tested if the proteins can be purified via the ITC method described in **2.2.3**.

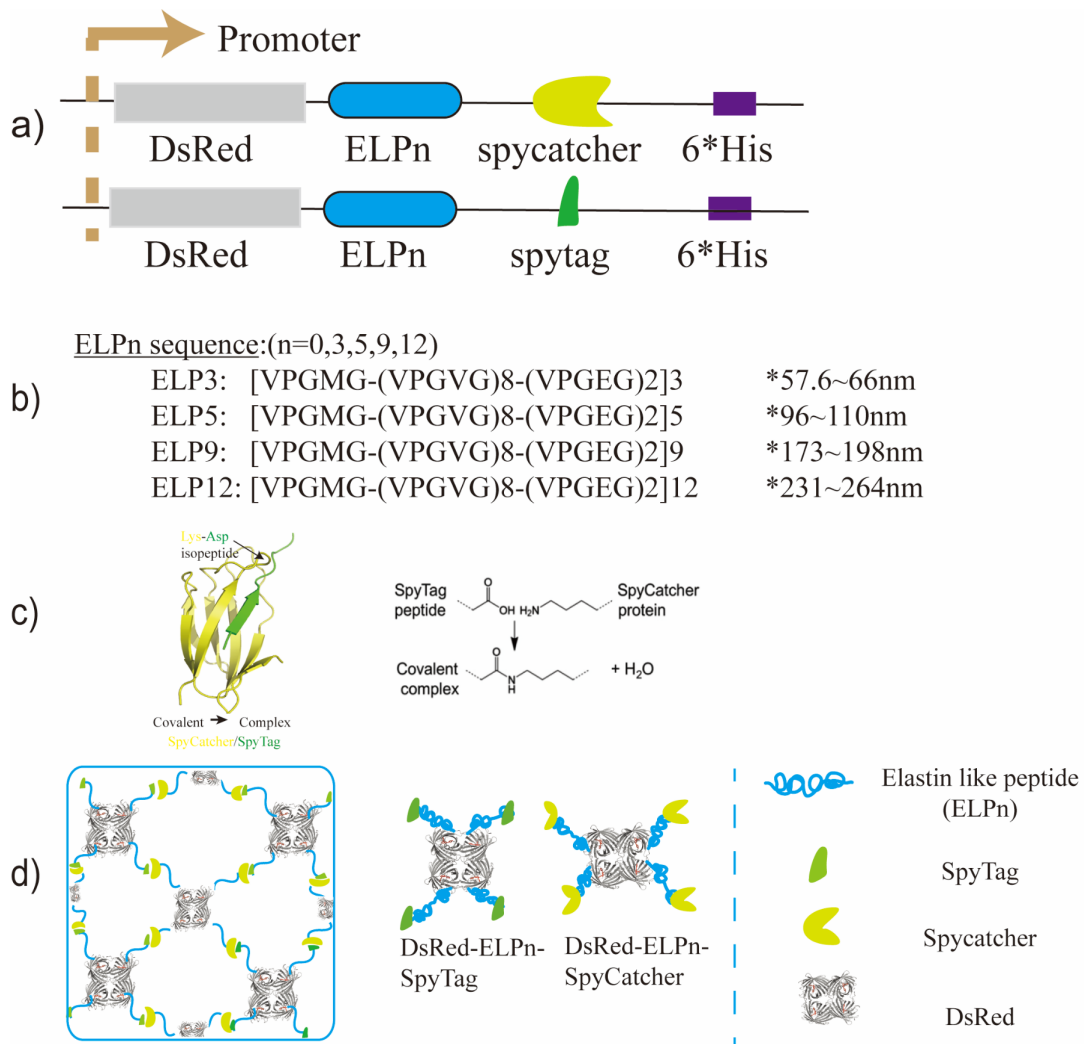


Figure 18. Components of the SpyCatcher-SpyTag cross-linked hydrogel. a) Fusion protein constructs. b) Amino acid sequence of the different ELPs. The predicted contour length of the different ELPs is given, considering that the distance between two amino acid is between 0.35 and 0.4 nm. c) Isopeptide bond formation between SpyCatcher and SpyTag (PDB ID 4MLS). d) Idealized hydrogel structure obtained after cross-linking DsRed-ELP_n-SpyCatcher-His and DsRed-ELP_n-SpyTag-His.

3.2.2 Protein expression, purification and characterization

The expression vectors were transformed into the *E. coli* strain BLR(DE3), which is frequently utilized for the expression of repetitive recombinant protein sequences. Both IMAC and ITC could be used for protein purification; however, it was found that the ITC method can be scaled up more easily. As both DsRed and the SpyCatcher domain remained functional during repeated heating-cooling cycles, ITC was the preferred method. The yields of the purified proteins are given in **Table 3**. For both DsRed-ELP_n-SpyCatcher-His and DsRed-ELP_n-SpyTag-His, the yield decreased with increasing ELP length. This is consistent with earlier results, obtained for ELP fusion proteins expressed in *E. coli*⁸² or plants.⁸³

Table 4. Yield of DsRed-ELP star proteins fused to SpyCatcher (SC) or SpyTag (ST).

The yield is given as the mass of purified protein per liter of bacterial culture.

Protein	ELP length (nm)	Yield (mg L ⁻¹)
DsRed(3CY)-linker-SC-His	0	150
DsRed(3CY)-ELP ₃ -SC-His	58-66	110
DsRed(3CY)-ELP ₅ -SC-His	96-110	99
DsRed(3CY)-ELP ₉ -SC-His	173-198	79
DsRed(3CY)-ELP ₁₂ -SC-His	231-264	54
DsRed(3CY)-linker-ST-His	0	140
DsRed(3CY)-ELP ₃ -ST-His	58-66	120
DsRed(3CY)-ELP ₅ -ST-His	96-110	81
DsRed(3CY)-ELP ₉ -ST-His	173-198	84
DsRed(3CY)-ELP ₁₂ -ST-His	231-264	61

The purified proteins were analyzed with SDS-PAGE to determine their purity and to confirm their molecular weight (**Figure 19** and **Table 4**). Most proteins appear as a single band and the purity appears sufficient for hydrogel synthesis. The apparent molecular weight of the protein bands does not match the calculated molecular weight, however. Especially the proteins containing ELP sequences migrate slower than what would be expected from their molecular weight.

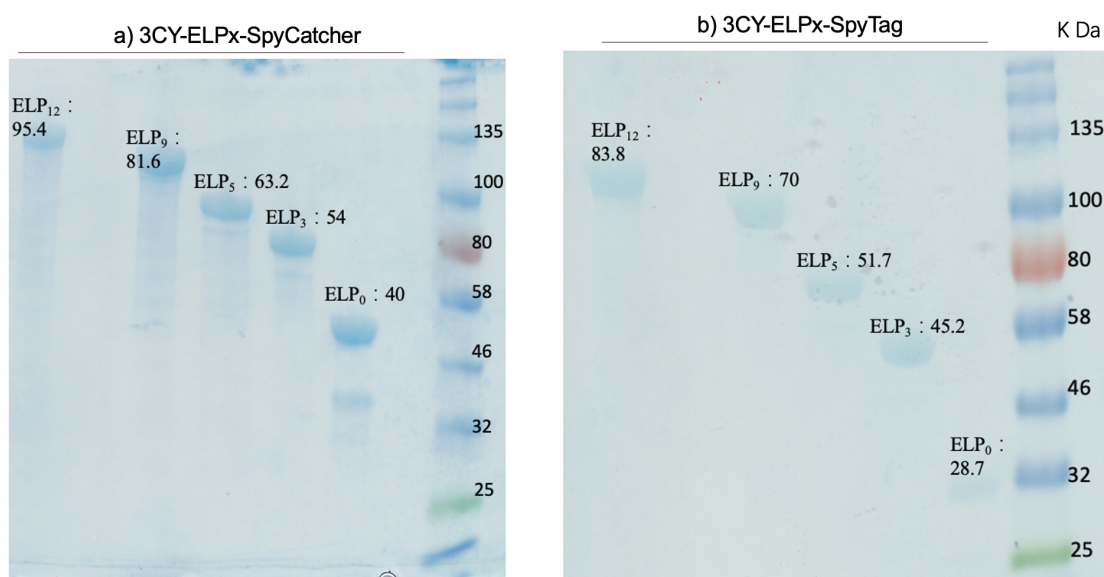


Figure 19. SDS-PAGE (12%) of all DsRed-ELP_n-SpyCatcher-His (a) and DsRed-ELP_n-SpyTag-His (b) proteins. The gel illustrates the apparent shift to larger molecular weights for the different ELP-containing proteins.

MALDI-TOF was thus used as a second characterization method to determine the molecular weight (**Table 4** and **appendix S3.2**). Mass spectra could be obtained for the proteins without any ELP sequence and for the proteins containing ELP₃ or ELP₅, but not for the proteins containing ELP₉ or ELP₁₂. The MALDI-TOF results confirm the molecular weight of the proteins.

Table 5. Molecular weight of DsRed-ELP star proteins fused to SpyCatcher (SC) or SpyTag (ST). For the calculated molecular weight (MW_{calc}) chromophore maturation is not considered. The measured mass (MW_{meas}) was obtained from MALDI-TOF.

Protein	MW_{calc} (Da)	MW_{meas} (Da)	Difference (%)
DsRed(3CY)-linker-SC-His	40513.30	40183.0	0.82
DsRed(3CY)-ELP ₃ -SC-His	54043.10	53880.8	0.30
DsRed(3CY)-ELP ₅ -SC-His	63235.84	62728.5	0.80
DsRed(3CY)-ELP ₉ -SC-His	81621.31	-	-
DsRed(3CY)-ELP ₁₂ -SC-His	95410.42	-	-
DsRed(3CY)-linker-ST-His	28749.63	28528.4	0.77
DsRed(3CY)-ELP ₃ -ST-His	42763.98	42167.9	1.39
DsRed(3CY)-ELP ₅ -ST-His	51956.72	51273.9	1.31
DsRed(3CY)-ELP ₉ -ST-His	70342.20	-	-
DsRed(3CY)-ELP ₁₂ -ST-His	83889.03	-	-

As a last method to determine protein size and solution properties, DLS was performed for DsRed-ELP₃-SpyCatcher-His and DsRed-ELP₃-SpyTag-His (**Figure 20**). Four different protein concentrations between 1.6 and 100 μM were analyzed. At all concentrations, the proteins showed a single, narrow peak with a hydrodynamic radius slightly above 10 nm. This corresponds well with the expected size of a tetrameric DsRed-ELP star protein.

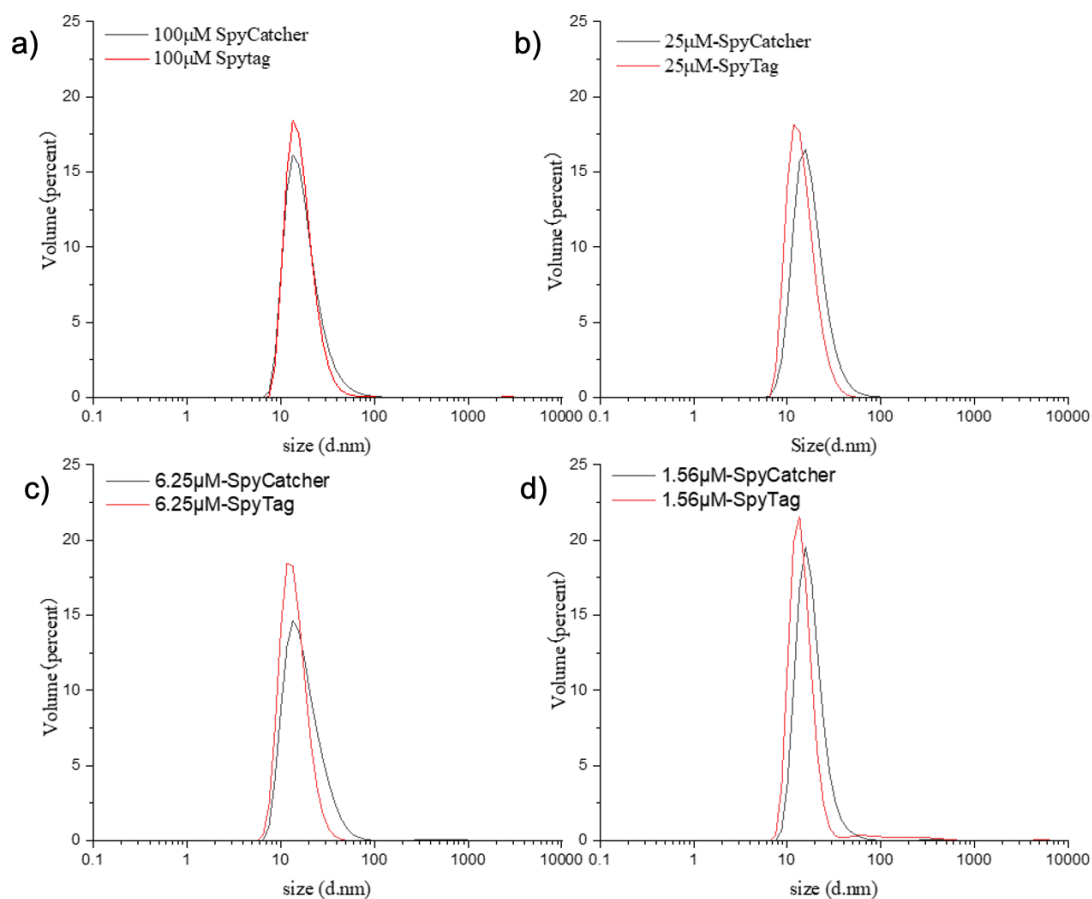


Figure 20. Dynamic light scattering of the DsRed-ELP₃ star proteins. The proteins were measured at concentrations of 100 μ M (a), 25 μ M (b), 6.25 μ M (c) and 1.56 μ M (d). The measurement was performed at 4°C.

For further characterization of the fusion proteins, their UV/VIS spectrum was measured to determine the fraction of “green” and “red” chromophores. It has been shown earlier that structural rearrangements around the chromophore can affect the kinetics of chromophore maturation as well as the brightness of DsRed variants.⁸⁴ It can thus not be excluded that fusing a dynamically fluctuating RCPP chain will have an effect on these important properties of DsRed. The spectra show no shift in the absorbance maxima of the “green” and “red” chromophores; however, the red:green ratio appears to depend on ELP length (**Figure 21**).

Interestingly, the fraction of “red” chromophores is higher for the proteins with a longer ELP chain.

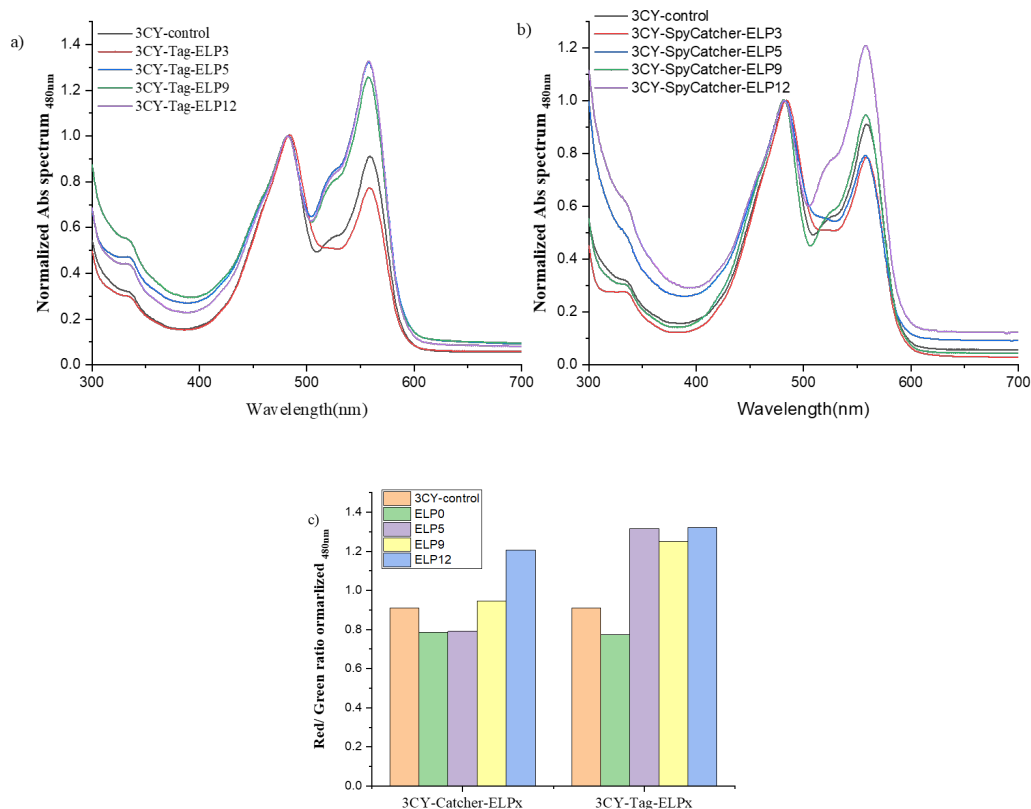


Figure 21. Spectroscopic characterization of the different DsRed-ELP star proteins. a) UV/VIS spectra of the DsRed-ELP_n-SpyTag-His proteins. The spectrum is normalized to the peak of the “green” chromophore. b) UV/VIS spectra of the DsRed-ELP_n-SpyCatcher-His proteins. The spectrum is normalized to the peak “green” chromophore. c) Ratio of the absorbance of the “red” and “green” chromophores.

3.2.3 Synthesis of hydrogels

For the synthesis of SpyCatcher-SpyTag cross-linked hydrogels, the lyophilized proteins were dissolved in different concentrations as indicated in **Table 1** in **2.4.2**. The solutions of the two hydrogel components were mixed in a 1: 1 molar ratio, yielding stoichiometric concentrations of SpyCatcher and SpyTag. Both the

SpyCatcher and SpyTag components primarily contained the same ELP length so that, in principle, hydrogels with 4 different RCPP lengths and 4 different protein concentrations can be obtained (**Figure 22a**). The total mass fraction of protein in the resulting hydrogels is given in **Table 6**. In some cases, also different ELP lengths were used, as this is an easy means to extend the tunable range of hydrogel properties.

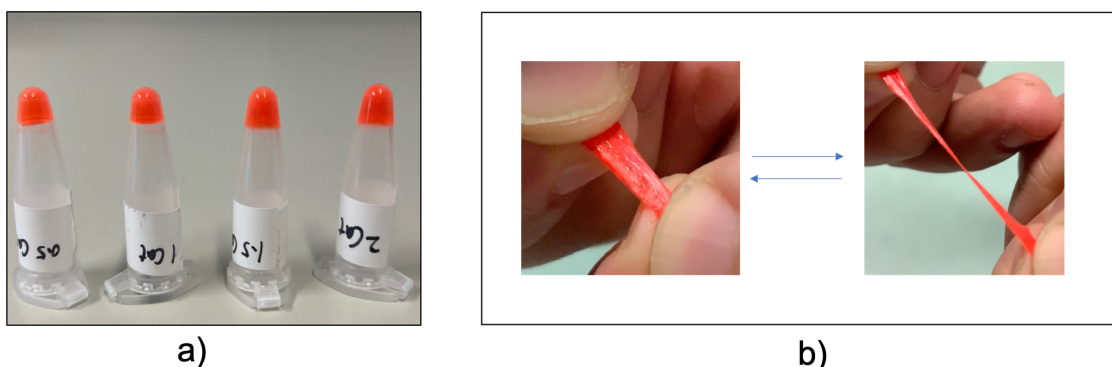


Figure 22. Synthesis and properties of the DsRed-ELP₅-SpyCatcher-His/DsRed-ELP₅-SpyTag-His hydrogel. a) Hydrogels formed after mixing different concentrations of the two protein components: 0.5 mM, 1.0 mM, 1.5 mM and 2 mM (from left to right). b) Simple mechanical test of the hydrogel.

All proteins were stored in lyophilized form and redissolved directly before preparing the hydrogels. It is important to note that the DsRed-ELP_n-SpyTag-His protein powder could be dissolved again easily. In contrast, some insoluble material remained when dissolving DsRed-ELP_n-SpyCatcher-His. The only difference between these proteins is the presence of the SpyCatcher domain. It thus appears likely that the SpyCatcher domain is partially aggregated as its concentration is now significantly higher than in the DLS measurements (**Figure 20**) In the future, optimized versions of the SpyCatcher sequence can be used to minimize this problem.^{45–47} For hydrogel preparation, the insoluble

fraction was left in the sample and possibly has an influence on the material properties as discussed further below.

Table 6. Total mass fraction of protein in the different SpyCatcher/SpyTag cross-linked hydrogels. The calculation is based on the weighted mass for each cross-link concentration (CC), as given in Table 1.

Protein	CC-0.5 mM mg mL ⁻¹	CC-1.0 mM mg mL ⁻¹	CC-1.5 mM mg mL ⁻¹	CC-2.0 mM mg mL ⁻¹
DsRed-ELP ₀	30	68	103	137
DsRed-ELP ₃	48	97	145	193
DsRed-ELP ₅	58	113	173	230
DsRed-ELP ₉	75	152	227	303
DsRed-ELP ₁₂	90	178	270	358

A simple mechanical test was performed to visualize the hydrogel properties (**Figure 22b**). When pulling the hydrogel manually, it can be stretched to at least twice of its original length without failure. Also in this simple experiment, no visible loss of red or an increase of green fluorescence could be detected. This is consistent with the results obtained for the DsRed-Cys/sPEG-Mal hydrogel described in **3.1**.

3.2.4 Influence of protein concentration and RCPP length on hydrogel properties

With the goal of understanding different molecular characteristics on bulk hydrogel properties, two different parameters were varied. These are the protein concentration and the length of the RCPP network chains. Increasing the protein concentration will increase the total protein mass fraction as well as the concentration of cross-links. As a result, the stiffness of the hydrogel is expected

to increase. Longer RCPP network chains are expected to increase the yield strain and the toughness of the material as individual network chains can be stretched to larger extensions before rupture.

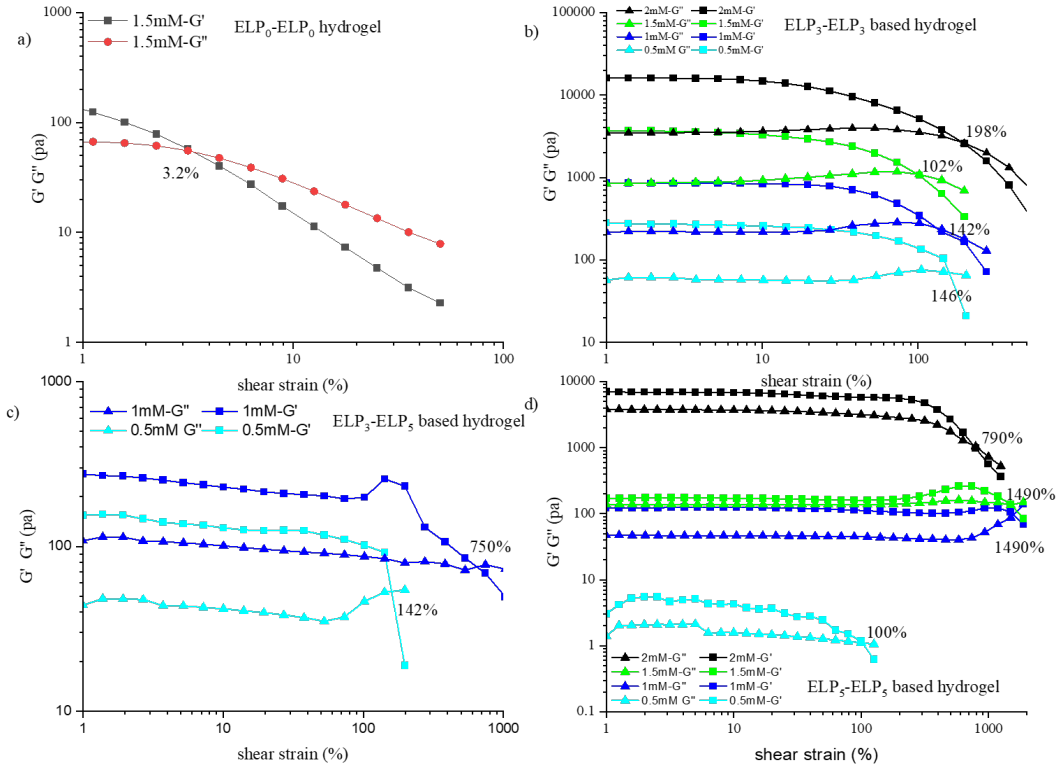


Figure 23. Amplitude sweeps of SpyCatcher/SpyTag cross-linked hydrogels, highlighting the effect of different protein concentrations. a) DsRed-ELP₀-SpyCatcher-His/DsRed-ELP₀-SpyTag-His hydrogel, measured at a cross-link concentration of 1.5 mM. b) Different concentrations of the DsRed-ELP₃-SpyCatcher-His/DsRed-ELP₃-SpyTag-His hydrogel. c) Different concentrations of a hydrogel where one component contained ELP₃ while the other component contained ELP₅. d) Different concentrations of the DsRed-ELP₅-SpyCatcher-His/DsRed-ELP₅-SpyTag-His hydrogel. The experiments were performed over a strain range from 1% to 2000% with an angular frequency of 10 rad s⁻¹.

Hydrogels were prepared from the DsRed-ELP star proteins with ELP₃ and ELP₅ and characterized with rheology. Samples prepared from star proteins with ELP₀ (i.e., the proteins with only the linker) were included for comparison. The proteins with ELP₉ and ELP₁₂ were not used for hydrogel synthesis because of their reduced expression yield. For the ELP₃-ELP₃ and ELP₅-ELP₅ containing star proteins, hydrogels were obtained at all 4 concentrations tested (**Figure 23**). In contrast, for ELP₀-ELP₀ gelation was only observed at cross-link concentrations above 1.5 mM (**Figure 23a**). For the ELP₃-ELP₃ hydrogel, a clear trend was observed where both G' and G'' increase with increasing protein concentration (**Figure 23b**), as expected for networks where the total polymer mass fraction and the cross-link concentration increase. The same trends were observed for hydrogels with ELP₃-ELP₅ (**Figure 23c**) and ELP₅-ELP₅ (**Figure 23d**).

For the highest protein concentration of 2 mM, a storage modulus of several thousand Pa is obtained for both the ELP₃-ELP₃ and ELP₅-ELP₅ hydrogels. This is higher than for many other recombinant protein-based hydrogels synthesized before, which partially also contained the SpyCatcher-SpyTag protein ligation system. This could be the result of a more ideal network formed from two tetrameric building blocks (which was not the case for most other hydrogels). It may also originate from the presence of aggregated SpyCatcher components that are still able to react with SpyTag. Small aggregates could increase the cross-functionality, which in turn increases the stiffness.^{17,19}

In addition to the storage modulus, the amplitude sweeps also report the yield point and the flow point (crossover between the G' and G'' curves). For the ELP₀-ELP₀ mixture, this crossover is at a strain below 10% (**Figure 23a**) while it lies above 100% for the ELP₃-ELP₃ hydrogel and increases to larger strains for the ELP₅-ELP₅ hydrogel. For protein concentrations above 0.5 mM, the flow point appears to be insensitive to the protein concentration (**Figure 23b** and

Figure 23d). These results suggest that that the yield point and flow point are primarily determined by the length of the RCPP chains.

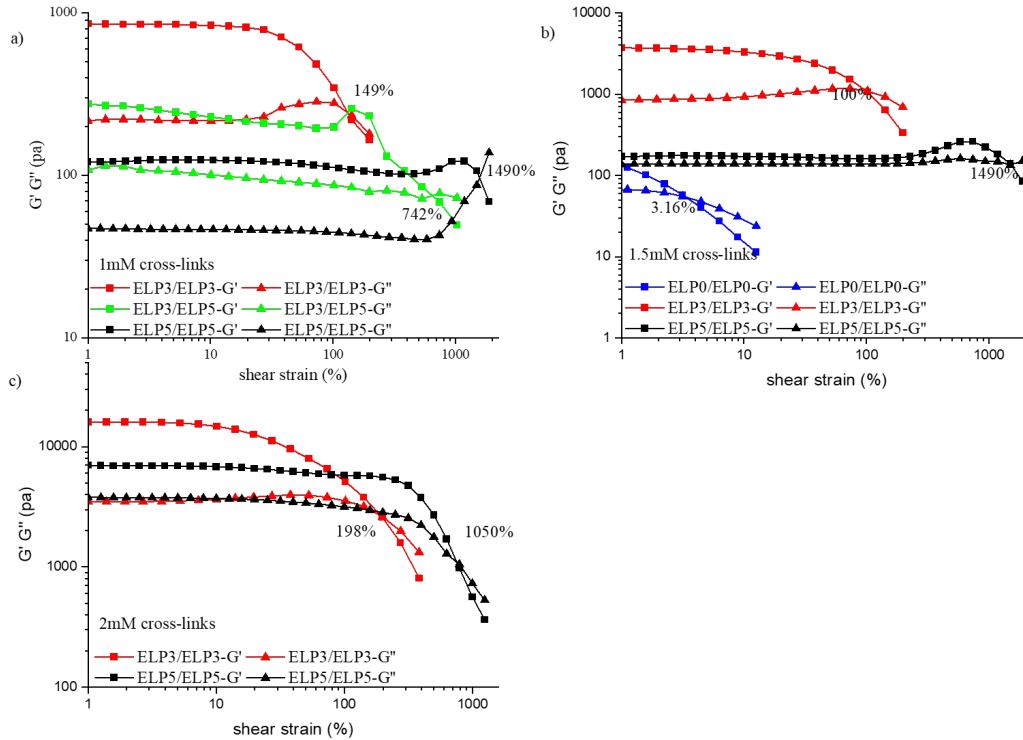


Figure 24. Amplitude sweeps of SpyCatcher/SpyTag cross-linked hydrogels, highlighting the effect of different RCPP lengths. a) Comparison of hydrogels with different ELP lengths, prepared at a concentration of 1.0 mM. b) Comparison of hydrogels with different ELP lengths, prepared at a concentration of 1.5 mM. c) Comparison of hydrogels with different ELP lengths, prepared at a concentration of 2.0 mM. The experiments were performed over a strain range from 1% to 2000% with an angular frequency of 10 rad s^{-1} .

This is confirmed when replotting the data to visualize the dependence of hydrogel properties as a function of RCPP length at a given protein concentration (**Figure 24**). At all protein concentrations (except 0.5 mM), the yield and flow points increase significantly with increasing ELP length. For example, for a

protein concentration of 1.0 mM (**Figure 24a**) the flow point increases from approximately 150% (ELP₃-ELP₃) to nearly 1500% (ELP₅-ELP₅). At the same time, increasing ELP length yields hydrogels with lower G' and a decreased ratio between G' and G'', suggesting that the material is more liquid. This result contradicts the fact that the cross-link concentration was maintained and the overall mass fraction of protein even increased. One possible explanation is that longer chains reduce the cross-linking efficiency and increase the number of defects in the network. The interpretation that less cross-links are formed for networks with the longer ELP chains is supported by the observation that the strain at the flow point showed a 10-fold increase while the length of the ELP chains hardly doubled. Overall, these results suggest that there may be an optimum ELP length to achieve efficient cross-linking.

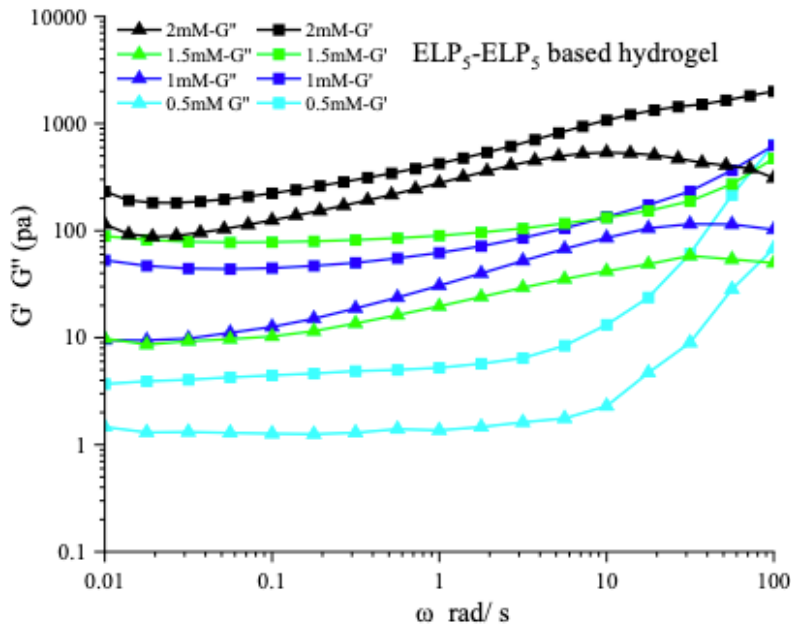


Figure 25. Frequency sweeps of DsRed-ELP₅-SpyCatcher-His/DsRed-ELP₅-SpyTag-His hydrogels, containing different protein concentrations. The angular frequency ranged from 0.01 to 100 rad s⁻¹. The strain amplitude was 5%.

Frequency sweeps were performed for the less efficiently cross-linked DsRed-ELP₅-SpyCatcher-His/DsRed-ELP₅-SpyTag-His hydrogels to determine if they display any stress relaxation (**Figure 25**). Over the entire frequency range tested, no crossover of the G' and G'' curves is observed, confirming the formation of an elastic material.

3.2.5 Determination of the fraction of SpyCatcher/SpyTag cross-links

As the fraction of cross-links formed appears to depend on the ELP length, an attempt was made to quantify the cross-linking efficiency. The SpyCatcher-SpyTag cross-linked DsRed-ELP star protein building blocks provide a unique opportunity to disassemble the network into its network chains (**Figure 26a**). Once the isopeptide bond between SpyCatcher and SpyTag formed, the only non-covalent interaction in the network is between the DsRed monomers. It should thus be possible to denature the DsRed tetramer with SDS and to visualize and quantify the disassembled fragments on SDS-PAGE.

The SDS-PAGE results of dissembled components are shown in **Figure 26b**. The gel shows 6 main bands. This is expected considering that 3 different fragments are formed (DsRed_{monomer}-SC/ST-DsRed_{monomer}, DsRed_{monomer}-SC and DsRed_{monomer}-ST) and that each fragment yields two bands (originating from DsRed). This makes it difficult to fully quantify this result, but the gel shows a clearly visible band of cross-linked network chains. This result forms an excellent basis for future work. The quantification of the cross-linking efficiency is usually not possible for hydrogels based on synthetic polymers, except specific cleavable bonds are introduced into the polymer backbone.^{85,86} Further developing this hydrogel platform introduced in this chapter may provide an excellent new strategy towards a better understanding of network structure.

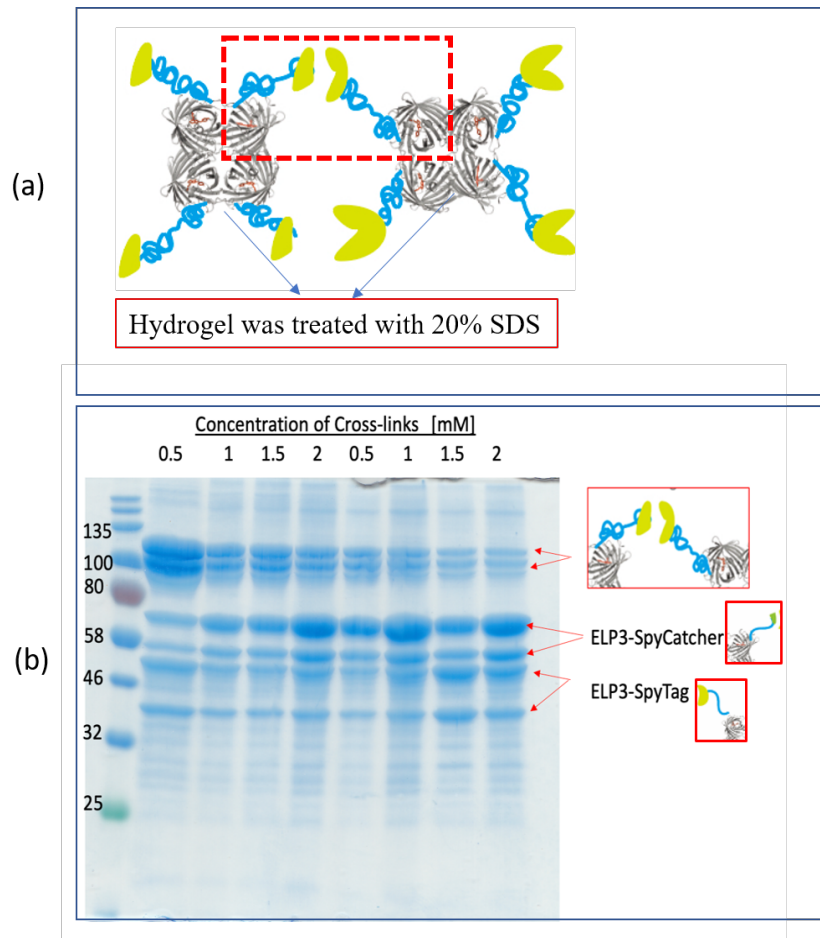


Figure 26. SDS-PAGE to determine the coupling efficiency of SpyCatcher and SpyTag in the hydrogel. a) Disassembly of the hydrogel into its network chains upon denaturation with SDS. b) SDS-PAGE of the disassembled DsRed-ELP₃-SpyCatcher-His/DsRed-ELP₃-SpyTag-His hydrogel.

3.3 Physically cross-linked DsRed-ELP_n star polymers (initial design)

3.3.1 Experimental setup and design

The goal of this chapter was to construct a series of recombinant protein-based hydrogels physically cross-linked via the heterodimeric CC A4B4. The hydrogel building blocks consisted of two DsRed-ELP star proteins, fused to either the CC-forming peptide A4 or B4 (**Figure 27**). The thermodynamic, kinetic and dynamic mechanical stabilities of A4B4 and several derivatives have been characterized.^{18,59,60,71,74,87} A4B4 has further been used as a physical cross-link for sPEG and polyisocyanopeptide hydrogels and it was intended to compare the properties of PEG-peptide hybrid hydrogels with structurally similar hydrogels based on protein-based star polymers.^{88,89}

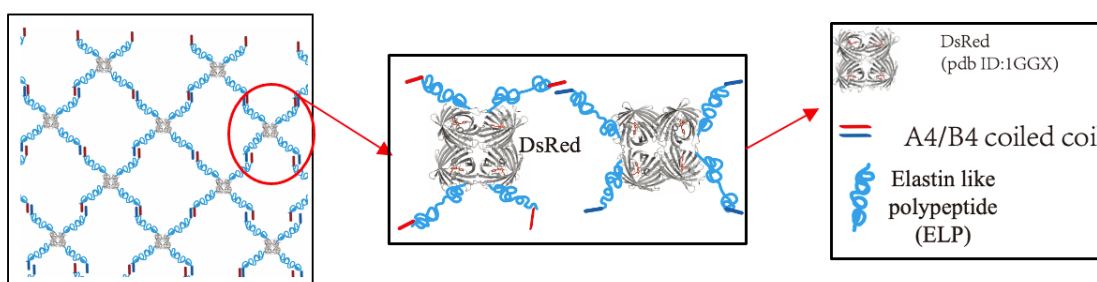


Figure 27. Physically cross-linked hydrogel based on DsRed-ELP star proteins, containing two different CC-forming peptides that fold into a heterodimeric CC.

The genes were designed in analogy to the DsRed-ELP star proteins introduced in **Chapter 3.2**. The initially designed constructs were intended to express the different components in the following order from N-terminus to C-terminus: His-DsRed(3CY)-ELP_n-A4 and B4-ELP_n-DsRed(3CY)-His. The position of A4 and B4 was chosen to provide the same RCPP attachment sites as for sPEG hydrogels previously characterized.⁸⁸ It is unknown, however, how the different locations of unstructured CC-forming peptides affect the expression of DsRed variants in *E. coli*.

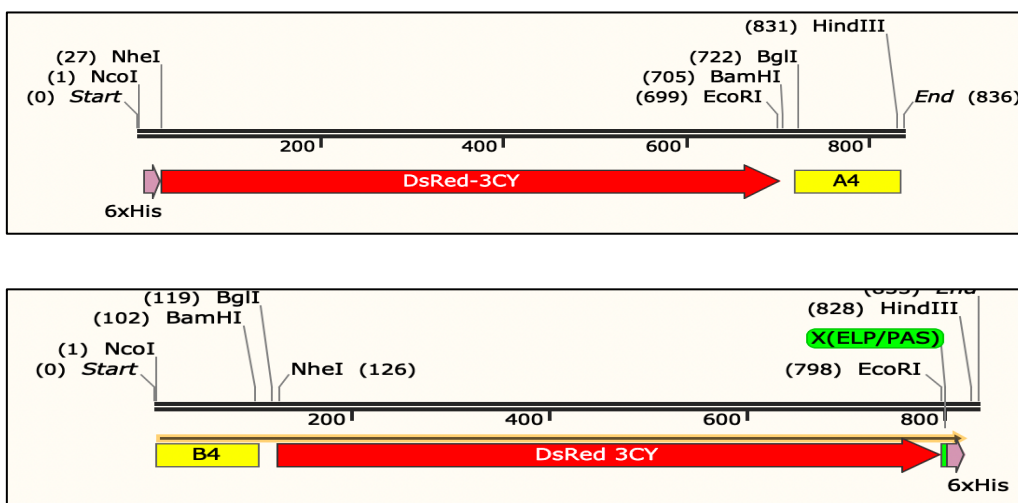


Figure 28. Expression cassettes for the star proteins His-DsRed(3CY)-linker-A4 and B4-linker-DsRed(3CY)-His. The previously used ELP fragments can be cloned via BamHI and BglI.

To facilitate cloning of these constructs, again two master plasmids (His-DsRed(3CY)-linker-A4 and B4-linker-DsRed(3CY)-His) were cloned. To utilize the same ELP fragments as in **Chapter 3.2**, a similar linker with BamHI and BglI restriction sites was designed. The gene constructs are shown in **Figure 28** and the full sequences are given in **appendix S1.3**.

3.3.2 Expression and characterization of the first generation of CC fusion proteins

Plasmids coding for the fusion proteins with ELP₅, ELP₉ and ELP₁₂ were transformed into BL21(DE3) and the proteins were expressed and purified as described (**Figure 29**). The molecular weight and yield of these proteins is given in **Table 7**. The yield was between 8 and 24 mg per liter of culture volume, which is much lower than for the SpyCatcher and SpyTag fusion proteins described in **Chapter 3.1**. This suggests that the unstructured and highly charged CC-forming peptides have a negative effect on the expression of these DsRed fusion proteins in *E. coli*.

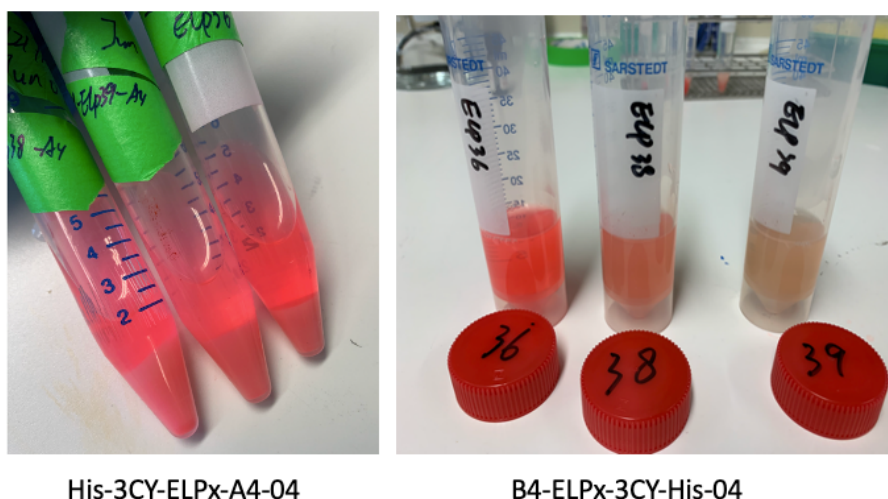


Figure 29. Expression test of His-DsRed(3CY)-ELP_n-A4 and B4-ELP_n-DsRed(3CY)-His. The samples show the non-cleared crude extracts. In the left image (His-DsRed(3CY)-ELP_n-A4), the order of samples is ELP₉, ELP₁₂ and ELP₅. In the right image (B4-ELP_n-DsRed(3CY)-His), the order of samples is ELP₅, ELP₉ and ELP₁₂.

Table 7. Molecular weight and yield of the DsRed-ELP star proteins fused to the CC-forming peptides A4 and B4. The yield is given as the mass of purified protein per liter of bacterial culture.

Protein	MW _{calc} (Da)	Yield (mg L ⁻¹)
His-DsRed(3CY)-linker-A4	30998.95	24
His-DsRed(3CY)-ELP ₅ -A4	53963.76	8
His-DsRed(3CY)-ELP ₉ -A4	72349.23	14
His-DsRed(3CY)-ELP ₁₂ -A4	86379.67	20
B4-linker-DsRed(3CY)-His	30911.32	20
B4-EPL ₅ -DsRed(3CY)-His	53876.14	16
B4-EPL ₉ -DsRed(3CY)-His	72261.61	10
B4-EPL ₁₂ -DsRed(3CY)-His	86292.05	-

Even though it has been shown earlier that the fusion of ELP sequences can improve the yield of difficult-to-express proteins, no general trend is seen for the

proteins expressed here. Combining the results in **Figure 29** and **Table 7**, it appears that the yield of the His-DsRed(3CY)-ELP_n-A4 is not strongly affected by the presence of the ELP sequences. In contrast, the yield clearly decreases with increasing ELP length for B4-ELP_n-DsRed(3CY)-His.

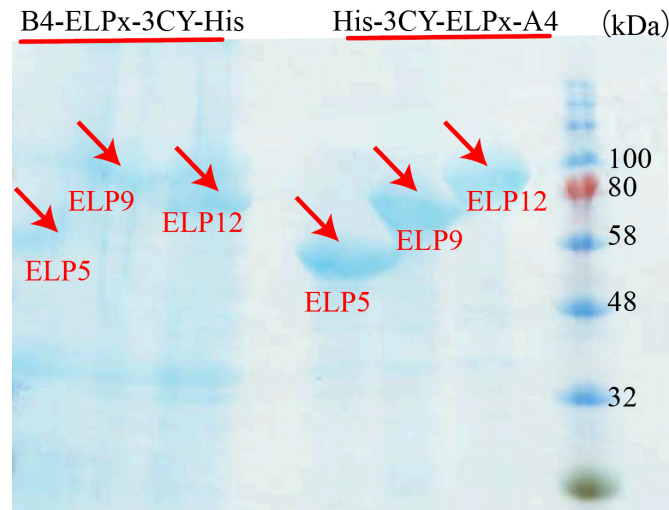


Figure 30. SDS-PAGE (12%) of the proteins His-DsRed(3CY)-ELP_n-A4 and B4-ELP_n-DsRed(3CY)-His. The purified His-DsRed(3CY)-ELP_n-A4 proteins yield a clearly defined band. In contrast, the B4-ELP_n-DsRed(3CY)-His are smeared out.

The purified protein variants were analyzed with SDS-PAGE (**Figure 30**). The bands of the fusion proteins with the C-terminal A4 peptide, His-DsRed(3CY)-ELP_n-A4, are well resolved and the proteins are rather pure. On the other hand, the bands for the fusion proteins with the N-terminal B4 peptide, B4-ELP_n-DsRed(3CY)-His, are smeared out. This may suggest that proteins with the B4 peptide have a tendency to aggregate. It has been shown earlier that the B4 peptide can form weak homodimers with a melting temperature around room temperature. Considering the tetravalent nature of the fusion proteins, this may be sufficient to induce the formation of larger aggregates.

Overall, this first design of fusion proteins shows that DsRed-ELP star proteins carrying CC-forming peptides are more difficult to express than fusion proteins with SpyCatcher and SpyTag. The N-terminal or C-terminal location of the CC-forming peptide and the histag does not seem to affect the yield of purified protein differently (**Table 7**). DsRed-ELP star proteins fused to the B4 peptide may form larger aggregates caused by the weak homodimerization of B4. At this point, it should be noted that each monomer of DsRed(3CY) contains a free Cys residue. This may further stabilize existing aggregates via the formation of disulfide bonds. This did not seem to present a problem in the other proteins; however, this Cys will be mutated in a new series of constructs introduced in the following chapter.

3.4 Physically cross-linked DsRed-ELP₃ and DsRed-PAS₈ star polymers

3.4.1 Experimental setup and design

The goal of this chapter was to improve the expression of the DsRed ELP star proteins fused to the CC-forming peptides described in **chapter 3.3**. This included a number of measures. These are:

- relocation of both CC-forming peptides to the C-terminus to facilitate a better comparison of the influence of A4 and B4 on expression yield,
- introduction of a modified B4 sequence with reduced homodimerization,
- introduction of the PAS RCPP sequence, which is known to well-expressed in *E. coli*,
- mutation of the Cys residue in position 117 of DsRed.T3 to Thr (as in DsRed-Express2),
- replacement of the expression strain BL21(DE3) with BLR(DE3),
- testing different inducer concentrations and expression temperatures.

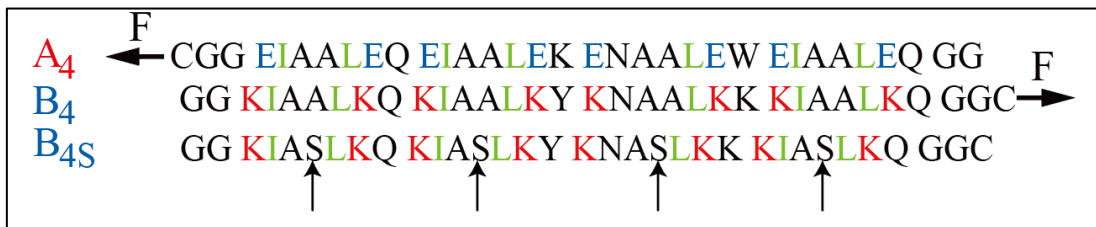


Figure 31. Sequences of the CC-forming peptides. The modification to reduce homodimer stability in B4 is indicated. In the c position of the CC heptad repeat, each Ala (A) was replaced with Ser (S). As Ser has a lower helix propensity, this reduced the thermodynamic stability of homodimeric as well as heterodimeric assemblies.

The modified B₄S sequence is shown in **Figure 31**. It has a lower overall helicity, which reduces the thermodynamic stability of the formed CC and also of possible homodimers.⁶⁰ A reduced stability of homodimers may decrease the tendency of

the fusion proteins to aggregate. The B4S peptide can still bind to A4 to form a CC.⁸⁹

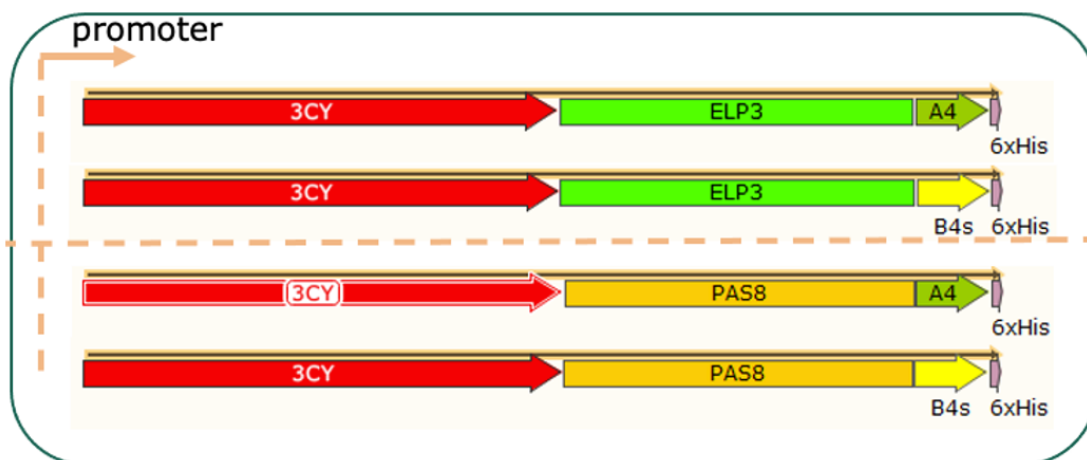


Figure 32. Expression cassette with the general layout of the DsRed_C117T-ELP_n/PAS_n-CC-His proteins. Instead of the wildtype DsRed.T3 protein a mutant was used where Cys in position 117 was replaced by Thr. Thr is the amino acid in the corresponding position of DsRed-Express2.

For the newly designed constructs, only the ELP₃ sequence was used. For the covalently cross-linked hydrogels in **Chapter 3.2**, this ELP length yielded the highest expression level and hydrogels with the highest ratio of G' to G". As indicated above, replacing the ELP sequence with the PAS polypeptide was tested. The PAS sequence is hydrophilic, and uncharged. PAS forms random coils without secondary structure and the biophysical properties of this biological polymer are comparable to those of PEG. In this project, the PAS sequence was designed such that its length was similar to ELP₃. The PAS sequence used contains 8 repeats of the amino acid sequence APAPASPAAPAPSAPAASPA. The gene design for all constructs is shown in **Figure 32**. The full protein sequences are given in **appendix S1.4** and their molecular weights are summarized in **Table 8**.

Table 8. Properties of the different DsRed_C117T-ELP_n/PAS_n-CC-His fusion proteins.

Protein	Isoelectric point	MW _{calc} (Da)
DsRed_C117T-ELP ₃ -A4-His	5.12	45138.45
DsRed_C117T-ELP ₃ -B4-His	6.71	45107.88
DsRed_C117T-ELP ₃ -B4S-His	6.71	45171.88
DsRed_C117T-PAS ₈ -A4-His	5.55	44609.14
DsRed_C117T-PAS ₈ -B4-His	8.86	44578.57
DsRed_C117T-PAS ₈ -B4S-His	8.86	44642.57

3.4.2. Expression and characterization of the redesigned CC fusion proteins

In total, 6 different fusion proteins with the general structure DsRed_C117T-ELP_n/PAS_n-CC-His were expressed and purified (**Table 8**). Expression was initially performed in BL21(DE3). An inducer concentration of 1 mM was used and cells were grown at 37°C for 3 h. **Figure 33** shows a semi-quantitative expression test. Comparing the intensity of the red color of DsRed, this experiment suggests that fusion proteins containing the B4 or B4S sequence show an overall higher expression than those containing the A4 sequence. The expression of the PAS-containing proteins is not better than that of the ELP-containing proteins.

The samples containing the ELP₃-containing proteins were further analyzed on SDS-PAGE (**Figure 34**). The gel confirms the low expression level of DsRed_C117T-ELP₃-A4-His. Very little protein is visible, both in the supernatant and in the pellet. In contrast, the overall expression yield of DsRed_C117T-ELP₃-B4-His and DsRed_C117T-ELP₃-B4S-His was much higher; however, most protein was found in the pellet. The proteins could form inclusion bodies or aggregate via B4 homodimerization. As no difference in the amount of soluble B4 and B4S fusion proteins was observed, inclusion body formation appears more likely.

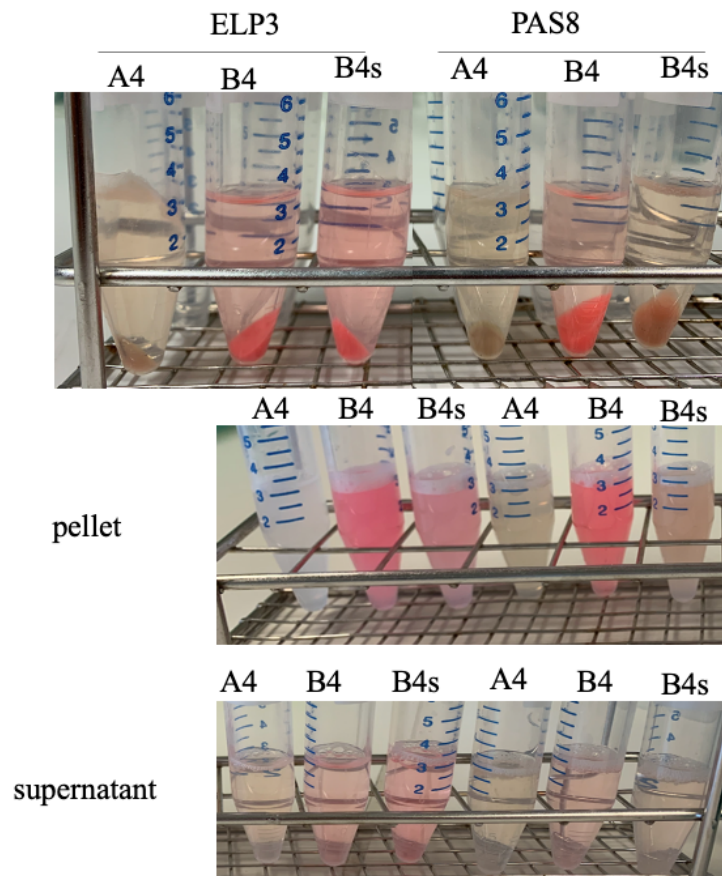


Figure 33. Visualization of protein expression for the DsRed_C117T-ELP_n/PAS_n-CC-His constructs. The top row shows the centrifuged cell lysate to highlight the red color of the pellet. The second row shows the resuspended pellet and the third row shows the supernatant containing soluble protein. The proteins were expressed in BL21(DE3), using 1 mM IPTG. Cells were grown at 37°C for 3 h after induction.

The proteins were purified as described and are shown in **Figure 34**. All proteins are reasonably pure, assuming that the lower-MW band again originates from fragmented DsRed. The yield of purified protein per liter of culture volume was similar to the proteins described in **Chapter 3.3**.

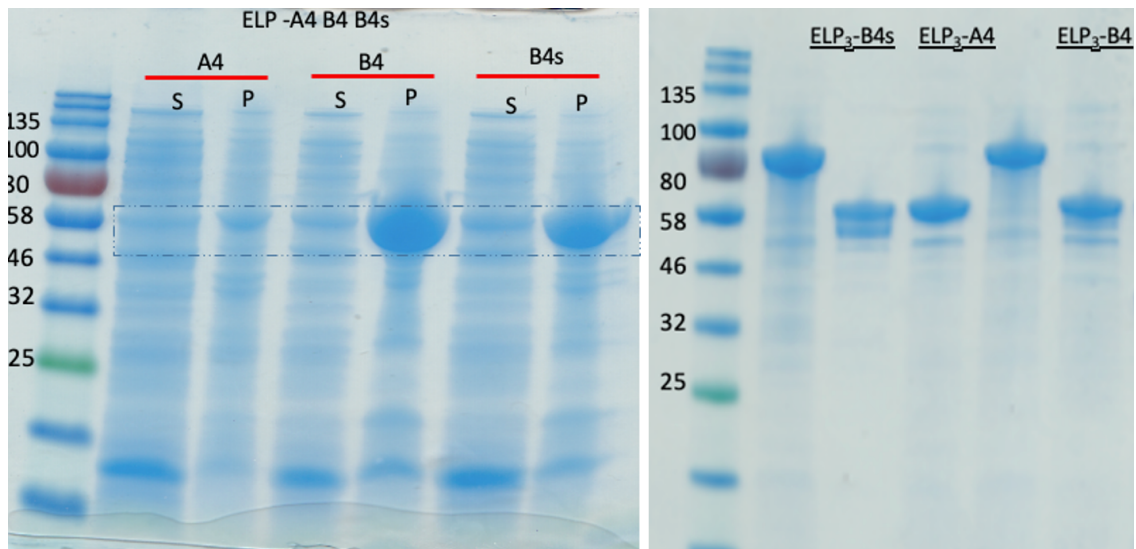


Figure 34. SDS-PAGE of the DsRed_C117T-ELP₃-CC-His proteins. Left: Comparison of the amount of soluble (supernatant, S) and insoluble (pellet, P) protein. Right: Purified proteins. The two proteins with a size above 80 kDa are not related to this project.

As a first step towards obtaining more overall and more soluble protein, BL21(DE3) was replaced with BLR(DE3). BLR, a recA-derivative of BL21, is known to be better suited for plasmids with repetitive sequences.⁹⁰ Taking advantage of the DsRed fusion protein, fluorescence of the growing cultures was monitored with a microplate reader (**Figure 33**). The ELP₃ and PAS₈ containing proteins fused to the A4 sequence do hardly show any increase in DsRed fluorescence (emission peak at 587 nm). The observed peak is scattered excitation light (535 nm) from the bacterial cells. A gradual increase in the fluorescence signal is observed for the fusion proteins containing the B4 or the B4S sequence. The data also shows, however, that chromophore maturation takes several hours, which is much longer than the time needed for these DsRed variants in the absence of a fusion partner.^{55–57} Furthermore, a difference in the chromophore maturation speed may exist for the fusion proteins containing either the ELP₃ or PAS₈ sequence. This suggests that C-terminal fusion partners have a strong influence on the expression and also the maturation speed of DsRed.

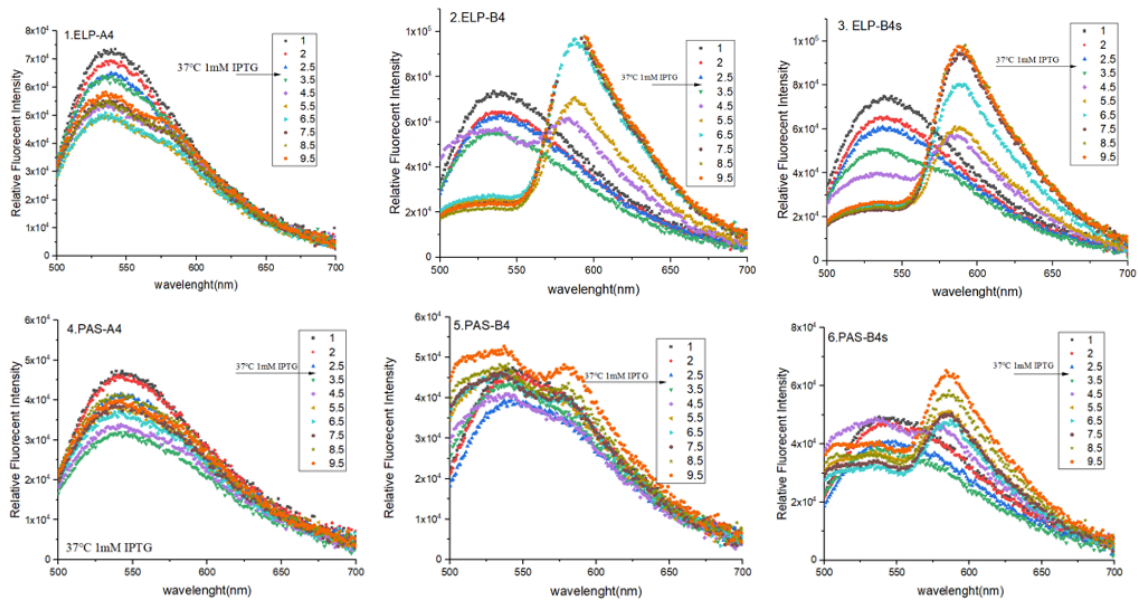


Figure 35. Increase of DsRed fluorescence in BLR(DE3) expression cultures. Expression was induced with 1 mM IPTG. Cultures were grown 37°C. For the recorded emission spectra, fluorescence was excited at 535 nm. The peak at 535 nm thus corresponds to light scattered by the bacterial cells.

The time evolution of DsRed fluorescence was subsequently compared for the protein DsRed_C117T-ELP₃-A4-His expressed in BLR(DE3) and BL21(DE) (**Figure 36**). A slightly better expression of the protein may be observed in BLR(DE3) so that this strain was used for all following experiments.

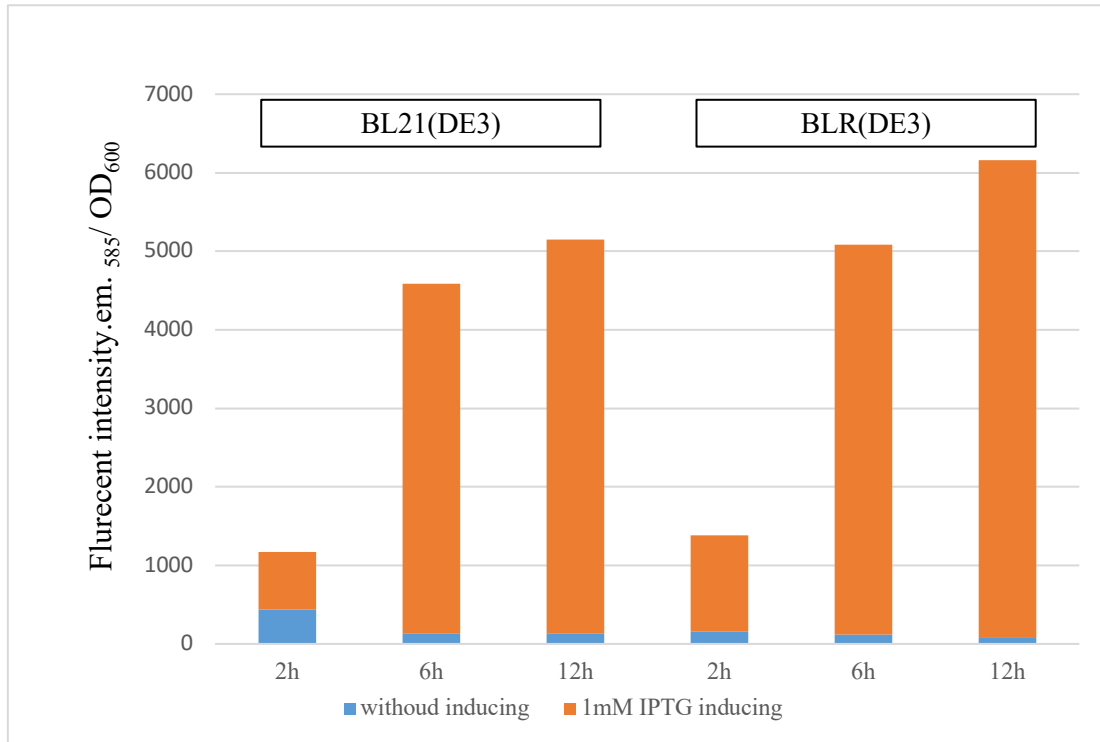


Figure 36. Comparison of the expression of DsRed_C117T-ELP₃-A4-His in BL21(DE3) and BLR(DE3). The fluorescence intensity of DsRed is slightly higher in BLR(DE3), suggesting that the yield of folded protein is increased. Expression was performed with 1 mM IPTG and cells were grown at 37°C.

A common strategy to improve the yield of soluble protein is to reduce the inducer concentration and to grow the cultures at a lower temperature. Here, the inducer concentration was reduced to 0.5 mM and the temperature was lowered to 16°C. For both parameters, no significant improvement for the expression of especially A4-containing fusion proteins was observed. It is currently unclear how C-terminal fusion partners affect DsRed expression and further research into this topic is needed. Eventually, a new gene design needs to be tested where the CC-forming sequences are relocated to the N-terminus.

3.4.3 Self-healing test of a CC-cross-linked hydrogel

For the two proteins DsRed_C117T-linker-A4-His and DsRed_C117T-ELP₃-B4S-His a sufficient amount of protein was obtained to prepare a hydrogel sample with a rather low protein concentration. The sample was characterized in a step strain experiment, which provides information about the reversibility of physical cross-link formation and thus self-healing. In a step strain experiment, an oscillatory strain is applied. The strain amplitude is suddenly switched between very low and very high values. At high strain values, (a fraction of) the cross-links are “broken” and can reform once the strain is lowered.

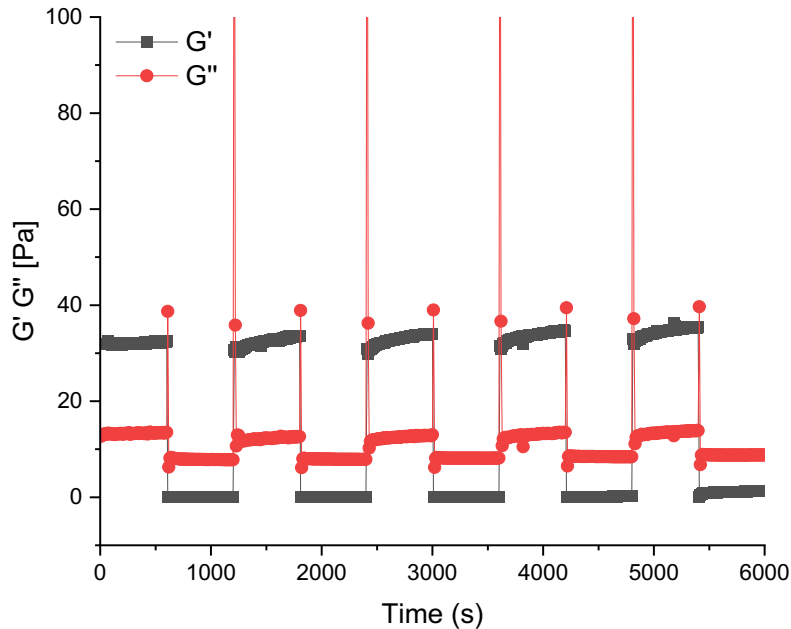


Figure 37. Step strain experiment of the CC cross-linked hydrogel. The cross-link concentration was 3.66 μM and the molar ratio of A4 and B4S was 1:1. The strain was set to an amplitude of 2000% to disrupt the formed network and switched back to an amplitude of 5% to monitor recovery. G' and G'' were measured at a constant angular frequency of 10 rad s^{-1} .

The step strain experiments revealed full recovery of G' within a very short time (~50 s) and over 5 cycles of the break-recovery process (**Figure 36**). This result suggests that the CCs successfully form reversible cross-links and that the CC-containing hydrogel is self-healing.

Despite these promising initial results, no more hydrogels were prepared and characterized. Unfortunately, the redesign of the gene constructs and all other measures tested did not improve the expression yield of the CC-containing ELP or PAS star proteins. More optimization is clearly needed until these hydrogel building blocks can be expressed and purified in sufficient quantities.

4. Discussion

4.1 Suitability of DsRed as a tetrameric core for protein-based hydrogels

The overall goal of this work was the development of chemically and physically cross-linked hydrogels based on recombinant star proteins. Such star protein building blocks can be used in analogy to sPEG, which is a frequent building block of hydrogels. One key component of such star proteins is the tetrameric core protein. In this work, the fluorescent protein DsRed was chosen. DsRed has been engineered for high expression yields in *E. coli*. Of particular interest was the fact that the DsRed tetramer is a mixture of monomers with “green” and “red” chromophores. Emission from the “green” chromophore is usually not observed as FRET occurs within the tetramer. This suggests that DsRed could possibly be engineered into a molecular force sensor. In other words, an increase in green fluorescence may be observed upon mechanical rupture of the tetramer. DsRed thus appeared as an ideal core protein with sensing function to read out core stability upon deformation.

In **Chapter 3.1**, 4 DsRed variants were designed based on DsRed.T3⁵⁵ and DsRed-Express2.⁵⁷ All variants were successfully expressed in *E. coli* with a high protein yield, especially the 3CY protein derived from DsRed.T3. To be suitable as a tetrameric core, the protein does not only need to express well. It also has to tolerate N-terminal and C-terminal fusion partners and be thermodynamically, kinetically and mechanically stable. DsRed.T3 has a higher fraction of “green” chromophores and was thus the first choice for hydrogel synthesis and to probe the response of the core protein to deformation inside the hydrogel.

The sequence of DsRed.T3 contains one Cys residue per monomer, which is located on the surface of the protein. It was thus possible to simply cross-link DsRed with sPEG-Mal to obtain a covalently cross-linked hydrogel. The cross-

linking reactions proceeds very quickly (**Figure 14**) and, as a result, probably yields an inhomogeneous hydrogel network. In the time sweep, the storage modulus also shows a plateau at only 100 to 200 Pa, which is low for a sPEG network with an sPEG cross-link concentration of 1.5 mM. This indeed suggests a high number of defects.

Using both amplitude sweeps and rotational stress-strain experiments, it was attempted to mechanically break the hydrogel and to observe a change in the spectral properties of DsRed. While shearing the sample, the fluorescence signal was monitored in a rheo-fluorescence setup. No clearly detectable change in DsRed fluorescence was observed. If DsRed tetramers are mechanically broken and green chromophores are generated, their number must be small. The more likely explanation, however, is that entangled polymer chains are pulled out from a weakly cross-linked network and that DsRed rupture does not occur. This suggests that the DsRed core tolerates force sufficiently well that other processes are more likely to occur upon deformation. Most probably, DsRed is sufficiently stable as a tetrameric core, an interpretation which is also supported by single-molecule mechanical experiments of the tetrameric protein streptavidin. To break a single streptavidin tetramer, a force of approximately 300 pN is required.⁶¹ It would, of course, be interesting to perform similar single-molecule experiments with DsRed. Eventually, the tetramer interface could also be engineered to obtain tetramers with different mechanical stabilities.

It should also be noted that limitations exist with the rheo-fluorescence setup that was used. The objective needs to be positioned at one specific location of the sample. If the material fails, cracks could initiate in other locations and would not be captured. This problem might be solved by combining fluorescence microscopy with AFM-based indentation or pulling experiments. In this way, it is

known that the maximum deformation happens close to the cantilever and that bond rupture most likely occurs in this region of the hydrogel sample.

4.2 Chemically cross-linked recombinant protein-based hydrogels

The goal of **Chapter 3.2** was to append the DsRed (DsRed.T3) core with ELPs to obtain a recombinant protein-based star polymer. Two protein stars were prepared, one that was “functionalized” with SpyCatcher and the other one with SpyTag. This protein ligation system spontaneously assembles and forms a covalent bond. In **Chapter 3.2**, it was successfully employed to covalently cross-link the two protein stars, yielding hydrogels with a storage modulus of several thousand Pa. SpyCatcher-SpyTag ligation has been utilized for the synthesis of a number of other hydrogels. But in most of these examples the interaction partners were inserted into linear RCPP chains, which most likely resulted in less regular networks than the more ordered tetrameric network prepared in this work.

Making use of a modular gene construct, protein stars with ELPs of different lengths could easily be cloned. The ELP length varied from approximately 60 to 260 nm. In combination with a construct without ELP, the length of network chains can thus be varied from 0 to above 500 nm. For comparison, the length of network chains in sPEG networks ranges from approximately 30 to 120 nm. Making use of this small library of DsRed-based hydrogel building blocks, the influence of the ELP length and the overall mass fraction of proteins on the resulting hydrogel properties was investigated. It was shown that the storage modulus increased with the overall mass fraction of protein as expected. More interestingly, the yield point and the flow point moved to higher strain values when the ELP length was increased. Increasing ELP length also decreased the coupling efficiency of the SpyCatcher and SpyTag system. This suggests that an ELP length-dependent trade-off exists between high stiffness and high toughness.

The use of DsRed-based protein stars did not only yield a novel biomaterial with tunable stiffness and toughness. It also provided a powerful method to detect the cross-linking efficiency in the network. For hydrogels made of synthetic polymers this is only possible when using polymers with engineered cleavable groups.^{85,86} The use of tetrameric core proteins thus opens up a new perspective for analyzing the efficiency of cross-linking in hydrogel networks, which is an important parameter that controls network topology and determines hydrogel stiffness.

Despite these initially highly promising results, the DsRed-ELP_n-SpyCatcher-His/DsRed-ELP_n-SpyTag-His hydrogel system still suffers from several limitations: (1) Even though the yield of purified protein is generally above 50 mg L⁻¹ of bacterial culture, the amount of protein is still the limiting factor for a more systematic analysis of how the properties of the molecular building blocks affect bulk material properties. Expression and purification need to be optimized and a scale-up from shake flask cultures to a fermenter may be needed. (2) In typical protein hydrogels, the protein concentrations are very high (i.e., >100 mg mL⁻¹). This concentration is close to the solubility limit of many proteins. A special focus thus needs to be on using highly soluble protein components. Here, the solubility limit of the SpyCatcher domain may have been reached and it will be interesting to test recently improved mutants of this protein.^{46,47,91} (3) The ability to characterize the cross-linking efficiency of the SpyCatcher-SpyTag protein ligation system has high potential; however, the fragmentation of DsRed complicates a fully quantitative analysis. Eventually other tetrameric fluorescent proteins can be used with a different chromophore structure. Also, other tetrameric protein building blocks, not based on fluorescent proteins, should provide the same possibility. (4) To achieve the goal of linking molecular and bulk material properties, rheology alone is not sufficient as a characterization method.

It should be tested if methods typically applied to tetrameric sPEG networks, such as small-angle neutron scattering⁶³ can also be applied to protein networks, which are of much higher complexity. This may also provide information about the presence of entanglements.

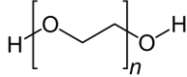
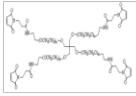
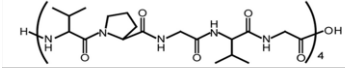
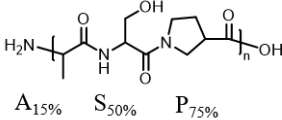
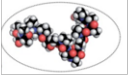
In the future, the DsRed-ELP_n-SpyCatcher-His/DsRed-ELP_n-SpyTag-His hydrogel system may find application as a material for fundamental studies of hydrogel properties in response to deformation. The mechanical properties of ELPs and the SpyCatcher-SpyTag adduct have been calibrated at the single-molecule level.^{50,78} As indicated in **Chapter 3.1** and **Chapter 4.1**, mechanical information about the DsRed tetramer is missing, but will hopefully be available in the near future. Making use of the sensitivity of ELPs to salt, pH and temperature, DsRed-ELP_n-SpyCatcher-His/DsRed-ELP_n-SpyTag-His may also be developed into stimulus-responsive or shape memory materials.

4.3 Physically cross-linked recombinant protein-based hydrogels

The main goal of **Chapter 3.3** and **Chapter 3.4** was to replace the covalent SpyCatcher-SpyTag cross-links with non-covalent CC cross-links. CCs are frequently used as dynamic physical cross-links in self-assembling and self-healing hydrogels. The second goal was to compare the performance of ELP and PAS RCPPs in comparison to PEG (**Table 9**). The A4B4 CC chosen in this work had already been used to cross-link sPEG. The CC fusion proteins were designed such that the CC-forming sequences were fused to the RCPP polymers at the same termini as they were coupled in these previously characterized sPEG networks. The A4 sequence was attached at its N-terminus while the B4-peptide was coupled at the C-terminus.⁸⁸ The DsRed-ELP_n-A4 fusion protein showed a low expression yield. At the same time, the B4-ELP-DsRed fusion protein had a

strong tendency to aggregate, which most likely originated from the tendency of the B4 sequence to form homodimers.

Table 9. Comparison of the RCPP proteins ELP and PAS to PEG. The figure of the PAS#1 structure was adapted from Breibeck et al.³⁶

Biopolymer	Composite	Structure	Source/sequence
Polyethylene glycol (4-arm-PEG) LC=63.6 arm		 Radius DLS(nm) 3.84±1.12	Chemical synthesis
Elastin Like Peptide (ELP) LC=66nm		?	[VPGMG-(VPGVG) ₈ -(VPGEG) ₂] ₃ Bio-synthesis
Proline-Serine-Alanine (PAS#1) LC=65nm		 Biopolymers, 2017	[A ₁₀ P ₇ S ₃] ₈ Bio-synthesis

A second-generation design of fusion proteins did not show any improved expression, especially for A4-containing proteins. Conley et al.⁸³ had shown that shorter ELPs can improve the protein yield. Thus, only ELP₃ was used instead of ELP₅, ELP₉ or ELP₁₂; however, without success. ELP₃ was also replaced with PAS₈. PAS is an RCPP sequence engineered to show high-level expression in *E. coli*. Again, no improvement could be achieved. A small improvement was obtained when using the expression strain BLR(DE3) instead of BL21(DE3). To reduce the aggregation tendency of the B4-containing proteins, the B4 sequence was replaced with B4S and the Cys in DsRed.T3 was removed. These modifications did not lead to any improvement in the yield of soluble protein. For both fusion proteins, lowering the inducer concentration and the temperature was also tested, but did not bring major improvements. It appears that the C-terminal fusion partner can have a large effect on the yield of DsRed fusion proteins, even

though the reason for these observations is currently unknown. The effect of C-terminal fusions partners is also confirmed when considering the maturation time of DsRed.T3, which is slower than the reported maturation time for improved DsRed variants without fusion partners.^{55,57} It is currently an open question how this problem can be overcome. At this moment, scaling up the expression culture appears as the only option to increase the amount of protein for hydrogel synthesis.

The obtained quantities of one A4- and one B4S-containing protein were finally used to fabricate a hydrogel, although with a very low protein concentration. These highly preliminary results suggest that the material is dynamically self-healing in a step-strain experiment. Once the expression level is optimized, the modular gene design allows the use of different well-characterized CCs.^{18,19,59,60,71,74} Most interestingly, the location of the CC-forming peptide at the N- or C-terminus of the fusion protein defines how the resulting CC will be mechanically loaded when inserted in a hydrogel under strain. It has been shown that CCs loaded in shear and unzip geometries rupture at different forces,^{59,71,92,93} which could be utilized to control the properties of hydrogels in the non-linear viscoelastic range. Considering that the second-generation constructs possess a histag next to the CC cross-link, a second type of cross-linking could possibly be implemented, using Histidine-metal coordination.¹⁹

5. Conclusions and Future Perspectives

In this thesis, the suitability of several protein structures to serve as building blocks in recombinant protein-based hydrogels was investigated. These included DsRed as a tetrameric core for protein-based star polymers, ELP and PAS sequences as RCPPs as well as SpyCatcher/SpyTag and CCs as chemical and physical cross-links, respectively. The DsRed variant DsRed.T3 was identified as a suitable core building block, primarily because of its excellent expression in *E. coli*. ELPs already find application in a wide range of different protein-based hydrogels. Their suitability to act as RCPPs in DsRed-based protein stars was confirmed in this work. The possible ELP alternative PAS did not show any improved expression, even though PAS sequences were developed to show high-level expression in *E. coli*. ELPs of different lengths were thus used as the main RCPPs in this work.

The SpyCatcher/SpyTag system served as a highly efficient covalent cross-link in DsRed-ELP_n-SpyCatcher-His/DsRed-ELP_n-SpyTag-His networks. Hydrogels with a storage modulus of several thousand Pa could be obtained, which is higher than what had been measured for many other recombinant protein-based hydrogels reported in the literature. Considering the modular gene design, a wide range of ELP lengths and thus hydrogel properties are easily accessible. Replacing the SpyCatcher/SpyTag system with a heterodimeric CC as a physical cross-link was a significant challenge as the CC-forming peptides had a large negative impact on the yield of soluble DsRed star proteins. It appears that C-terminal fusion partners affect the expression (and possibly also chromophore maturation of DsRed). The underlying reasons are currently unknown and further optimization is necessary before CC-cross-linked hydrogels can be prepared.

Physically cross-linked and modular recombinant protein-based hydrogels are promising candidates for the application as extracellular matrix mimics in tissue engineering. Further directions of research could focus on the following aspects. Mechanically calibrated molecular building blocks could be used to control the linear and non-linear viscoelastic properties of hydrogels at a bulk level. This could ultimately allow for the recombinant synthesis of hydrogels with tunable mechanical properties that can be used to direct the fate of cells. Recombinant hydrogels are easily functionalized with cell-adhesive sites, such as the RGD motif. The location and density of cell attachment sites can thus be programmed at the molecular level, again based on a modular fusion protein design. Last but not least, mechanoresponsive protein units can be inserted to serve as molecular force sensors. These include FRET-based sensors, previously inserted into the focal adhesion proteins talin and vinculin as well as the adherens junction protein catenin. Last but not least, DsRed can potentially be engineered to become a molecular force sensor itself after its response to mechanical forces has been studied at the single-molecule level. In summary, recombinant protein-based hydrogel have an enormous potential for applications in cell biology and also in the area of smart materials. One important prerequisite is that the number of suitable and characterized protein building blocks is increased. This thesis has contributed to this growing field and also highlighted current bottlenecks with characterizing the potential and limitations of a number of building blocks.

6. References

- (1) Wichterle, O.; Lím, D. Hydrophilic Gels for Biological Use. *Nature* **1960**, *185*, 117–118. <https://doi.org/10.1038/185117a0>.
- (2) Ullah, F.; Othman, M. B. H.; Javed, F.; Ahmad, Z.; Akil, H. Md. Classification, Processing and Application of Hydrogels: A Review. *Mater. Sci. Eng. C* **2015**, *57*, 414–433. <https://doi.org/10.1016/j.msec.2015.07.053>.
- (3) Dessì, M.; Borzacchiello, A.; Mohamed, T. H. A.; Abdel-Fattah, W. I.; Ambrosio, L. Novel Biomimetic Thermosensitive β -Tricalcium Phosphate/Chitosan-Based Hydrogels for Bone Tissue Engineering: β -TCP/Chitosan-Based Hydrogels for Bone Tissue Engineering. *J. Biomed. Mater. Res* **2013**, *101*, 2984–2993. <https://doi.org/10.1002/jbm.a.34592>.
- (4) Chaudhuri, O.; Gu, L.; Klumpers, D.; Darnell, M.; Bencherif, S. A.; Weaver, J. C.; Huebsch, N.; Lee, H.; Lippens, E.; Duda, G. N.; Mooney, D. J. Hydrogels with Tunable Stress Relaxation Regulate Stem Cell Fate and Activity. *Nat. Mater.* **2016**, *15* (3), 326–334. <https://doi.org/10.1038/nmat4489>.
- (5) Jansen, K. A.; Licup, A. J.; Sharma, A.; Rens, R.; MacKintosh, F. C.; Koenderink, G. H. The Role of Network Architecture in Collagen Mechanics. *Biophysical Journal* **2018**, *114* (11), 2665–2678. <https://doi.org/10.1016/j.bpj.2018.04.043>.
- (6) Shalumon, K. T.; Liao, H.-T.; Kuo, C.-Y.; Wong, C.-B.; Li, C.-J.; P.A., M.; Chen, J.-P. Rational Design of Gelatin/Nanohydroxyapatite Cryogel Scaffolds for Bone Regeneration by Introducing Chemical and Physical Cues to Enhance Osteogenesis of Bone Marrow Mesenchymal Stem

Cells. *Mater. Sci. Eng. C* **2019**, *104*, 109855.

<https://doi.org/10.1016/j.msec.2019.109855>.

- (7) Kim, S.; Min, S.; Choi, Y. S.; Jo, S.-H.; Jung, J. H.; Han, K.; Kim, J.; An, S.; Ji, Y. W.; Kim, Y.-G.; Cho, S.-W. Tissue Extracellular Matrix Hydrogels as Alternatives to Matrigel for Culturing Gastrointestinal Organoids. *Nat Commun* **2022**, *13* (1), 1692. <https://doi.org/10.1038/s41467-022-29279-4>.
- (8) Romano, N. H.; Sengupta, D.; Chung, C.; Heilshorn, S. C. Protein-Engineered Biomaterials: Nanoscale Mimics of the Extracellular Matrix. *Biochim. Biophys. Acta, Gen. Subj.* **2011**, *1810*, 339–349. <https://doi.org/10.1016/j.bbagen.2010.07.005>.
- (9) Lapenta, F.; Aupič, J.; Strmšek, Ž.; Jerala, R. Coiled Coil Protein Origami: From Modular Design Principles towards Biotechnological Applications. *Chem. Soc. Rev.* **2018**, *47*, 3530–3542. <https://doi.org/10.1039/C7CS00822H>.
- (10) Zhang, W.-B.; Sun, F.; Tirrell, D. A.; Arnold, F. H. Controlling Macromolecular Topology with Genetically Encoded SpyTag–SpyCatcher Chemistry. *J. Am. Chem. Soc.* **2013**, *135* (37), 13988–13997. <https://doi.org/10.1021/ja4076452>.
- (11) Zakeri, B.; Fierer, J. O.; Celik, E.; Chittock, E. C.; Schwarz-Linek, U.; Moy, V. T.; Howarth, M. Peptide Tag Forming a Rapid Covalent Bond to a Protein, through Engineering a Bacterial Adhesin. *Proc. Natl. Acad. Sci. U.S.A.* **2012**, *109*, E690–E697. <https://doi.org/10.1073/pnas.1115485109>.
- (12) Kersey, F. R.; Loveless, D. M.; Craig, S. L. A Hybrid Polymer Gel with Controlled Rates of Cross-Link Rupture and Self-Repair. *J. R. Soc. Interface* **2007**, *4* (13), 373–380. <https://doi.org/10.1098/rsif.2006.0187>.

- (13) Murphy, W. L.; Dillmore, W. S.; Modica, J.; Mrksich, M. Dynamic Hydrogels: Translating a Protein Conformational Change into Macroscopic Motion. *Angew. Chem. Int. Ed.* **2007**, *46*, 3066–3069. <https://doi.org/10.1002/anie.200604808>.
- (14) Fullenkamp, D. E.; He, L.; Barrett, D. G.; Burghardt, W. R.; Messersmith, P. B. Mussel-Inspired Histidine-Based Transient Network Metal Coordination Hydrogels. *Macromolecules* **2013**, *46* (3), 1167–1174. <https://doi.org/10.1021/ma301791n>.
- (15) Appel, E. A.; Forster, R. A.; Koutsioubas, A.; Toprakcioglu, C.; Scherman, O. A. Activation Energies Control the Macroscopic Properties of Physically Cross-Linked Materials. *Angew. Chem., Int. Ed.* **2014**, *53* (38), 10038–10043. <https://doi.org/10.1002/anie.201403192>.
- (16) Grindy, S. C.; Learsch, R.; Mozhdehi, D.; Cheng, J.; Barrett, D. G.; Guan, Z.; Messersmith, P. B.; Holten-Andersen, N. Control of Hierarchical Polymer Mechanics with Bioinspired Metal-Coordination Dynamics. *Nat. Mater.* **2015**, *14*, 1210–1216. <https://doi.org/10.1038/nmat4401>.
- (17) Li, Q.; Barrett, D. G.; Messersmith, P. B.; Holten-Andersen, N. Controlling Hydrogel Mechanics via Bio-Inspired Polymer-Nanoparticle Bond Dynamics. *ACS Nano* **2016**, *10*, 1317–1324. <https://doi.org/10.1021/acsnano.5b06692>.
- (18) Tunn, I.; De Léon, A. S.; Blank, K. G.; Harrington, M. J. Tuning Coiled Coil Stability with Histidine-Metal Coordination. *Nanoscale* **2018**, *10*, 22725–22729. <https://doi.org/10.1039/C8NR07259K>.
- (19) Tunn, I.; Harrington, M. J.; Blank, K. G. Bioinspired Histidine–Zn²⁺ Coordination for Tuning the Mechanical Properties of Self-Healing Coiled

Coil Cross-Linked Hydrogels. *Biomimetics* **2019**, *4*, 25.

<https://doi.org/10.3390/biomimetics4010025>.

- (20) Wu, J.; Li, P.; Dong, C.; Jiang, H.; Bin Xue; Gao, X.; Qin, M.; Wang, W.; Bin Chen; Cao, Y. Rationally Designed Synthetic Protein Hydrogels with Predictable Mechanical Properties. *Nature Communications* **2018**, *9* (1), 620. <https://doi.org/10.1038/s41467-018-02917-6>.
- (21) Yang, Z.; Kou, S.; Wei, X.; Zhang, F.; Li, F.; Wang, X.-W.; Lin, Y.; Wan, C.; Zhang, W.-B.; Sun, F. Genetically Programming Stress-Relaxation Behavior in Entirely Protein-Based Molecular Networks. *ACS Macro Lett.* **2018**, *7*, 1468–1474. <https://doi.org/10.1021/acsmacrolett.8b00845>.
- (22) Yang, Z.; Yang, Y.; Wang, M.; Wang, T.; Fok, H. K. F.; Jiang, B.; Xiao, W.; Kou, S.; Guo, Y.; Yan, Y.; Deng, X.; Zhang, W.-B.; Sun, F. Dynamically Tunable, Macroscopic Molecular Networks Enabled by Cellular Synthesis of 4-Arm Star-like Proteins. *Matter* **2020**, *2*, 233–249. <https://doi.org/10.1016/j.matt.2019.09.013>.
- (23) Klimek, K.; Ginalska, G. Proteins and Peptides as Important Modifiers of the Polymer Scaffolds for Tissue Engineering Applications—A Review. *Polymers* **2020**, *12*, 844. <https://doi.org/10.3390/polym12040844>.
- (24) Sakai, T.; Matsunaga, T.; Yamamoto, Y.; Ito, C.; Yoshida, R.; Suzuki, S.; Sasaki, N.; Shibayama, M.; Chung, U. Design and Fabrication of a High-Strength Hydrogel with Ideally Homogeneous Network Structure from Tetrahedron-like Macromonomers. *Macromolecules* **2008**, *41*, 5379–5384. <https://doi.org/10.1021/ma800476x>.
- (25) Lake, G. J. Fatigue and Fracture of Elastomers. *Rubber Chem. Technol.* **1995**, *68*, 435–460. <https://doi.org/10.5254/1.3538750>.

- (26) Cappello, J.; Crissman, J.; Dorman, M.; Mikolajczak, M.; Textor, G.; Marquet, M.; Ferrari, F. Genetic Engineering of Structural Protein Polymers. *Biotechnol. Prog.* **1990**, *6*, 198–202.
<https://doi.org/10.1021/bp00003a006>.
- (27) Urry, D. W.; Gowda, D. C.; Parker, T. M.; Luan, C.-H.; Reid, M. C.; Harris, C. M.; Pattanaik, A.; Harris, R. D. Hydrophobicity Scale for Proteins Based on Inverse Temperature Transitions. *Biopolymers* **1992**, *32*, 1243–1250.
<https://doi.org/10.1002/bip.360320913>.
- (28) Lee, J.; Macosko, C. W.; Urry, D. W. Mechanical Properties of Cross-Linked Synthetic Elastomeric Polypentapeptides. *Macromolecules* **2001**, *34*, 5968–5974. <https://doi.org/10.1021/ma0017844>.
- (29) Dinerman, A. A.; Cappello, J.; Ghandehari, H.; Hoag, S. W. Swelling Behavior of a Genetically Engineered Silk-Elastinlike Protein Polymer Hydrogel. *Biomaterials* **2002**, *23*, 4203–4210.
[https://doi.org/10.1016/S0142-9612\(02\)00164-3](https://doi.org/10.1016/S0142-9612(02)00164-3).
- (30) Sun, F.; Zhang, W.-B.; Mahdavi, A.; Arnold, F. H.; Tirrell, D. A. Synthesis of Bioactive Protein Hydrogels by Genetically Encoded SpyTag-SpyCatcher Chemistry. *Proc. Natl. Acad. Sci. U.S.A.* **2014**, *111*, 11269–11274. <https://doi.org/10.1073/pnas.1401291111>.
- (31) Liu, X.; Yang, X.; Yang, Z.; Luo, J.; Tian, X.; Liu, K.; Kou, S.; Sun, F. Versatile Engineered Protein Hydrogels Enabling Decoupled Mechanical and Biochemical Tuning for Cell Adhesion and Neurite Growth. *ACS Appl. Nano Mater.* **2018**, *1*, 1579–1585.
<https://doi.org/10.1021/acsanm.8b00077>.
- (32) Schellenberger, V.; Wang, C.; Geething, N. C.; Spink, B. J.; Campbell, A.; To, W.; Scholle, M. D.; Yin, Y.; Yao, Y.; Bogin, O.; Cleland, J. L.;

- Silverman, J.; Stemmer, W. P. C. A Recombinant Polypeptide Extends the in Vivo Half-Life of Peptides and Proteins in a Tunable Manner. *Nat. Biotechnol.* **2009**, *27*, 1186–1190. <https://doi.org/10.1038/nbt.1588>.
- (33) Podust, V. N.; Balan, S.; Sim, B.-C.; Coyle, M. P.; Ernst, U.; Peters, R. T.; Schellenberger, V. Extension of in Vivo Half-Life of Biologically Active Molecules by XTEN Protein Polymers. *J. Controlled Release* **2016**, *240*, 52–66. <https://doi.org/10.1016/j.jconrel.2015.10.038>.
- (34) Binder, U.; Skerra, A. PASylation®: A Versatile Technology to Extend Drug Delivery. *Curr. Opin. Colloid Interface Sci.* **2017**, *31*, 10–17. <https://doi.org/10.1016/j.cocis.2017.06.004>.
- (35) Gebauer, M.; Skerra, A. Prospects of PASylation® for the Design of Protein and Peptide Therapeutics with Extended Half-Life and Enhanced Action. *Bioorg. Med. Chem.* **2018**, *26*, 2882–2887. <https://doi.org/10.1016/j.bmc.2017.09.016>.
- (36) Breibeck, J.; Skerra, A. The Polypeptide Biophysics of Proline/Alanine-Rich Sequences (PAS): Recombinant Biopolymers with PEG-like Properties. *Biopolymers* **2018**, *109*, e23069. <https://doi.org/10.1002/bip.23069>.
- (37) Huang, Y.-S.; Wen, X.-F.; Wu, Y.-L.; Wang, Y.-F.; Fan, M.; Yang, Z.-Y.; Liu, W.; Zhou, L.-F. Engineering a Pharmacologically Superior Form of Granulocyte-Colony-Stimulating Factor by Fusion with Gelatin-like-Protein Polymer. *Eur. J. Pharm. Biopharm.* **2010**, *74*, 435–441. <https://doi.org/10.1016/j.ejpb.2009.12.002>.
- (38) Li, L.; Tong, Z.; Jia, X.; Kiick, K. L. Resilin-like Polypeptide Hydrogels Engineered for Versatile Biological Function. *Soft Matter* **2013**, *9*, 665–673. <https://doi.org/10.1039/C2SM26812D>.

- (39) Urry, D. W.; Luan, C. H.; Parker, T. M.; Gowda, D. C.; Prasad, K. U.; Reid, M. C.; Safavy, A. Temperature of Polypeptide Inverse Temperature Transition Depends on Mean Residue Hydrophobicity. *J. Am. Chem. Soc.* **1991**, *113* (11), 4346–4348. <https://doi.org/10.1021/ja00011a057>.
- (40) Li, N. K.; Quiroz, F. G.; Hall, C. K.; Chilkoti, A.; Yingling, Y. G. Molecular Description of the LCST Behavior of an Elastin-Like Polypeptide. *Biomacromolecules* **2014**, *15*, 3522–3530. <https://doi.org/10.1021/bm500658w>.
- (41) Rincón, A. C.; Molina-Martinez, I. T.; De Las Heras, B.; Alonso, M.; Bañez, C.; Rodríguez-Cabello, J. C.; Herrero-Vanrell, R. Biocompatibility of Elastin-like Polymer Poly(VPAVG) Microparticles: In Vitro And In Vivo Studies. *J. Biomed. Mater. Res.* **2006**, *78A* (2), 343–351. <https://doi.org/10.1002/jbm.a.30702>.
- (42) Tarakanova, A.; Huang, W.; Weiss, A. S.; Kaplan, D. L.; Buehler, M. J. Computational Smart Polymer Design Based on Elastin Protein Mutability. *Biomaterials* **2017**, *127*, 49–60. <https://doi.org/10.1016/j.biomaterials.2017.01.041>.
- (43) Breibeck, J.; Serafin, A.; Reichert, A.; Maier, S.; Küster, B.; Skerra, A. PAS-Cal: A Generic Recombinant Peptide Calibration Standard for Mass Spectrometry. *J. Am. Soc. Mass Spectrom.* **2014**, *25*, 1489–1497. <https://doi.org/10.1007/s13361-014-0902-3>.
- (44) Zakeri, B.; Howarth, M. Spontaneous Intermolecular Amide Bond Formation between Side Chains for Irreversible Peptide Targeting. *J. Am. Chem. Soc.* **2010**, *132*, 4526–4527. <https://doi.org/10.1021/ja910795a>.
- (45) Keeble, A. H.; Banerjee, A.; Ferla, M. P.; Reddington, S. C.; Anuar, I. N. A. K.; Howarth, M. Evolving Accelerated Amidation by SpyTag/SpyCatcher to

- Analyze Membrane Dynamics. *Angew. Chem. Int. Ed.* **2017**, *56* (52), 16521–16525. <https://doi.org/10.1002/anie.201707623>.
- (46) Hinrichsen, M.; Lenz, M.; Edwards, J. M.; Miller, O. K.; Mochrie, S. G. J.; Swain, P. S.; Schwarz-Linek, U.; Regan, L. A New Method for Post-Translationally Labeling Proteins in Live Cells for Fluorescence Imaging and Tracking. *Protein Engineering, Design and Selection* **2017**, *30* (12), 771–780. <https://doi.org/10.1093/protein/gzx059>.
- (47) Keeble, A. H.; Turkki, P.; Stokes, S.; Khairil Anuar, I. N. A.; Rahikainen, R.; Hytönen, V. P.; Howarth, M. Approaching Infinite Affinity through Engineering of Peptide–Protein Interaction. *Proc. Natl. Acad. Sci. U.S.A.* **2019**, *116* (52), 26523–26533. <https://doi.org/10.1073/pnas.1909653116>.
- (48) Hatlem, D.; Trunk, T.; Linke, D.; Leo, J. C. Catching a SPY: Using the SpyCatcher-SpyTag and Related Systems for Labeling and Localizing Bacterial Proteins. *IJMS* **2019**, *20* (9), 2129. <https://doi.org/10.3390/ijms20092129>.
- (49) Kang, H. J.; Coulibaly, F.; Clow, F.; Proft, T.; Baker, E. N. Stabilizing Isopeptide Bonds Revealed in Gram-Positive Bacterial Pilus Structure. *Science* **2007**, *318*, 1625–1628. <https://doi.org/10.1126/science.1145806>.
- (50) Guo, Z.; Hong, H.; Sun, H.; Zhang, X.; Wu, C.-X.; Li, B.; Cao, Y.; Chen, H. SpyTag/SpyCatcher Tether as a Fingerprint and Force Marker in Single-Molecule Force Spectroscopy Experiments. *Nanoscale* **2021**, *13*, 11262–11269. <https://doi.org/10.1039/D1NR01907D>.
- (51) Gao, X.; Fang, J.; Xue, B.; Fu, L.; Li, H. Engineering Protein Hydrogels Using SpyCatcher-SpyTag Chemistry. *Biomacromolecules* **2016**, *17*, 2812–2819. <https://doi.org/10.1021/acs.biomac.6b00566>.

- (52) Kou, S.; Yang, Z.; Luo, J.; Sun, F. Entirely Recombinant Protein-Based Hydrogels for Selective Heavy Metal Sequestration. *Polym. Chem.* **2017**, *8*, 6158–6164. <https://doi.org/10.1039/C7PY01206C>.
- (53) Wang, R.; Yang, Z.; Luo, J.; Hsing, I.-M.; Sun, F. B₁₂-Dependent Photoresponsive Protein Hydrogels for Controlled Stem Cell/Protein Release. *Proc. Natl. Acad. Sci. U.S.A.* **2017**, *114*, 5912–5917. <https://doi.org/10.1073/pnas.1621350114>.
- (54) Apostolovic, B.; Danial, M.; Klok, H.-A. Coiled Coils: Attractive Protein Folding Motifs for the Fabrication of Self-Assembled, Responsive and Bioactive Materials. *Chem. Soc. Rev.* **2010**, *39*, 3541–3575. <https://doi.org/10.1039/b914339b>.
- (55) Bevis, B. J.; Glick, B. S. Rapidly Maturing Variants of the Discosoma Red Fluorescent Protein (DsRed). *Nat. Biotechnol.* **2002**, *20*, 83–87. <https://doi.org/10.1038/nbt0102-83>.
- (56) Sørensen, M.; Lippuner, C.; Kaiser, T.; Mißlitz, A.; Aebischer, T.; Bumann, D. Rapidly Maturing Red Fluorescent Protein Variants with Strongly Enhanced Brightness in Bacteria. *FEBS Lett.* **2003**, *552*, 110–114. [https://doi.org/10.1016/S0014-5793\(03\)00856-1](https://doi.org/10.1016/S0014-5793(03)00856-1).
- (57) Strack, R. L.; Strongin, D. E.; Bhattacharyya, D.; Tao, W.; Berman, A.; Broxmeyer, H. E.; Keenan, R. J.; Glick, B. S. A Noncytotoxic DsRed Variant for Whole-Cell Labeling. *Nat. Methods* **2008**, *5*, 955–957. <https://doi.org/10.1038/nmeth.1264>.
- (58) Solovyev, I. D.; Gavshina, A. V.; Katti, A. S.; Chizhik, A. I.; Vinokurov, L. M.; Lapshin, G. D.; Ivashina, T. V.; Khrenova, M. G.; Kireev, I. I.; Gregor, I.; Enderlein, J.; Savitsky, A. P. Monomerization of the Photoconvertible Fluorescent Protein SAASoti by Rational Mutagenesis of Single Amino

Acids. *Sci. Rep.* **2018**, *8*, 15542. <https://doi.org/10.1038/s41598-018-33250-z>.

- (59) Goktas, M.; Luo, C.; Sullan, R. M. A.; Bergues-Pupo, A. E.; Lipowsky, R.; Vila Verde, A.; Blank, K. G. Molecular Mechanics of Coiled Coils Loaded in the Shear Geometry. *Chem. Sci.* **2018**, *9* (20), 4610–4621. <https://doi.org/10.1039/c8sc01037d>.
- (60) López-García, P.; Goktas, M.; Bergues-Pupo, A. E.; Kokschi, B.; Varón Silva, D.; Blank, K. G. Structural Determinants of Coiled Coil Mechanics. *Phys. Chem. Chem. Phys.* **2019**, *21*, 9145–9149. <https://doi.org/10.1039/C9CP00665F>.
- (61) Kim, M.; Wang, C.-C.; Benedetti, F.; Rabbi, M.; Bennett, V.; Marszalek, P. E. Nanomechanics of Streptavidin Hubs for Molecular Materials. *Adv. Mater.* **2011**, *23*, 5684–5688. <https://doi.org/10.1002/adma.201103316>.
- (62) Sacchetti, A.; Subramaniam, V.; Jovin, T.; Alberti, S. Oligomerization of DsRed Is Required for the Generation of a Functional Red Fluorescent Chromophore. *FEBS Lett.* **2002**, *525*, 13–19. [https://doi.org/10.1016/S0014-5793\(02\)02874-0](https://doi.org/10.1016/S0014-5793(02)02874-0).
- (63) Sakai, T.; Matsunaga, T.; Yamamoto, Y.; Ito, C.; Yoshida, R.; Suzuki, S.; Sasaki, N.; Shibayama, M.; Chung, U. Design and Fabrication of a High-Strength Hydrogel with Ideally Homogeneous Network Structure from Tetrahedron-like Macromonomers. *Macromolecules* **2008**, *41* (14), 5379–5384. <https://doi.org/10.1021/ma800476x>.
- (64) Xu, X.; Xu, Z.; Yang, X.; He, Y.; Lin, R. Construction and Characterization of a Pure Protein Hydrogel for Drug Delivery Application. *Int. J. Biol. Macromol.* **2017**, *95*, 294–298. <https://doi.org/10.1016/j.ijbiomac.2016.11.028>.

- (65) Zhang, X.; Chu, X.; Wang, L.; Wang, H.; Liang, G.; Zhang, J.; Long, J.; Yang, Z. Rational Design of a Tetrameric Protein to Enhance Interactions between Self-Assembled Fibers Gives Molecular Hydrogels. *Angew. Chem. Int. Ed.* **2012**, *51*, 4388–4392. <https://doi.org/10.1002/anie.201108612>.
- (66) Gu, Y.; Zhao, J.; Johnson, J. A. A (Macro)Molecular-Level Understanding of Polymer Network Topology. *Trends in Chemistry* **2019**, *1* (3), 318–334. <https://doi.org/10.1016/j.trechm.2019.02.017>.
- (67) Wheeldon, I. R.; Calabrese Barton, S.; Banta, S. Bioactive Proteinaceous Hydrogels from Designed Bifunctional Building Blocks. *Biomacromolecules* **2007**, *8*, 2990–2994. <https://doi.org/10.1021/bm700858p>.
- (68) Knoff, D. S.; Kim, S.; Fajardo Cortes, K. A.; Rivera, J.; Cathey, M. V. J.; Altamirano, D.; Camp, C.; Kim, M. Non-Covalently Associated Streptavidin Multi-Arm Nanohubs Exhibit Mechanical and Thermal Stability in Cross-Linked Protein-Network Materials. *Biomacromolecules* **2022**, *23*, 4130–4140. <https://doi.org/10.1021/acs.biomac.2c00544>.
- (69) Jiang, B.; Liu, X.; Yang, C.; Yang, Z.; Luo, J.; Kou, S.; Liu, K.; Sun, F. Injectable, Photoresponsive Hydrogels for Delivering Neuroprotective Proteins Enabled by Metal-Directed Protein Assembly. *Sci. Adv.* **2020**, *6*, eabc4824. <https://doi.org/10.1126/sciadv.abc4824>.
- (70) Li, H.; Cao, Y. Protein Mechanics: From Single Molecules to Functional Biomaterials. *Acc. Chem. Res.* **2010**, *43*, 1331–1341. <https://doi.org/10.1021/ar100057a>.
- (71) López-García, P.; Araujo, A. D.; Bergues-Pupo, A. E.; Tunn, I.; Fairlie, D. P.; Blank, K. G. Fortified Coiled Coils: Enhancing Mechanical Stability with

Lactam or Metal Staples. *Angew. Chem. Int. Ed.* **2021**, *60*, 232–236.

<https://doi.org/10.1002/anie.202006971>.

- (72) Norioka, C.; Inamoto, Y.; Hajime, C.; Kawamura, A.; Miyata, T. A Universal Method to Easily Design Tough and Stretchable Hydrogels. *NPG Asia Mater.* **2021**, *13*, 34. <https://doi.org/10.1038/s41427-021-00302-2>.
- (73) Grindy, S. C.; Learsch, R.; Mozhdehi, D.; Cheng, J.; Barrett, D. G.; Guan, Z.; Messersmith, P. B.; Holten-Andersen, N. Control of Hierarchical Polymer Mechanics with Bioinspired Metal-Coordination Dynamics. *Nat Mater* **2015**, *14* (12), 1210–1216. <https://doi.org/10.1038/nmat4401>.
- (74) Tsirigoni, A.; Goktas, M.; Atris, Z.; Valleriani, A.; Vila Verde, A.; Blank, K. G. Chain Sliding versus β -Sheet Formation upon Shearing Single α -Helical Coiled Coils. *Macromolecular Bioscience* **2023**, 2200563. <https://doi.org/10.1002/mabi.202200563>.
- (75) Makyła, K.; Müller, C.; Lörcher, S.; Winkler, T.; Nussbaumer, M. G.; Eder, M.; Bruns, N. Fluorescent Protein Senses and Reports Mechanical Damage in Glass-Fiber-Reinforced Polymer Composites. *Adv. Mater.* **2013**, *25* (19), 2701–2706. <https://doi.org/10.1002/adma.201205226>.
- (76) Zocchi, G. Controlling Proteins Through Molecular Springs. *Annu. Rev. Biophys.* **2009**, *38* (1), 75–88. <https://doi.org/10.1146/annurev.biophys.050708.133637>.
- (77) Gump, H.; Puchner, E. M.; Zimmermann, J. L.; Gerland, U.; Gaub, H. E.; Blank, K. Triggering Enzymatic Activity with Force. *Nano Lett.* **2009**, *9*, 3290–3295. <https://doi.org/10.1021/nl9015705>.
- (78) Ott, W.; Jobst, M. A.; Bauer, M. S.; Durner, E.; Milles, L. F.; Nash, M. A.; Gaub, H. E. Elastin-like Polypeptide Linkers for Single-Molecule Force

Spectroscopy. *ACS Nano* **6AD**, 11 (6), 6346–6354.

<https://doi.org/10.1021/acsnano.7b02694>.

- (79) Fong, B. A.; Wu, W.-Y.; Wood, D. W. Optimization of ELP-Intein Mediated Protein Purification by Salt Substitution. *Protein Expression Purif.* **2009**, 66, 198–202. <https://doi.org/10.1016/j.pep.2009.03.009>.
- (80) Hassouneh, W.; Christensen, T.; Chilkoti, A. Elastin-Like Polypeptides as a Purification Tag for Recombinant Proteins. *Curr. Protoc. Protein Sci.* **2010**, 61, 6.11.1-6.11.16. <https://doi.org/10.1002/0471140864.ps0611s61>.
- (81) Gross, L. A.; Baird, G. S.; Hoffman, R. C.; Baldrige, K. K.; Tsien, R. Y. The Structure of the Chromophore within DsRed, a Red Fluorescent Protein from Coral. *Proc. Natl. Acad. Sci. U.S.A.* **2000**, 97, 11990–11995. <https://doi.org/10.1073/pnas.97.22.11990>.
- (82) Meyer, D. E.; Trabbic-Carlson, K.; Chilkoti, A. Protein Purification by Fusion with an Environmentally Responsive Elastin-Like Polypeptide: Effect of Polypeptide Length on the Purification of Thioredoxin. *Biotechnol. Prog.* **2001**, 17, 720–728. <https://doi.org/10.1021/bp010049o>.
- (83) Conley, A. J.; Joensuu, J. J.; Jevnikar, A. M.; Menassa, R.; Brandle, J. E. Optimization of Elastin-like Polypeptide Fusions for Expression and Purification of Recombinant Proteins in Plants. *Biotechnol. Bioeng.* **2009**, 103, 562–573. <https://doi.org/10.1002/bit.22278>.
- (84) Strongin, D. E.; Bevis, B.; Khuong, N.; Downing, M. E.; Strack, R. L.; Sundaram, K.; Glick, B. S.; Keenan, R. J. Structural Rearrangements near the Chromophore Influence the Maturation Speed and Brightness of DsRed Variants. *Protein Eng., Des. Sel.* **2007**, 20, 525–534. <https://doi.org/10.1093/protein/gzm046>.

- (85) Wang, J.; Lin, T.-S.; Gu, Y.; Wang, R.; Olsen, B. D.; Johnson, J. A. Counting Secondary Loops Is Required for Accurate Prediction of End-Linked Polymer Network Elasticity. *ACS Macro Lett.* **2018**, *7*, 244–249. <https://doi.org/10.1021/acsmacrolett.8b00008>.
- (86) Wang, J.; Wang, R.; Gu, Y.; Sourakov, A.; Olsen, B. D.; Johnson, J. A. Counting Loops in Sidechain-Crosslinked Polymers from Elastic Solids to Single-Chain Nanoparticles. *Chem. Sci.* **2019**, *10*, 5332–5337. <https://doi.org/10.1039/C9SC01297D>.
- (87) Thomas, F.; Boyle, A. L.; Burton, A. J.; Woolfson, D. N. A Set of de Novo Designed Parallel Heterodimeric Coiled Coils with Quantified Dissociation Constants in the Micromolar to Sub-Nanomolar Regime. *J. Am. Chem. Soc.* **2013**, *135* (13), 5161–5166. <https://doi.org/10.1021/ja312310g>.
- (88) Grad, E. M.; Tunn, I.; Voerman, D.; de Léon, A. S.; Hammink, R.; Blank, K. G. Influence of Network Topology on the Viscoelastic Properties of Dynamically Crosslinked Hydrogels. *Front. Chem.* **2020**, *8*, 536. <https://doi.org/10.3389/fchem.2020.00536>.
- (89) Dånmark, S.; Aronsson, C.; Aili, D. Tailoring Supramolecular Peptide-Poly(Ethylene Glycol) Hydrogels by Coiled Coil Self-Assembly and Self-Sorting. *Biomacromolecules* **6AD**, *17* (6), 2260–2267. <https://doi.org/10.1021/acs.biomac.6b00528>.
- (90) Zhou, Y.; Huo, S.; Loznik, M.; Göstl, R.; Boersma, A. J.; Herrmann, A. Controlling Optical and Catalytic Activity of Genetically Engineered Proteins by Ultrasound. *Angew. Chem. Int. Ed.* **2021**, *60* (3), 1493–1497. <https://doi.org/10.1002/anie.202010324>.
- (91) Keeble, A. H.; Banerjee, A.; Ferla, M. P.; Reddington, S. C.; Anuar, I. N. A. K.; Howarth, M. Evolving Accelerated Amidation by SpyTag/SpyCatcher to

Analyze Membrane Dynamics. *Angew. Chem. Int. Ed.* **2017**, 56 (52), 16521–16525. <https://doi.org/10.1002/anie.201707623>.

- (92) Bornschlögl, T.; Rief, M. Single Molecule Unzipping of Coiled Coils: Sequence Resolved Stability Profiles. *Phys. Rev. Lett.* **2006**, 96 (11), 118102. <https://doi.org/10.1103/PhysRevLett.96.118102>.
- (93) Dietz, H.; Bornschlögl, T.; Heym, R.; König, F.; Rief, M. Programming Protein Self Assembly with Coiled Coils. *New J. Phys.* **2007**, 9 (11), 424.

7. Appendix

S1. Amino acid sequences

S1.1 Sequences of the DsRed variants used in Chapter 3.1

DsRed.T3 (3CY)

MVASSDVIKEFMRFKVRMEGSVNGHEFEIEGEGEGRPYEGTQTAKLKVTKG
GPLPFAWDILSPQFQYGSKVYVKHPADIPDYKKLSFPEGFKWERVMNFEDGG
VVTVTQDSSLQDGC**C**FIYKVKFIGVNFPSDGPVMQKKTMGWEPSTERLYPRDG
VLKGEIHKALKLKDGGHYLVEFKSIYMAKKPVQLPGYYYYVDSKLDITSHNEDYT
IVEQYERTEGRHHLFLEFH¹⁰HHHHH

DsRed Express2 (2TH)

MDSTENVIKPFMRFKVHMEGSVNGHEFEIEGEGEGKPYEGTQTAKLQVTKGG
PLPFAWDILSPQFQYGSKVYVKHPADIPDYKKLSFPEGFKWERVMNFEDGGV
VTVTQDSSLQDGT**T**FIYHVKFIGVNFPSDGPVMQKKT¹⁰LGWEPSTERLYPRDGV
LKGEIHKALKLKGGGHYLVFVKSIYMAKKPVKLP¹⁰GYYYYYVDSKLDITSHNEDYTV
VEQYERAEARHHLFQEF¹⁰HHHHH

DsRed Express2 (2CH)

MDSTENVIKPFMRFKVHMEGSVNGHEFEIEGEGEGKPYEGTQTAKLQVTKGG
PLPFAWDILSPQFQYGSKVYVKHPADIPDYKKLSFPEGFKWERVMNFEDGGV
VTVTQDSSLQDGC**C**FIYHVKFIGVNFPSDGPVMQKKT¹⁰LGWEPSTERLYPRDGV
LKGEIHKALKLKGGGHYLVFVKSIYMAKKPVKLP¹⁰GYYYYYVDSKLDITSHNEDYTV
VEQYERAEARHHLFQEF¹⁰HHHHH

DsRed Express2 (2THG)

MDSTENVIKPFMRFKVHMEGSVNGHEFEIEGEGEGKPYEGTQTAKLQVTKGG
PLPFAWDILSPQFQYGSKVYVKHPADIPDYKKLSFPEGFKWERVMNFEDGGV

VTVTQDSSLQDGTFIYHVKFIGVNFPSDGPVMQKKT LGWEPSTERLYPRDGV
LKGEIHKALKLKGGGHYLVEFKSIYMAKKPVKLPGYYYVDSKLDITSHNEDYTV
VEQYERAEARHHLFQEFHHHHHHGGC

DsRed(3CY)-ELP₉-ST-His

sequence as DsRed(3CY)-ELP₃-ST-His, but with **9 repeats** of the ELP sequence printed in bold

DsRed(3CY)-ELP₁₂-ST-His

sequence as DsRed(3CY)-ELP₃-ST-His, but with **12 repeats** of the ELP sequence printed in bold

S1.3 Sequences of the DsRed-ELP star proteins used in chapter 3.3

His-DsRed(3CY)-linker-A4

MGHHHHHHASSEDVIKEFMRFKVRMEGSVNGHEFEIEGEGEGRPYEGTQTA
KLKVTKGGPLPFAWDILSPQFQYGSKVYVKHPADIPDYKKLSFPEGFKWERV
MNFEDGGVVTVTQDSSLQDGCIFYKVKFIGVNFPSDGPVMQKKTMGWEPST
ERLYPRDGV LKGEIHKALKLKDGGHYLVEFKSIYMAKKPVQLPGYYYVDSKLDI
TSHNEDYTIVEQYERTEGRHHLFLEFGSGGPGWQGGEIAALEQEIAALEKENA
ALEWEIAALEQGG

B4-DsRed(3CY)-linker-His

MGGKIAALKQKIAALKYKNAALKKKIAALKQGGGSGGPGWQASSEDVIKEFMR
FKVRMEGSVNGHEFEIEGEGEGRPYEGTQTAKLKVTKGGPLPFAWDILSPQF
QYGSKVYVKHPADIPDYKKLSFPEGFKWERVMNFEDGGVVTVTQDSSLQDG
CFIYKVKFIGVNFPSDGPVMQKKTMGWEPSTERLYPRDGV LKGEIHKALKLKD
GGHYLVEFKSIYMAKKPVQLPGYYYVDSKLDITSHNEDYTIVEQYERTEGRHH
LFLEFH HHHHHH

His-DsRed(3CY)-ELP₅-A4

MGHHHHHHASSEDVIKEFMRFKVRMEGSVNGHEFEIEGEGEGRPYEGTQTA
KLKVTKGGPLPFAWDILSPQFQYGSKVYVKHPADIPDYKKLSFPEGFKWERV
MNFEDGGVVTVTQDSSLQDGCIFYKVKFIGVNFPSDGPVMQKKTMGWEPST
ERLYPRDGV LKGEIHKALKLKDGGHYLVEFKSIYMAKKPVQLPGYYYVDSKLDI
TSHNEDYTIVEQYERTEGRHHLFLEFGSGHG**VGVPGMGVPGVGVPGVPG**
VGVPGVPGVGVPGVGVPGVGVPGVGVPGEGVPGEGVPGVGVPGMGVPGVGP
GVGVPGVGVPGVGVPGVGVPGVGVPGVGVPGEGVPGEGVPGVGVPGMGV
PGVGVPGVGVPGVGVPGVGVPGVGVPGVGVPGVGVPGEGVPGEGVPGVGV
VPGMGVPGVGVPGVGVPGVGVPGVGVPGVGVPGVGVPGVGVPGEGVPGE

GVPGVGVPGMGVPGVGVPGVPGVGVPGVPGVGVPGVPGVGVPGVPGVGVPGVPG
EGVPGEGVPGWQQGGEIAALEQEIAALEKENAALEWEIAALEQGG

B4-DsRed(3CY)-ELP₅-His

MGGKIAALKQKIAALKYKNAALKKKIAALKQGGGSGHG**VGVPGMGVPGVGVP**
GVGVPGVGVPGVPGVGVPGVPGVGVPGVPGEGVPGEGVPGVGVPGMGV
PGVGVPGVPGVGVPGVPGVGVPGVPGVGVPGVPGEGVPGEGVPGVG
VPGMGVPGVGVPGVPGVGVPGVPGVGVPGVPGVGVPGVPGEGVPGE
GVPGVGVPGMGVPGVGVPGVPGVGVPGVPGVGVPGVPGVGVPGVPGVGVP
EGVPGEGVPGVGVPGMGVPGVGVPGVPGVGVPGVPGVGVPGVPGVGVP
GVGVPGEGVPGEGVPGWQASSEDVIKEFMRFKVRMEGSVNGHEFEIEGEGE
GRPYEGTQTAKLKVTKGGPLPFAWDILSPQFQYGSKVYVKHPADIPDYKKLSF
PEGFKWERVMNFEDGGVVTVTQDSSLQDGCFIYKVKFIGVNFPSDGPVMQK
KTMGWEPSTERLYPRDGVLKGEIHKALKLKDGGHYLVEFKSIYMAKKPVQLP
GYYYVDSKLDITSHNEDYTIVEQYERTEGRHHLFLEFHHHHHH

S1.4 Sequences of the DsRed-ELP and DsRed-PAS star proteins used in chapter 3.4

DsRed_C117T-ELP₃-A4-His

MVASSDVIKEFMRFKVRMEGSVNGHEFEIEGEGEGRPYEGTQTAKLKVTKG
GPLPFAWDILSPQFQYGSKVYVKHPADIPDYKKLSFPEGFKWERVMNFEDGG
VVTVTQDSSLQDGTFIYKVKFIGVNFPSDGPVMQKKTMGWEPSTERLYPRDG
VLKGEIHKALKLKDGGHYLVEFKSIYMAKKPVQLPGYYYVDSKLDITSHNEDYT
IVEQYERTEGRHHLFLEFGSGHG**VGVPGMGVPGVGVPGVGVPGVGVPGVGV**
VPGVGVPGVGVPGVGVPGEGVPGEVPGVGVPGMGVPGVGVPGVGVPGV
GVPGVGVPGVGVPGVGVPGVGVPGEGVPGEVPGVGVPGMGVPGVGVPG
VGVPGVGVPGVGVPGVGVPGVGVPGVGVPGEGVPGEVPGWQLGGEIAAL
EQEIAALEKENAALEWEIAALEQGGVDHHHHHH

DsRed_C₁₁₇T-ELP₃-B4-His

MVASSDVIKEFMRFKVRMEGSVNGHEFEIEGEGEGRPYEGTQTAKLKVTKG
GPLPFAWDILSPQFQYGSKVYVKHPADIPDYKKLSFPEGFKWERVMNFEDGG
VVTVTQDSSLQDGTFIYKVKFIGVNFPSDGPVMQKKTMGWEPSTERLYPRDG
VLKGEIHKALKLKDGGHYLVEFKSIYMAKKPVQLPGYYYVDSKLDITSHNEDYT
IVEQYERTEGRHHLFLEFGSGHG**VGVPGMGVPGVGVPGVGVPGVGVPGVGV**
VPGVGVPGVGVPGVGVPGEGVPGEVPGVGVPGMGVPGVGVPGVGVPGV
GVPGVGVPGVGVPGVGVPGVGVPGEGVPGEVPGVGVPGMGVPGVGVPG
VGVPGVGVPGVGVPGVGVPGVGVPGVGVPGEGVPGEVPGWQLGGKIAAL
KQKIAALKYKNAALKKKIAALKQGGVDHHHHHH

DsRed_C₁₁₇T-ELP₃-B4S-His

MVASSDVIKEFMRFKVRMEGSVNGHEFEIEGEGEGRPYEGTQTAKLKVTKG
GPLPFAWDILSPQFQYGSKVYVKHPADIPDYKKLSFPEGFKWERVMNFEDGG

VVTVTQDSSLQDGTFIYKVKFIGVNFPSDGPVMQKKTMGWEPSTERLYPRDG
VLKGEIHKALKLKDGGHYLVEFKSIYMAKKPVQLPGYYYVDSKLDITSHNEDYT
IVEQYERTEGRHHLFLEFGSGHG**VGVPGMGVPGVGVPGVGVPGVGVPGVGV**
VPGVGVPGVGVPGVGVPGEGVPGEVPGVGVPGMGVPGVGVPGVGVPGV
GVPGVGVPGVGVPGVGVPGVGVPGEGVPGEVPGVGVPGMGVPGVGVPG
VGVPGVGVPGVGVPGVGVPGVGVPGVGVPGEGVPGEVPGWQLGGKISAL
KQKISALKYKNSALKKKISALKQGGVDHHHHHH

DsRed_C₁₁₇T-PAS₈-A4-His

MVASEDVIKEFMRFKVRMEGSVNGHEFEIEGEGEGRPYEGTQTAKLKVTKG
GPLPFAWDILSPQFQYGSKVYVKHPADIPDYKKLSFPEGFKWERVMNFEDGG
VVTVTQDSSLQDGTFIYKVKFIGVNFPSDGPVMQKKTMGWEPSTERLYPRDG
VLKGEIHKALKLKDGGHYLVEFKSIYMAKKPVQLPGYYYVDSKLDITSHNEDYT
IVEQYERTEGRHHLFLEFGSG**APAPASPAAPAPSAPAASPAAPAPASPAAPA**
PSAPAASPAAPAPASPAAPAPSAPAASPAAPAPASPAAPAPSAPAASPAAPAP
ASPAAPAPSAPAASPAAPAPASPAAPAPSAPAASPAAPAPASPAAPAPSAPAA
SPAAPAPASPAAPAPSAPAASPAAPAWQLGGEIAALEQEIAALEKENAALEWE
IAALEQGGVDHHHHHH

DsRed_C₁₁₇T-PAS₈-B4-His

MVASEDVIKEFMRFKVRMEGSVNGHEFEIEGEGEGRPYEGTQTAKLKVTKG
GPLPFAWDILSPQFQYGSKVYVKHPADIPDYKKLSFPEGFKWERVMNFEDGG
VVTVTQDSSLQDGTFIYKVKFIGVNFPSDGPVMQKKTMGWEPSTERLYPRDG
VLKGEIHKALKLKDGGHYLVEFKSIYMAKKPVQLPGYYYVDSKLDITSHNEDYT
IVEQYERTEGRHHLFLEFGSG**APAPASPAAPAPSAPAASPAAPAPASPAAPA**
PSAPAASPAAPAPASPAAPAPSAPAASPAAPAPASPAAPAPSAPAASPAAPAP
ASPAAPAPSAPAASPAAPAPASPAAPAPSAPAASPAAPAPASPAAPAPSAPAA

SPAAPAPASPAAPAPSAPAASPAAPAWQLGGKIAALKQKIAALKYKNAALKKKI
AALKQGGVDHHHHHH

DsRed_C117T-PAS₈-B4S-His

MVASSDVIKEFMRFKVRMEGSVNGHEFEIEGEGEGRPYEGTQTAKLKVTKG
GPLPFAWDILSPQFQYGSKVYVKHPADIPDYKKLSFPEGFKWERVMNFEDGG
VVTVTQDSSLQDGTFIYKVKFIGVNFPSDGPVMQKKTMGWEPSTERLYPRDG
VLKGEIHKALKLKDGGHYLVEFKSIYMAKKPVQLPGYYYYVDSKLDITSHNEDYT
IVEQYERTEGRHHLFLEFGSG**APAPASPAAPAPSAPAASPAAPAPASPAAPA**
PSAPAASPAAPAPASPAAPAPSAPAASPAAPAPASPAAPAPSAPAASPAAPAP
ASPAAPAPSAPAASPAAPAPASPAAPAPSAPAASPAAPAPASPAAPAPSAPAA
SPAAPAPASPAAPAPSAPAASPAAPAWQLGGKISALKQKISALKYKNSALKKKI
SALKQGGVDHHHHHH

S2. List of primers

Table S1. Primers for gene sequencing

Name	Sequence (5'-3')
Removal - <i>Bgl</i> I - fwd	TGGCACGACAGGTTTCCCGA
Removal - <i>Bgl</i> I - rev	AACTCTCTCAGGGCCAGG
T7	TAATACGACTCACTATAGGG
T7term	TGCTAGTTATTGCTCAGCGG

S3. MALDI-TOF of the proteins used

S3.1 MALDI-TOF of the DsRed variants used in chapter 3.1

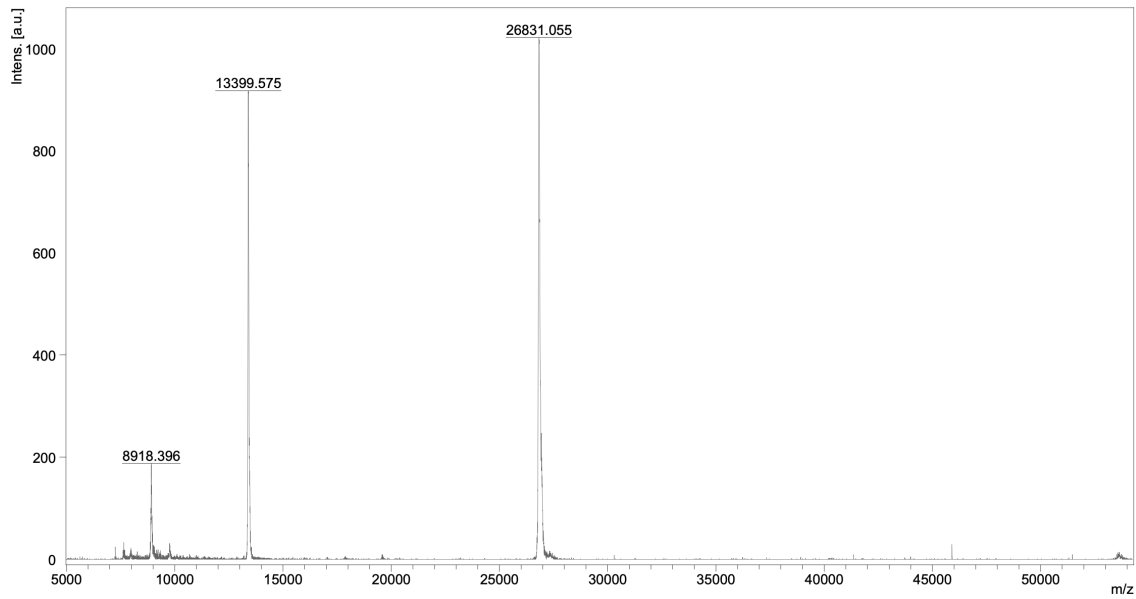


Figure S1. MALDI-TOF spectrum of DsRed 3CY (measured: 26831.1 Da; calculated: 27007.65 Da)

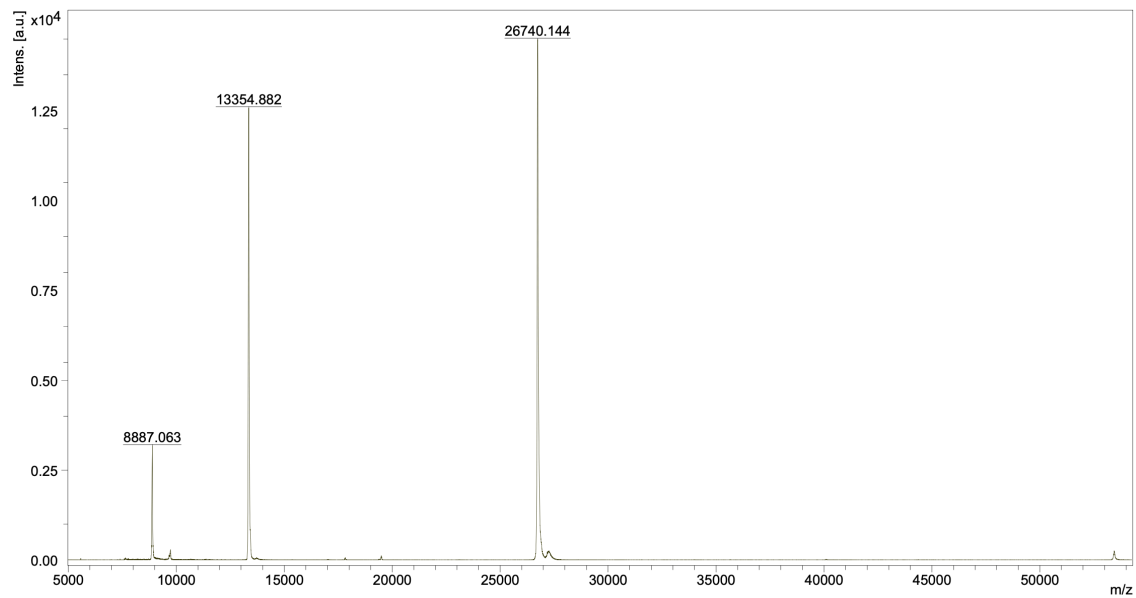


Figure S2. MALDI-TOF spectrum of DsRed 2TH (measured: 26740.1 Da; calculated: 26802.32 Da).

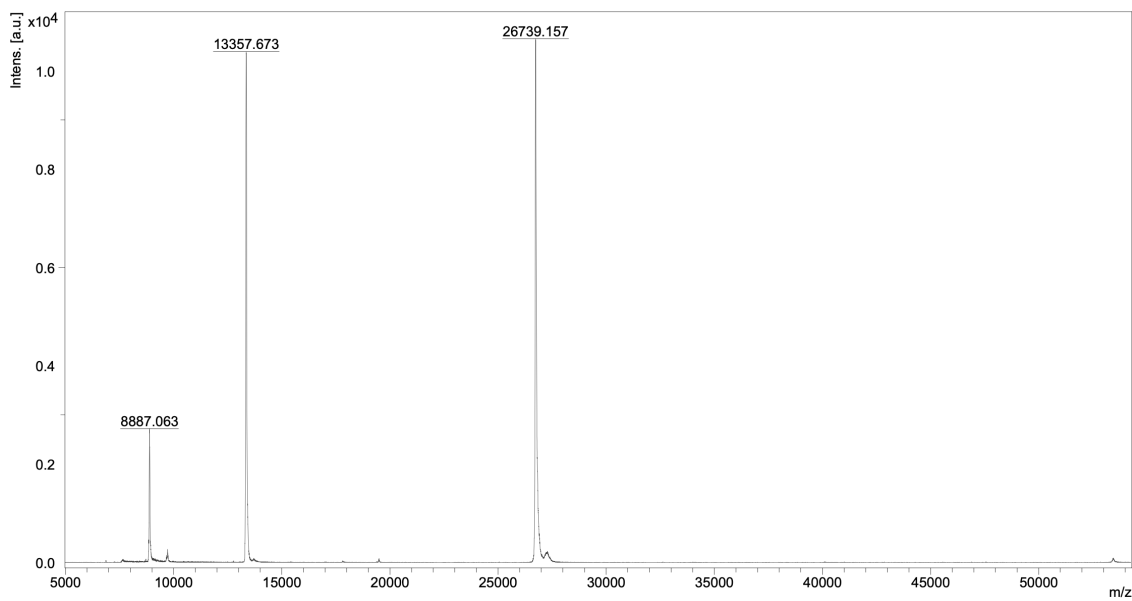


Figure S3. MALDI-TOF spectrum of DsRed 2CH (measured: 26739.2 Da; calculated: 26804.35 Da)

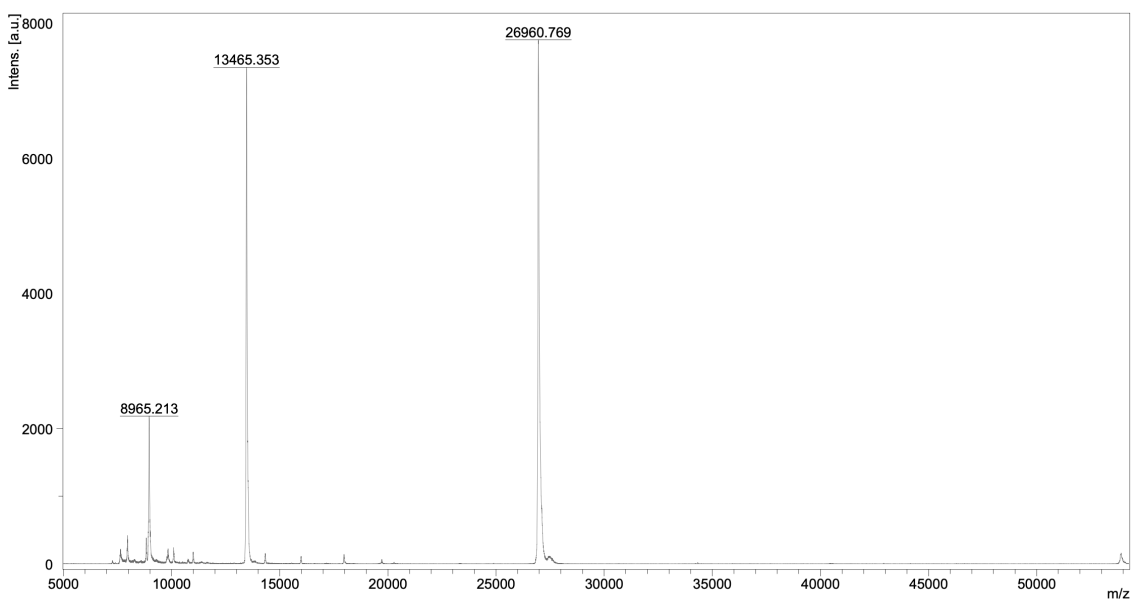


Figure S4. MALDI-TOF spectrum of DsRed 2THG (measured: 26960.8 Da; calculated: 27019.5 Da)

S3.2 MALDI-TOF of the DsRed-ELP star proteins used in chapter 3.2

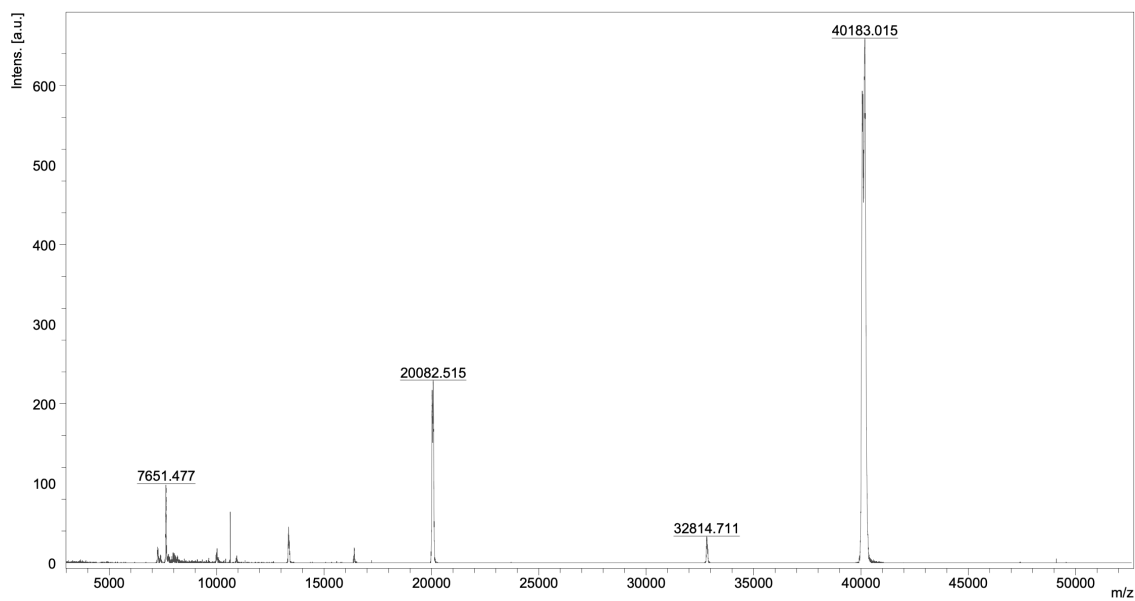


Figure S5. MALDI-TOF spectrum of DsRed(3CY)-ELP₀-SC-His (measured: 40183.0 Da; calculated: 40513.30 Da)

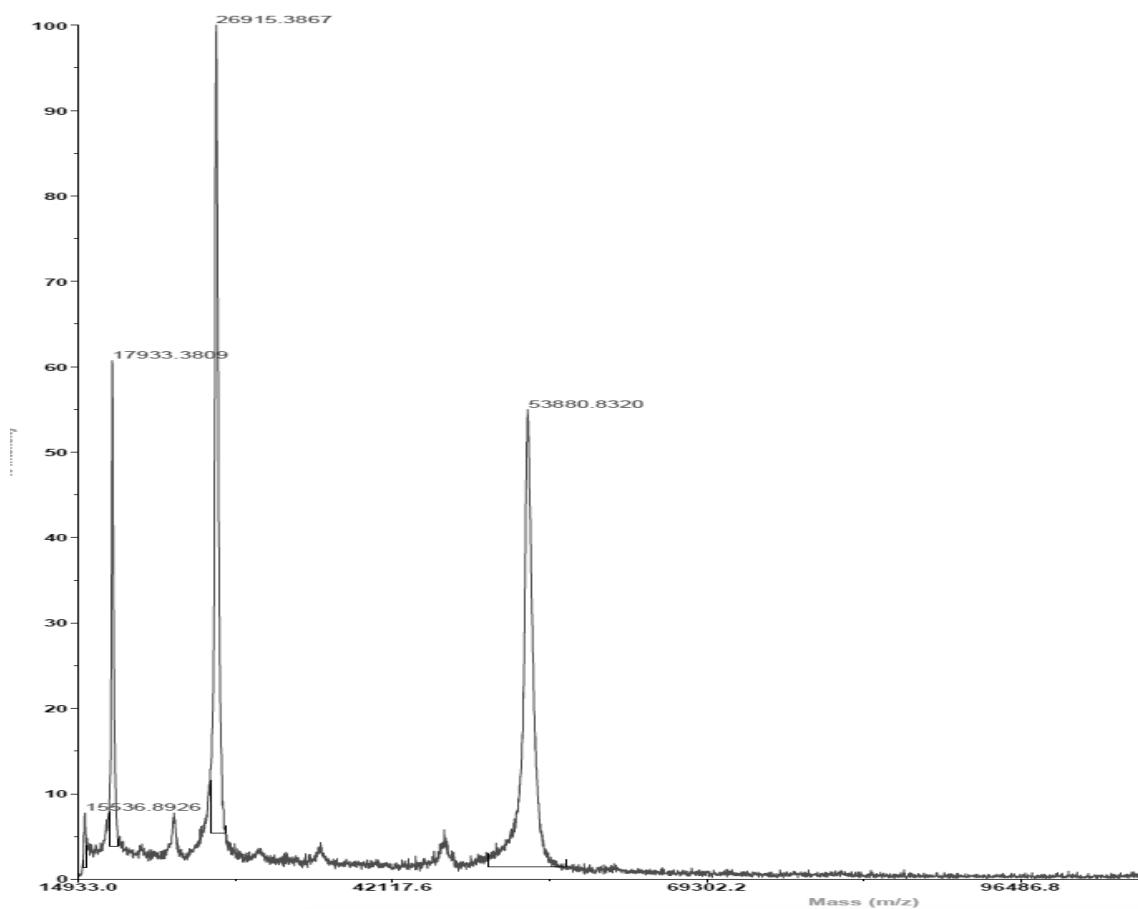


Figure S6. MALDI-TOF spectrum of DsRed(3CY)-ELP₃-SC-His (measured: 53880.8 Da; calculated: 54043.1 Da)

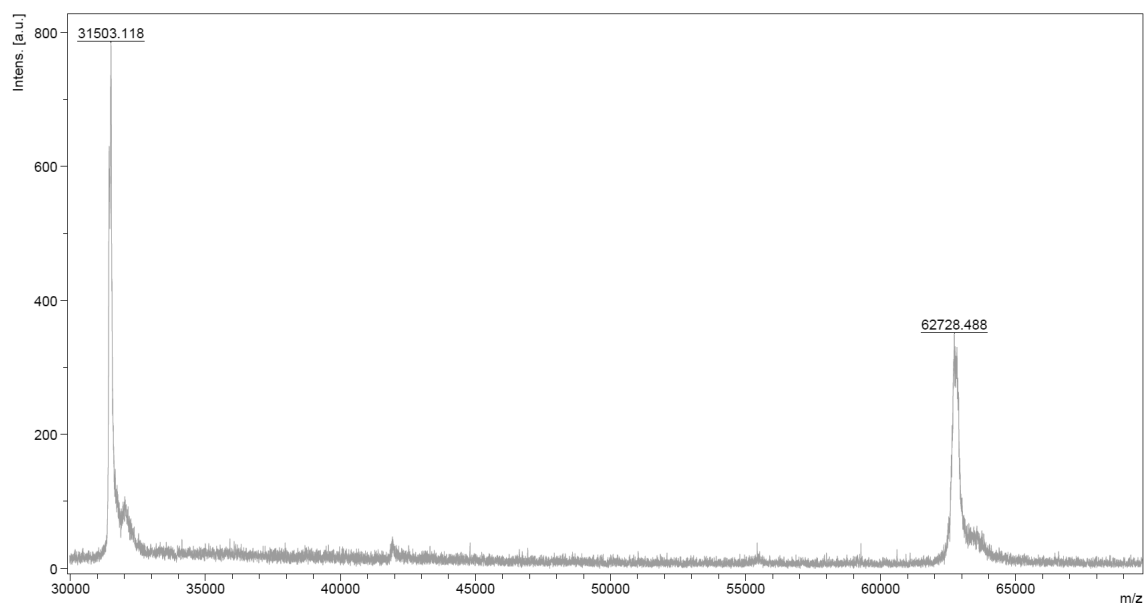


Figure S7. MALDI-TOF spectrum of DsRed(3CY)-ELP₅-SC-His (measured: 62728.5; calculated: 63235.8 Da).

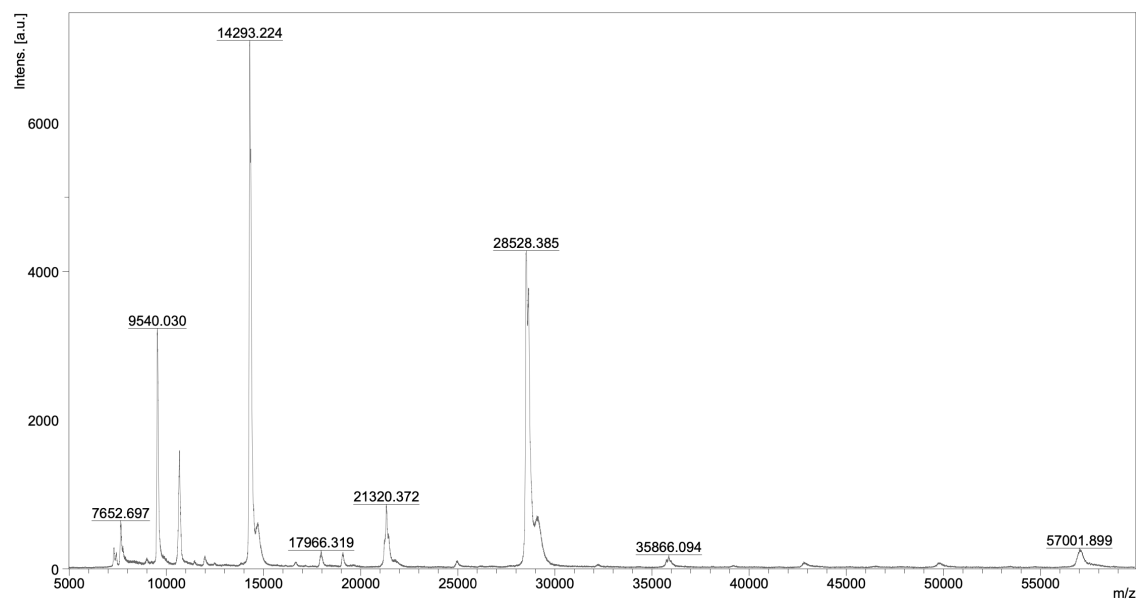


Figure S8. MALDI-TOF spectrum of DsRed(3CY)-ELP₀-ST-His (measured: 28528.4 Da; calculated: 28749.63 Da).

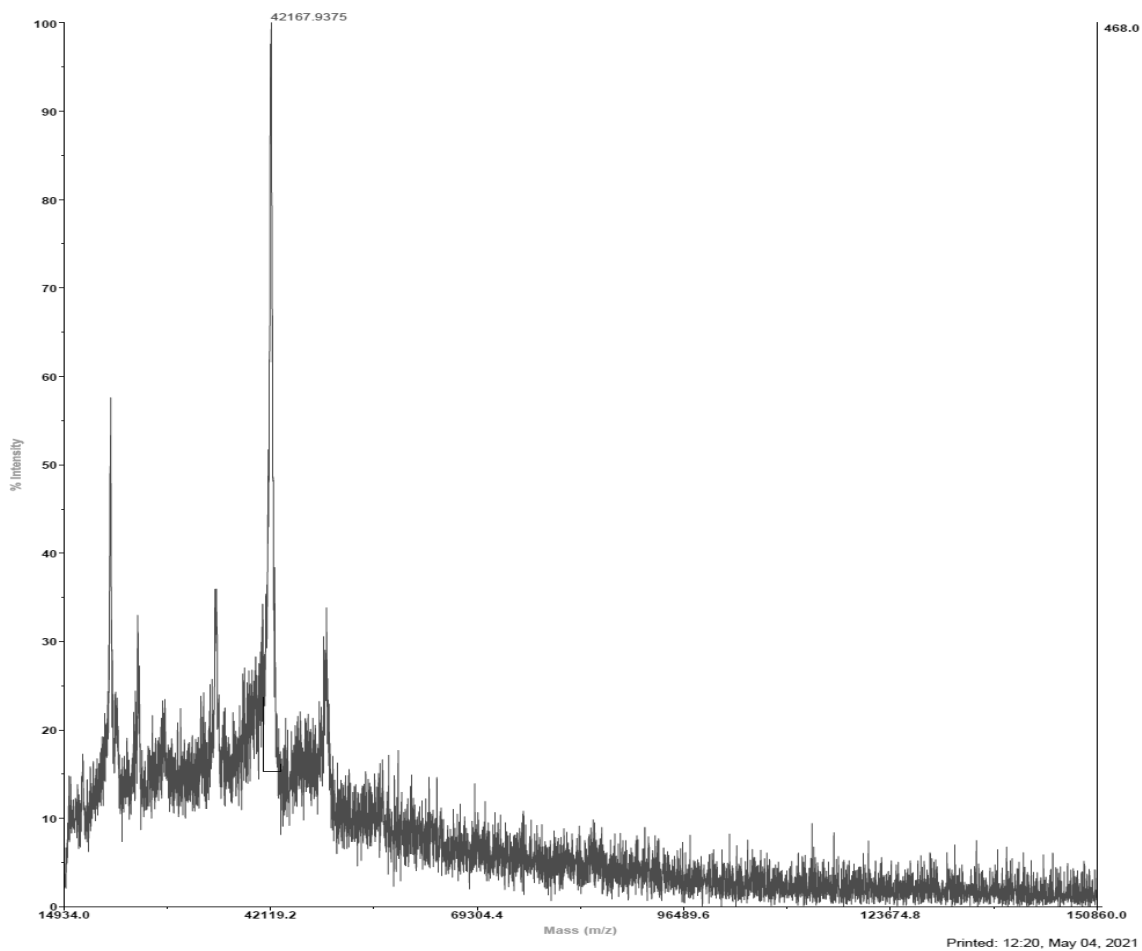


Figure S9. MALDI-TOF spectrum of DsRed(3CY)-ELP₃-ST-His (measured. 42167.9 Da; calculated. 42763.98 Da).

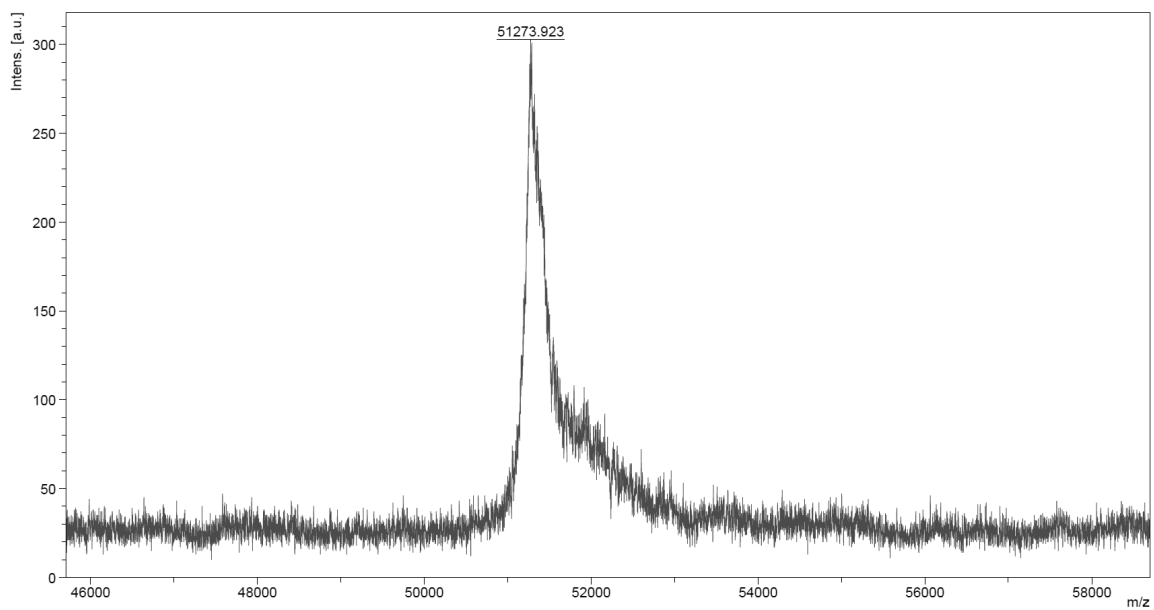


Figure S10. MALDI-TOF spectrum of DsRed(3CY)-ELP₅-SC (measured: 51273.9 Da; calculated: 51956.72 Da).